

Middle East Journal of Science

www.dergipark.org.tr/mejs

MEJS

VOLUME 8

ISSUE 2

DECEMBER

2022

E-ISSN

2618-6136



Copyright © 2022

Email : bilgumus@gmail.com

Visit our home page on www.dergipark.org.tr/mejs

MEJS is an open access journal. This journal licensed under creative common 4.0 International (CC BY 4.0) license. You are free to share and adapt for any purpose, even commercially.

Under the following terms:

Attribution — You must give appropriate credit, provide a link to the license, and indicate if changes were made. You may do so in any reasonable manner, but not in any way that suggests the licensor endorses you or your use.

No additional restrictions — You may not apply legal terms or technological measures that legally restrict others from doing anything the license permits.

Notices:

You do not have to comply with the license for elements of the material in the public domain or where your use is permitted by an applicable exception or limitation.

No warranties are given. The license may not give you all of the permissions necessary for your intended use. For example, other rights such as publicity, privacy, or moral rights may limit how you use the material.



Editor-in-Chief

Zülküf GÜLSÜN

Atomic and Molecular Physics, NMR Spectroscopy
(Prof.Dr., General Director of INSERA, Dicle Teknokent, Dicle University, Diyarbakır, TURKEY))
zulkufgulsun@gmail.com

Language Editor

Dr. Mustafa BULUT

Dicle University Vocational School, Diyarbakır/TURKEY
mbulut@dicle.edu.tr

Co-Editor

Bilal GÜMÜŞ

Dicle University Faculty of Engineering, Dep. of Electrical and Electronics Engineering, Diyarbakır/TURKEY
bilgumus@dicle.edu.tr

Members of Editorial Board and their fields

Abdülkadir MASKAN

Field: Physics Education, Science Education

(Prof.Dr., Dicle University, Faculty of Education, Turkey) akmaskan@dicle.edu.tr

Abdulselam ERTAŞ

Field: Natural products, Pharmacognosy^[SEP] (Assoc.Prof.Dr., Dicle University, Faculty of Pharmacy, Department of Pharmacognosy, Turkey) abdulselamertas@hotmail.com

Abdullah SESSİZ

Field: Agricultural Machinery and Technologies Engineering

(Prof.Dr., Dicle University, Faculty of Agriculture, Turkey) asesiz@dicle.edu.tr

Ahmad ALI

Field: Biotechnology, DNA Extraction, Molecular Biology, Lifesciences

(PhD., University of Mumbai, Dep. of Life Sciences, Mumbai, INDIA) ahmadali@mu.ac.in

Ahmet ALTINDAL

Field: Condensed Matter Physics, Electronic Structure, Thin Films and Low-Dimensional Structures

(Prof.Dr., YILDIZ Technical University, Faculty of Arts and Sciences, Turkey) altindal@yildiz.edu.tr

Ahmet ONAY

Field: Botany, General Biology

(Prof.Dr., Dicle University, Faculty of Science, Dep. of Biology, Turkey) ahmeto@dicle.edu.tr

Alexander PANKOV

Field: Partial Differential Equations, Nonlinear Analysis and Critical Point Theory, Mathematical Physics, Applied Mathematics

(Prof.Dr., Morgan State University, USA) alexander.pankov@morgan.edu

Ali YILMAZ

Field: Atomic and Molecular Physics, Biophysics, NMR Spectroscopy

(Prof.Dr., Retirad, Turkey) yilmz.ali@gmail.com

Arun Kumar Narayanan NAIR

Field: Polymer Chemistry, Computer Simulation

(PhD., King Abdullah University of Science and Technology, Saudi Arabia) anarayanannair@gmail.com

Azeez Abdullah BARZINJY

Field: Material Science, Physics

(Associate Prof.Dr., Materials Science, Department of Physics, Salahaddin University, IRAQ)

azeez.azeez@su.edu.krd

Bayram DEMİR

Field: Nuclear Physics, Nuclear Medicine, Medical Imaging

(Prof.Dr., İstanbul University, Faculty of Science, Turkey) bayramdemir69@yahoo.com

Birol OTLUDİL

Field: General Biology, Pharmaceutical Biology, Science Education

(Prof.Dr., Dicle University, Faculty of Education, Turkey) birolotludil@dicle.edu.tr

Enver SHERIFI

Field: Herbolgy, Biology, Agricultural Science

(Prof.Dr., University of Prishtina, Kosovo) e_sherifi@yahoo.com

Feyyaz DURAP

Field: Inorganic Chemistry

(Prof.Dr., Dicle University, Faculty of Science, Dep. of Chemistry, TURKEY) fdurap@dicle.edu.tr

Gültekin ÖZDEMİR

Field: Agricultural Science, Horticulture

(Prof.Dr., Dicle University, Faculty of Agriculture, Department of Horticulture, Turkey) gozdemir@gmail.com

Hamdi TEMEL

Field: Pharmaceutical Chemistry

(Prof.Dr., Dicle University, Fac. of Pharmacy, Dep. of Pharmaceutical Chemistry, Turkey)

htemelh@hotmail.com

Hasan Çetin ÖZEN

Field: Botany, General Biology

(Prof.Dr., Dicle University, Faculty of Science, Dep. of Biology, Turkey) hasancetino@gmail.com

Hasan İÇEN

Field: Veterinary Internal Disease

(Prof.Dr., Dicle University, Faculty of Veterinary, Dep. of Internal Disease, TURKEY) hasanicen@dicle.edu.tr

Hasan KÜÇÜKBAY

Field: Organic Chemistry, Peptide Chemistry, Heterocyclic Chemistry, Medicinal Chemistry

(Prof.Dr., İnönü University, Faculty of Science and Letters, Dep. of Chemistry, Turkey)

hkucukbay@gmail.com

Hadice Budak GÜMGÜM

Field: Atomic and Molecular Physics, NMR Spectroscopy

(Prof.Dr., Dicle University, Faculty of Science, Dep. of Physics, TURKEY) hbudak@gmail.com

Hüseyin ALKAN

Field: Protein Separation Techniques, Pharmacy

(Assoc.Prof.Dr., Dicle University Faculty of Pharmacy, Department of Biochemistry, TURKEY)

mhalkan@dicle.edu.tr

Ishtiaq AHMAD

Field: Numerical Analysis, Computer Engineering

(PhD., Austrian Institute of Technology, Austria) ishtiaq.ahmad.fl@ait.ac.at

İlhan DAĞADUR

Field: Mathematics, Analysis and Functions Theory

(Prof.Dr., Mersin University Faculty of Arts and Sciences, Dep. of Mathematics, Turkey)

ilhandagdur@yahoo.com; idadagdur@mersin@edu.tr

İsmail YENER

Field: Analytical Techniques, Pharmacy

(PhD., Dicle University, Faculty of Pharmacy, Department of Analytical Chemistry, Turkey)

ismail.yener@dicle.edu.tr

Javier FOMBONA

Field: Science Education

(Prof.Dr., University of Oviedo, Spain) fombona@uniovi.es

Jonnalagadda Venkateswara RAO

Field: Algebra, General Mathematics

(Prof.Dr., School of Science & Technology, United States International University, Nairobi, KENYA)

drjvenkateswararao@gmail.com

Lotfi BENSAPHLA-TALET

Field: Ecology, Hydrobiology

(Assoc. Prof.Dr., Department of Biology, Faculty of Natural Sciences and Life, University Oran1-Ahmed

BENBELLA, Algeria) btlotfi1977@gmail.com

M.Aydın KETANİ

Field: Veterinary, Histology and Embryology

(Prof.Dr., Dicle University, Fac. of Veterinary, Dep. of Histology and Embryology, TURKEY)

Mohammad ASADI

Field: Agriculture, Entomology, Pesticides toxicology

(Dr., Department of Plant Protection, Faculty of Agriculture and Natural Resources,

University of Mohaghegh Ardabili, Ardabil, IRAN) assadi20@gmail.com

Mukadder İĞDİ ŞEN

Field: Astronautics Engineering

(Dr., Trakya University, Edirne Vocational College of Technical Sciences, Turkey)

mukaddersen@trakya.edu.tr

Murat AYDEMİR

Field: Inorganic Chemistry

(Prof.Dr., Dicle University, Faculty of Science, Dep. of Chemistry, TURKEY) aydemir@dicle.edu.tr

Murat HÜDAVERDİ

Field: High Energy and Plasma Physics

(Dr., Yıldız Technical University, Faculty of Science and Letters, Dep. of Physics, TURKEY)

hudaverd@yildiz.edu.tr

Müge SAKAR

Field: General Mathematics

(Assoc.Prof.Dr., Dicle University, Turkey) mugesakar@hotmail.com

Mustafa AVCI

Field: General Mathematics

(Assoc.Prof.Dr., Batman University, Turkey) mustafa.avci@batman.edu.tr

Nuri ÜNAL

Field: High Energy and Plasma Physics

(Retired Prof.Dr., Akdeniz University, Faculty of Science, Turkey) nuriunal@akdeniz.edu.tr

Özlem GÜNEY

Field: Mathematics, Analysis and Functions Theory

(Prof.Dr., Dicle University, Faculty of Science, Dep. of Mathematics, Turkey) ozlemg@dicle.edu.tr

Petrica CRISTEA

Field: Computational Physics, Condensed Matter Physics, Electromagnetism

(Assoc.Prof.Dr., University of Bucharest, Faculty of Physics, Romania) pcristea@fizica.unibuc.ro

Sanaa M. AL-DELAIMY

Field: Atomic and Molecular Physics, General Physics

(Ph.D., Physics Department, Education College for Pure Sciences, Mosul University, Mosul, Iraq)

sadelaimy@yahoo.com

Selahattin GÖNEN

Field: Physics Education, Science Education

(Prof.Dr., Dicle University, Faculty of Education, Turkey) sgonen@dicle.edu.tr

Şemsettin OSMANOĞLU

Field: Atomic and Molecular Physics, ESR Spectroscopy

(Retired Prof.Dr., Dicle University, Faculty of Science, Dep. of Physics) sems@dicle.edu.tr

Sezai ASUBAY

Field: Solid State Physics

(Prof.Dr., Dicle University, Faculty of Science, Dep. of Physics, Turkey) sezai.asubay@gmail.com

Süleyman DAŞDAĞ

Field: Biophysics

(Prof.Dr., İstanbul Medeniyet University, Faculty of Medicine, Dep. of Biophysics, Turkey)

sdasdag@gmail.com

Tamraz H. TAMRAZOV

Field: Biological Sciences

(Assoc.Prof.Dr., Department of Plant Physiology and Biotechnology, Research Institute of Crop Husbandry,
Ministry of Agriculture of the Republic of Azerbaijan)

tamraz.tamrazov@mail.ru

Yusuf ZEREN

Field: Mathematics, Topology

(Assoc.Prof.Dr., Yıldız Technical University, Faculty of Science and Letters, Dep. of Mathematics, TURKEY)

yzeren@yildiz.edu.tr

Z. Gökay KAYNAK

Field: Nuclear Physics

(Retired Prof.Dr., Uludag University, Faculty of Science, Dep. of Physics, Turkey) kaynak@uludag.edu.tr



CONTENTS

Research Articles

- 1- REMOVAL OF HEAVY METALS FROM SYNTHETIC ACIDIC MINE WATER USING RECYCLED AGGREGATES77-83
Gulsen TOZSIN
- 2 - EVALUATION OF SERUM VITAMIN D LEVELS ACCORDING TO SEASON, AGE, AND GENDER IN MARDIN PROVINCE AND ITS SURROUNDINGS..... 84-90
Ahmet DÜNDAR
- 3- THE CHANGES IN HOFFBAUER AND SYNCYTIOTROPHOBLAST CELLS IN SERIOUS PREECLAMPSIA COMPLICATED WITH HELLP SYNDROME (ULTRASTRUCTURAL AND IMMUNOHISTOCHEMICAL STUDY)..... 91-98
Yusuf NERGİZ, Şebnem NERGİZ, Fırat AŞIR, Engin DEVECİ, Erdal SAK, Sıddık EVSEN, Selçuk TUNİK, Uğur ŞEKER
- 4- MODIFICATION OF ASPERGILLUS NIGER ATCC 11414 GROWTH FOR THE ENHANCEMENT OF PROTEASE PRODUCTION BY THE EFFECT OF NATURAL MICROPARTICLES..... 99-105
Hasan Bugra COBAN
- 5- DYNAMIC SUBSTANCE RESEARCH IN DOMESTIC AND IMPORTED BLACK TEA SOLD IN TURKEY..... 106-111
Kasım TAKIM, Mehmet Emin AYDEMİR
- 6- SOLUTION FOR STEKLOV BOUNDARY VALUE PROBLEM INVOLVING THE $p(x)$ -LAPLACIAN OPERATORS 112- 121
Zehra YÜCEDAĞ, Vahup MURAD
- 7- DETERMINATION OF BIOACTIVITIES OF *Convallaria Majalis* L. (LILY OF THE VALLEY), ISOLATING PHARMACEUTICAL ACTIVE INGREDIENTS AND INVESTIGATION ITS INDUSTRIAL USAGE..... 122- 137
Nazan DEMİR, Sıla Nezahat DAŞDEMİR, Alevcan KAPLAN, Yaşar DEMİR
- 8- SOME NOVEL SCHIFF BASE DERIVATIVES AS PROMISING CHOLINESTERASE INHIBITORS WITH ANTIOXIDANT ACTIVITY AGAINST ALZHEIMER'S DISEASE: SYNTHESIS, CHARACTERIZATION AND BIOLOGICAL EVALUATION 138- 146
Ercan ÇINAR, Mehmet BOĞA, Giray TOPAL, Reşit ÇAKMAK

- 9- SYNTHESIS OF NOVEL BIS(PHOSPHINO)AMINE-RUII(ACAC)₂ COMPLEXES, AND INVESTIGATION OF CATALYTIC ACTIVITY IN TRANSFER HYDROGENATION.....** 147- 156
Duygu ELMA KARAKAŞ, Uğur IŞIK, Murat AYDEMİR, Feyyaz DURAP, Akın BAYSAL

Review Articles

- 10- HIROTA METHOD AND SOLITON SOLUTIONS** 157-172
Barış YAPIŞKAN

- 11-THE CHEMISTRY MECHANISM OF HAIR DYES.....** 173-193
Arzu YILDIRIM, Belinda DEMİR, Berfin AK İZGİ, Büşra Nur ERKOL, Çağla ÖZSU, Gülşah EŞLİK AYDEMİR, Mine MUSTAFAOĞLU, Murat KIZIL, Nubar AYHAN, Sevil EMEN

**REMOVAL OF HEAVY METALS FROM SYNTHETIC ACIDIC MINE WATER USING RECYCLED AGGREGATES****Gulsen TOZSIN*** 

Department of Metallurgical and Materials Engineering, Ataturk University, 25240, Erzurum, Turkey

*Corresponding author: gulsentozsin@gmail.com

Abstract: Acid mine drainage (AMD), a highly acidic and sulfate (SO_4^{2-})-rich solution, is an environmental concern related to the release of metal-containing wastewater from mining areas into the environment. In this study, recycled aggregates (RA) produced from concrete debris were used in the treatment of acidic mine water contaminated with heavy metals. For a model synthetic acidic mine water with a pH of 2.31, SO_4^{2-} and iron (Fe) concentrations of 5200 mg L^{-1} and 700 mg L^{-1} , respectively, RA increased the pH value to 11.18 and reduced the SO_4^{2-} and Fe concentrations by 90.51% and 100%, respectively, at RA/AMD ratio of 100 mg L^{-1} after 300 minutes of shaking at room temperature in batch experiments. The test results also showed that 100% of copper (Cu), zinc (Zn), manganese (Mn), silver (Pb), and cobalt (Co) concentrations were removed at this ratio and shaking time. This study demonstrates that RA has significant potential to neutralize acidity and remove heavy metals from AMD, a serious problem for ecological systems and health.

Keywords: Acid mine drainage, Heavy metals, Recycled aggregates, Batch experiment.

Received: April 13, 2022

Accepted: September 19, 2022

1. Introduction

Acid mine drainage (AMD) is a significant environmental problem caused by sulfide mining operations. AMD process starts when sulfide minerals react with oxygen and water [1-5]. Acidic mine waters have low pH because of the oxidation of sulfide minerals to produce sulfuric acid (1) and contain elevated concentrations of SO_4^{2-} , Fe, and other dissolved metals [6-9].



Heavy metal contamination in the aqueous environment is a serious problem for ecological systems and health. If AMD is not controlled, its formation can continue for hundreds of years even after the mine is closed [10-13]. AMD with low pH and high concentrations of heavy metals can be remedied using a process such as adsorption, ion exchange, membrane separation, electrochemical approach, or precipitation [14]. These acidic waters are generally treated with alkaline materials such as recycled aggregates (RA), which increase the pH of aqueous systems and precipitate heavy metals [15, 17].

The concrete industry is one of the leading sectors using the natural resource in the world. The demolition process produces very large quantities of concrete debris and causes great concern for the environment and the economy. Concrete contains 70% aggregates and the industry consumes about 7 billion tons of aggregates every year [18]. After the demolition process, RA produced from concrete debris is mainly composed of a mixture of hydrated cement paste and aggregates. Alkaline materials

like RA generated from concrete debris can be used in neutralizing acidic water and immobilizing heavy metals [19, 20]. The utilization of RA reduces the amount of waste in landfills, thus preserving natural resources and contributing to greater environmental sustainability. This study aimed to investigate the effect of different RA/AMD ratios and shaking times on changes in pH value and SO_4^{2-} , Fe, Cu, Zn, Mn, Pb, and Co concentrations in acidic water.

2. Materials and Methods

RA used in this study was obtained from Istanbul Environmental Management Industry and Trade Company (ISTAC), Istanbul, Turkey. The sample was crushed and sieved below 150 microns. A synthetic AMD solution was prepared by dissolving metal sulfates (FeSO_4 , CuSO_4 , ZnSO_4 , MnSO_4 , PbSO_4 , and CoSO_4) (MERCK, analytical grade) in distilled water. Batch experiments were conducted to evaluate the treatment efficacy by monitoring pH change, and SO_4^{2-} and metal removal rates. Powdered RA samples with masses 20, 40, 60, 80, and 100 g were added to the synthetic AMD solution having a volume of 1000 mL. These rates were adjusted to 2, 4, 6, 8, and 10 g of RA samples in 100 ml of AMD solution and placed in 250 ml Erlenmeyer flasks.

RA and AMD mixtures were agitated in an orbital shaker with continuous agitation at a speed of 180 rpm at room temperature (25°C) for 300 minutes. 10 mL samples were withdrawn using a syringe every 30 minutes, filtered, and stored in sterile tubes at 4°C. The solutions were analyzed to determine the pH value and SO_4^{2-} , Fe, Cu, Zn, Mn, Pb, and Co concentrations.

The chemical composition of RA was determined by X-ray fluorescence (XRF-Philips pW 1400) and reported in wt.%. Solution pH was measured using an Orion model 209 pH meter. The heavy metal concentrations were determined using inductively coupled plasma optical emission spectroscopy (ICP-OES-Perkin Elmer Optima DV 7000). The SO_4^{2-} concentration was measured using a UV/Vis spectrophotometer according to method 375.4 of EPA [21].

3. Results and Discussion

3.1. RA and Synthetic AMD Characterization

The chemical composition of RA is given in Table 1. RA is mainly comprised of CaO (36.28%), SiO_2 (25.88%), Al_2O_3 (5.05%), Fe_2O_3 (2.35%), and MgO (2.18%). A synthetic AMD solution has a composition of $5200 \pm 50 \text{ mg L}^{-1}$ SO_4^{2-} , $700 \pm 20 \text{ mg L}^{-1}$ Fe, $50 \pm 5 \text{ mg L}^{-1}$ Cu, Zn, and Mn; $5 \pm 0.5 \text{ mg L}^{-1}$ Pb and Co; and pH of 2.31 (Table 2).

Table 1. Chemical composition of the RA (%)

CaO	SiO_2	Al_2O_3	Fe_2O_3	MgO	K_2O	SO_3	Na_2O	TiO_2	MnO
36.28	25.88	5.05	2.35	2.18	1.00	0.63	0.62	0.26	0.07
P_2O_5	SrO	ZnO	Cl	BaO	ZrO_2	Cr_2O_3	NiO	CuO	LOI
0.06	0.06	0.05	0.05	0.03	0.03	0.02	0.01	0.01	25.38

LOI: Loss of ignition

Table 2. Chemical composition of synthetic AMD (pH = 2.31)

Component	Source	Concentration (mg L ⁻¹)
Fe	FeSO ₄ ·7H ₂ O	700±20
Cu	CuSO ₄ ·5H ₂ O	50±5
Zn	ZnSO ₄ ·7H ₂ O	50±5
Mn	MnSO ₄ ·H ₂ O	50±5
Pb	PbSO ₄ ·H ₂ O	5±0.5
Co	CoSO ₄ ·7H ₂ O	5±0.5
SO ₄ ²⁻	-	5200±50

3.2. The pH Changes of Synthetic AMD

The time-dependent variations in the pH value, Fe and SO₄²⁻ concentrations measured during batch tests conducted at different RA/AMD ratios are given in Figure 1. The pH increased rapidly at the first 30 minutes and reached an almost steady state for all dose applications. The pH value was measured as 5.57 with a minimum RA dose (20 g L⁻¹) application and increased from 2.31 to 11.18 with a maximum RA (100 g L⁻¹) application after 300 minutes of shaking. The increase in pH value was due to the dissolution of CaO present in RA having high alkalinity. Name and Sheridan [22] state that a high amount of CaO in compounds reacts with water to form calcium hydroxide (Ca(OH)₂) and the dissolution of Ca(OH)₂ generates the alkalinity.

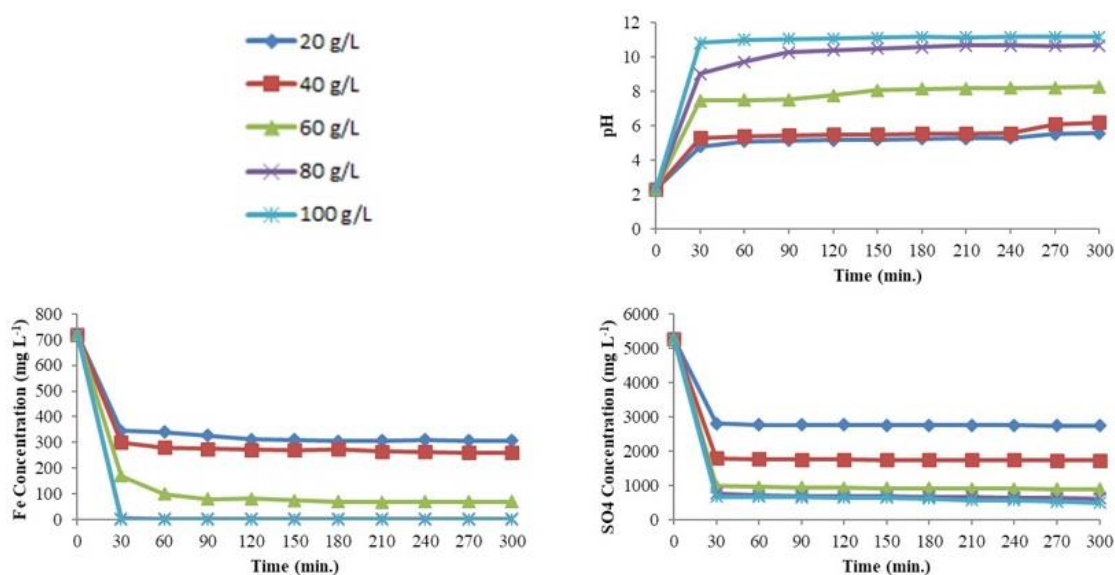


Figure 1. The changes of pH value, Fe, and SO₄²⁻ concentrations at different RA/AMD ratios and shaking times.

3.3. Removal of SO₄²⁻ and Heavy Metals

SO₄²⁻ and Fe concentrations decreased with an increase in RA/AMD ratios. The concentrations dropped very quickly in the first 30 minutes. The removal rate was a function of the RA/AMD ratio with higher ratios showing the highest removal rate. SO₄²⁻ concentration decreased from 5200 mg L⁻¹ to 501 mg L⁻¹ while Fe concentration decreased from 700 mg L⁻¹ to 0.001 mg L⁻¹ at RA/AMD ratio of 100 mg L⁻¹ after 300 minutes of shaking. The pH value of 11.18 was recorded at this ratio (Figure 1). SO₄²⁻ and Fe concentrations were reduced by 90.51% and 100%, respectively, at RA/AMD ratio of 100 mg L⁻¹ at the end of 300 minutes (Table 3). SO₄²⁻ removal is pH-dependent. The drop in the concentration of SO₄²⁻ at high pH is due to the precipitation process [23]. RA, as a calcium-rich neutralizing agent, removed

the SO_4^{2-} ions in the acidic mine waters by precipitation. Madzivire et al. [24] explained the SO_4^{2-} ions concentration could be controlled by the precipitation of gypsum ($\text{CaSO}_4 \cdot 2\text{H}_2\text{O}$) at low pH and ettringite ($\text{Ca}_6\text{Al}_2(\text{SO}_4)_3 \cdot 32\text{H}_2\text{O}$) at high pH.

Table 3. Removal efficiencies of SO_4^{2-} and heavy metals at different RA/AMD ratios and shaking times

		Removal efficiency (%)									
RA/AMD ratio		30	60	90	120	150	180	210	240	270	300
		(minutes)									
SO₄	20 g L⁻¹	46.76	47.39	47.46	47.52	47.67	47.71	47.77	47.78	47.82	47.82
	40 g L⁻¹	65.85	66.36	66.59	66.67	66.86	66.88	66.93	66.95	67.03	67.05
	60 g L⁻¹	81.42	81.86	82.05	82.18	82.42	82.48	82.69	82.80	82.94	83.03
	80 g L⁻¹	85.44	86.63	86.88	86.93	87.03	87.16	87.18	87.78	88.05	88.31
	100 g L⁻¹	87.27	87.37	87.42	87.65	87.80	88.16	89.05	89.07	89.83	90.51
Fe	20 g L⁻¹	52.08	52.78	54.44	56.67	56.94	57.64	57.36	56.94	57.22	57.36
	40 g L⁻¹	58.33	61.11	61.81	62.22	62.50	61.94	63.19	63.33	63.89	63.89
	60 g L⁻¹	76.39	86.11	88.89	88.61	89.58	90.28	90.56	90.28	90.28	90.28
	80 g L⁻¹	100.00	100.00	100.00	100.00	100.00	100.00	100.00	100.00	100.00	100.00
	100 g L⁻¹	100.00	100.00	100.00	100.00	100.00	100.00	100.00	100.00	100.00	100.00
Cu	20 g L⁻¹	100.00	100.00	100.00	100.00	100.00	100.00	100.00	100.00	100.00	100.00
	40 g L⁻¹	100.00	100.00	100.00	100.00	100.00	100.00	100.00	100.00	100.00	100.00
	60 g L⁻¹	100.00	100.00	100.00	100.00	100.00	100.00	100.00	100.00	100.00	100.00
	80 g L⁻¹	100.00	100.00	100.00	100.00	100.00	100.00	100.00	100.00	100.00	100.00
	100 g L⁻¹	100.00	100.00	100.00	100.00	100.00	100.00	100.00	100.00	100.00	100.00
Zn	20 g L⁻¹	98.54	100.00	100.00	100.00	100.00	100.00	100.00	100.00	100.00	100.00
	40 g L⁻¹	100.00	100.00	100.00	100.00	100.00	100.00	100.00	100.00	100.00	100.00
	60 g L⁻¹	100.00	100.00	100.00	100.00	100.00	100.00	100.00	100.00	100.00	100.00
	80 g L⁻¹	100.00	100.00	100.00	100.00	100.00	100.00	100.00	100.00	100.00	100.00
	100 g L⁻¹	100.00	100.00	100.00	100.00	100.00	100.00	100.00	100.00	100.00	100.00
Mn	20 g L⁻¹	83.78	89.49	91.37	93.91	95.72	96.84	97.71	98.22	98.60	100.00
	40 g L⁻¹	98.83	100.00	100.00	100.00	100.00	100.00	100.00	100.00	100.00	100.00
	60 g L⁻¹	100.00	100.00	100.00	100.00	100.00	100.00	100.00	100.00	100.00	100.00
	80 g L⁻¹	100.00	100.00	100.00	100.00	100.00	100.00	100.00	100.00	100.00	100.00
	100 g L⁻¹	100.00	100.00	100.00	100.00	100.00	100.00	100.00	100.00	100.00	100.00
Pb	20 g L⁻¹	100.00	100.00	100.00	100.00	100.00	100.00	100.00	100.00	100.00	100.00
	40 g L⁻¹	100.00	100.00	100.00	100.00	100.00	100.00	100.00	100.00	100.00	100.00
	60 g L⁻¹	100.00	100.00	100.00	100.00	100.00	100.00	100.00	100.00	100.00	100.00
	80 g L⁻¹	100.00	100.00	100.00	100.00	100.00	100.00	100.00	100.00	100.00	100.00
	100 g L⁻¹	100.00	100.00	100.00	100.00	100.00	100.00	100.00	100.00	100.00	100.00
Co	20 g L⁻¹	91.44	95.20	96.40	97.56	98.34	98.70	98.56	98.76	99.04	100.00
	40 g L⁻¹	100.00	100.00	100.00	100.00	100.00	100.00	100.00	100.00	100.00	100.00
	60 g L⁻¹	100.00	100.00	100.00	100.00	100.00	100.00	100.00	100.00	100.00	100.00
	80 g L⁻¹	100.00	100.00	100.00	100.00	100.00	100.00	100.00	100.00	100.00	100.00
	100 g L⁻¹	100.00	100.00	100.00	100.00	100.00	100.00	100.00	100.00	100.00	100.00

Initial concentrations: SO_4^{2-} = 5200 mg/L; Fe = 700 mg/L; Cu = 50 mg/L; Zn = 50 mg/L; Mn = 50 mg/L; Pb = 5 mg/L; Co = 5 mg/L.

All the soluble Fe was removed using RA, which was attributed to the formation of various precipitates. Name and Sheridan [22] explained that the potential-pH diagram for Fe-S-H₂O system indicated that Fe(OH)₃ and Fe(OH)₂ were formed as precipitates. Rose [25] also explained that more Fe

precipitates such as (FeOOH), (Fe₂O₃), and (Fe₅O₈H₄H₂O) could be formed at different pH values. Soluble Fe was removed from the AMD as a form of different insoluble compounds. The results indicated that RA is well suited for pH increase as well as SO₄²⁻ and Fe reductions. Cu, Zn, Mn, Pb, and Co were also totally removed from acidic water at RA/AMD ratio of 100 mg L⁻¹ after 300 minutes of shaking (Table 3). Rodríguez-Jordá et al. [26] stated that heavy metals could be removed from AMD by precipitation using alkaline materials.

4. Conclusion

RA was used in this study as a neutralizing agent for the treatment of AMD. The results clearly indicated that RA reduced the acidity, SO₄²⁻, Fe, and other heavy metals (Cu, Zn, Mn, Pb, and Co) concentrations. The removal rate of SO₄²⁻ and heavy metals increased parallel to the RA/AMD ratios. SO₄²⁻ and heavy metal removal was very rapid in the first 30 minutes. The results show that RA could be effectively used as an alternative alkaline material to neutralize acidity and remove heavy metals from AMD.

Conflict of Interest: The author declares no conflict of interest.

Compliance with Research and Publication Ethics: This work was carried out by obeying research and ethics rules.

The Declaration of Ethics Committee Approval: The author declares that this document does not require ethics committee approval or any special permission. Our study does not cause any harm to the environment.

References

- [1] Akcil, A., Koldas, S., “Acid Mine Drainage (AMD): causes, treatment and case studies”, *Journal of Cleaner Production*, 14 (12-13), 1139-1145, 2006.
- [2] Zhu, M., Legg, B., Zhang, H., Gilbert, B., Ren, Y., Banfield, J.F., Waychunas, G.A., “Early stage formation of iron oxyhydroxides during neutralization of simulated acid mine drainage solutions”, *Environmental Science and Technology*, 46, 8140-8147, 2012.
- [3] Tolonen, E.T., Sarpola, A., Hu, T., Rämö, J., Lassi, U., “Acid mine drainage treatment using by-products from quicklime manufacturing as neutralization chemicals”, *Chemosphere*, 117, 419–424, 2014.
- [4] Demers, I., Benzaazoua, M., Mbonimpa, M., Bouda, M., Bois, D., and Gagnon, M., “Valorisation of acid mine drainage treatment sludge as remediation component to control acid generation from mine wastes, part 1: Material characterization and laboratory kinetic testing”, *Minerals Engineering*, 76, 109–116, 2015.
- [5] Turingan, C.O.A., Cordero, K.S., Santos, A.L., Tan, G.S.L., Tabelin, C.B., Alorro, R.D., Orbecido, A.H., “Acid mine drainage treatment using a process train with laterite mine waste, concrete waste, and limestone as treatment media”, *Water*, 14, 1-21, 2022.
- [6] Smith, M.W., Skema, V.W., “Evaluating the potential for acid mine drainage remediation through remaining in the Tangascootack Creek watershed, Clinton County, Pennsylvania”, *Minerals Engineering*, 41–48, 2001.
- [7] Nieto, J.M., Sarmiento, A.M., Olias, M., Canovas, C.R., Riba, I., Kalman, J., Delvalls, T.A., “Acid mine drainage pollution in the Tinto and Odiel rivers (Iberian Pyrite Belt, SW Spain) and

- bioavailability of the transported metals to the Huelva Estuary”, *Environmental International*, 33, 445-455, 2007.
- [8] Tozsın, G., Arol, A.I., Cayci, G., “Evaluation of pyritic tailings from a copper concentration plant for calcareous sodic soil reclamation”, *Physicochemical Problems of Mineral Processing*, 50 (2), 693-704, 2014.
- [9] Esmali, A., Mobini, M., Eslami, H., “Removal of heavy metals from acid mine drainage by native natural clay minerals, batch and continuous studies”, *Applied Water Science*, 9, 1-6, 2019.
- [10] Cheng, S., Dempsey, B.A., Logan, B.E., “Electricity generation from synthetic acid-mine drainage (AMD) water using fuel cell technologies”, *Environmental Science and Technology*, 41, 8149-8153, 2007.
- [11] Laus, R., Geremias, R., Vasconcelos, H.L., Laranjeira, M.C.M., Favere, V.T., “Reduction of acidity and removal of metal ions from coal mining effluents using chitosan microspheres”, *Journal of Hazardous Materials*, 149, 471-474, 2007.
- [12] Sahinkaya, E., Hasar, H., Kaksonen, A.H., Rittmann, B.E., “Performance of a sulfide-oxidizing, sulfur-producing membrane biofilm reactor treating sulfide-containing bioreactor effluent”, *Environmental Science and Technology*, 45 (9), 4080–4087, 2011.
- [13] Sun, W., Sun, X., Li, B., Xu, R., Young, L.Y., Dong, Y., Zhang, M., Kong, T., Xiao, E., Wang, Q., “Bacterial response to sharp geochemical gradients caused by acid mine drainage intrusion in a terrace: Relevance of C, N, and S cycling and metal resistance”, *Environmental International*, 138, 105601, 2020.
- [14] Fu, F., Wang, Q., “Removal of heavy metal ions from wastewaters: A review”, *Journal of Environmental Management*, 92, 407-418, 2011.
- [15] Johnson, D.B., and Hallberg, K.B., “Acid mine drainage remediation options: A review”, *Science of the Total Environment*, 338 (1-2), 3-14, 2005.
- [16] Papirio, S., Villa-Gomez, D.K., Esposito, G., Pirozzi, F., Lens, P.N.L., “Acid mine drainage treatment in fluidized-bed bioreactors by sulfate-reducing bacteria: A critical review”, *Critical Reviews in Environmental Science and Technology*, 43, 2545-2580, 2013.
- [17] Mahedi, M., Dayioglu, A.Y., Cetin, B., Jones, S., “Remediation of Acid Mine Drainage with Recycled Concrete Aggregates and Fly Ash”, *Journal of Environmental Geotechnics*, 1-14, 2020.
- [18] Bogas, J.A., de Brito, J., Figueiredo, J.M., “Mechanical characterization of concrete produced with recycled lightweight expanded clay aggregate concrete”, *Journal of Cleaner Production*, 89, 187-195, 2015.
- [19] Silva, R.V., de Brito, J., Dhir, R.K., “Prediction of the shrinkage behavior of recycled aggregate concrete: A review”, *Construction and Building Materials*, 77, 327–339, 2015.
- [20] Zhao, T., Remond, S., Damidot, D., Xu, W., “Influence of fine recycled concrete aggregates on the properties of mortars”, *Construction and Building Materials*, 81, 179-186, 2015.
- [21] EPA, *Sulfate turbidimetric. Method 375.4, Methods for the chemical analysis of water and wastes*, EPA/600/4–79/020. US Environmental Protection Agency, Washington DC, USA, 1979.
- [22] Name, T., and Sheridan, C., “Remediation of acid mine drainage using metallurgical slags”, *Minerals Engineering*, 64, 15-22, 2014.

- [23] Nogueira, E.W., de Godoi, L.A.G., Yabuki, L.N.M., Brucha, G., Damianovic, M.H.R.Z., “Sulfate and metal removal from acid mine drainage using sugarcane vinasse as electron donor: Performance and microbial community of the down-flow structured-bed bioreactor”, *Bioresource Technology*, 330, 124968, 2021.
- [24] Madzivire, G., Gitari, W.M., Vadapalli, V.R.K., Ojumu, T.V., and Petrik, L.F., “Fate of sulphate removed during the treatment of circum-neutral mine water and acid mine drainage with coal fly ash: Modelling and experimental approach”, *Minerals Engineering*, 24, 1467-1477, 2011.
- [25] Rose, A.W., *Advances in passive treatment of coal mine drainage*, Penn State University, University Park, PA, 2010.
- [26] Rodríguez-Jordá, M.P., Garrido, F., García-González, M.T., “Effect of the addition of industrial by-products on Cu, Zn, Pb and As leachability in a mine sediment”, *Journal of Hazardous Materials*, 213 (214), 46-54, 2012.

**EVALUATION OF SERUM VITAMIN D LEVELS ACCORDING TO SEASON, AGE, AND GENDER IN MARDIN PROVINCE AND ITS SURROUNDINGS****Ahmet DÜNDAR** Mardin Artuklu University, Health Sciences Vocational School, Mardin, Türkiye
Corresponding author; ahmetdundar83@hotmail.com

Abstract: Vitamin D is a steroid in character and fat-soluble vitamin. It is produced primarily from cholesterol in the skin and is also taken up in a small amount in the diet. 25(OH)D₃ levels are used as an indirect measure of vitamin D levels. Our aim was to investigate the variation in serum 25(OH)D₃ levels of patients admitted to the hospital in and around Mardin based on gender, season, and age. 25(OH)D₃ concentrations were evaluated at Mardin Training and Research Hospital between 01.01.2017 and 31.12.2019. Our study established subgroups according to gender, season, age, and 25(OH)D₃ status. 25(OH)D₃ concentration was measured using the chemiluminescence method. A significant decrease was observed in the 25(OH)D₃ levels of female (13.62±11.53 ng/ml) patients compared to male patients (12.14±9.38 ng/ml). A significant increase was detected in the summer and autumn seasons compared to winter and spring (p<0.001). There was no significant difference between age and serum 25(OH)D₃ concentration (p>0.05). 25(OH)D₃ status was shown to be 60.5% in the severe deficiency group. As a result, it has been shown that the vitamin D profile in Mardin and its surroundings is low in all seasons and in all age groups. For this reason, consuming food sources rich in vitamin D and taking supplements indicate that the importance of sunlight in vitamin D metabolism should be emphasized.

Keywords: Vitamin D, Gender, Age, Seasons, Sunlight

Received: January 8, 2022

Accepted: November 07, 2022

1. Introduction

Vitamin D is known to have important functions in maintaining bone health by regulating calcium and phosphorus metabolism [1]. In epidemiological studies, it has been stated that it is associated with diabetes mellitus, cardiovascular diseases, cancer, multiple sclerosis, autoimmune diseases, and psychiatric and infectious diseases [2-6]. It has also been reported to be associated with the pathophysiology of Parkinson's disease [7]. In autoimmune diseases and multiple cancers, vitamin D stimulates apoptosis and sensitizes cells to chemotherapy by reducing angiogenesis [8]. Vitamin D levels are used as a measure of 25(OH)D₃ levels in patients. Serum levels of 25(OH)D₃ are classified as adequate, insufficient, and deficient [9].

There are two forms of vitamin D: vitamin D₂ in plants and vitamin D₃ in animals [10]. The difference between vitamins D₂ and D₃, which act as prohormones, lies in the structure of their side chains; theoretically, they are used by the body in the same way [11]. Vitamins D₂ and D₃ are biologically inactive. 7-dehydrocholesterol, an intermediate product of cholesterol from epidermal cells in the skin, turns into pre-vitamin D₃ molecules as a result of exposure to sunlight. Vitamin D, taken from the outside, is activated by two hydroxylation mechanisms. The first mechanism takes place in the

liver and forms 25(OH)D₃. This variant of vitamin D makes up the majority of circulating storage forms. The half-life of this molecule is approximately 2–3 weeks. A second hydroxylation reaction occurs in the kidneys, and with this conversion, 1,25(OH)₂D₃ is formed. The half-life of calcitriol is approximately 4–6 hours [12-14].

This study aims to investigate the variation of 25(OH)D₃ levels between gender, season, and age in patients admitted to the hospital in and around Mardin province.

2. Materials and methods

The vitamin D results of patients who applied to Mardin Training and Research Hospital between 01.01.2017-31.12.2019 were evaluated. Chronic renal failure, hypertension, diabetes mellitus, vitamin D supplementation, acute and chronic inflammation, and thyroid dysfunction were determined as exclusion criteria. The study was approved with the permission of the scientific researchers and Publication Ethics Committee of Mardin Artuklu University (11.08.2021 issue no: 7/6). A total of 3,679 patients (female = 2,865; male = 814) were included in our study and grouped according to age, gender, season, and vitamin D status. 25(OH)D₃ concentrations were classified according to the season: spring, summer, autumn, or winter. In terms of age, they were divided into three subgroups: 18–39 years, 40–69 years, and 70 years. They were then further categorised into four groups for the evaluation of vitamin D status: the I-Severe deficiency group, II-Deficiency group, III-Insufficiency group, and IV-Normal group [15]. Serum 25(OH)D₃ levels were determined with the ADVIA Centaur XP brand device using the chemiluminescence method.

2.1. Statistical analysis

Statistical analysis was performed using the SPSS (v. 23) program. The compatibility of the data with the normal distribution was checked with the Kolmogorov - Smirnov test and visual graphics. Since the data were not normally distributed, Mann Whitney-U was used to compare paired groups, and Kruskal Wallis Test was used to compare more than two groups. In the comparison with the Kruskal-Wallis Test, 2-comparisons were made with the Mann-Whitney-U test by making Bonferroni correction in order to understand from which group the statistical difference originated. In all statistical analyzes, those with a p-value below 5% were statistically significant.

3. Results

Descriptive statistics, mean, and standard deviation values are given in the tables. The demographic data of the patients and the mean 25(OH)D₃ level are given in Table 1. It has been demonstrated that the mean 25(OH)D₃ level in female patients (12.14± 9.38 ng/ml) was lower than in male patients (13.62 ± 11.53 ng/ml) and was statistically significant. (p<0.001). Table 1

Regarding the seasons, 25(OH)D₃ levels were 10.82 ± 8.31 ng/ml in spring, 13.66 ± 9.90 ng/ml in summer, 15.04 ± 11.41 ng/ml in autumn, and 10.58 ± 9.16 ng/ml in winter. It was determined that the summer and autumn seasons were higher than the winter and spring seasons and were statistically significant (p<0.001). Table 2

25(OH)D₃ concentration by age was 12.54 ± 10.92 ng/ml in patients aged 18–39 and 12.16 ± 8.64 ng/ml aged 40–69 years, respectively, and in patients aged 18–39 years and above 13.32 ± 9.30 ng/ml. No statistically significant difference was found between age and 25(OH)D₃ concentration. (p>0.05). When analysing 25(OH)D₃ status, 60.5% (n=2.224) of the severe deficiency group, 25.5% (n=939) of the deficiency group, 10.4% (n=383) of the inadequacy group, and 3.6% of the normal group (n=133) were observed. Table 3

While the 25(OH)D₃ concentration was observed as the lowest month with a 9.45±8.20 ng/ml level in February, October was observed to be the highest month with 18.11 ± 10.83 ng/ml. Table 4

Table 1. Serum 25(OH)D₃ (ng/ml) levels according to gender

Gender	n	(%)	(M±SD)	p
Female	2865	(77,9)	12,14± 9,38	0,000
Male	814	(22,1)	13,62 ± 11,53	

M:Mean SD; standard deviation *=p<0.001

Table 2. Serum 25(OH)D₃ (ng/ml) levels according to seasons

Seasons	n	%	(M±SD)	P
Spring	924	(25,1)	10,82±8,31	Group 1-3
Summer	888	(24,1)	13,66±9,90	Group 1-2 Group 2-3
Autumn	894	(24,3)	15,04±11,41	Group 2-4 Group 3-4
Winter	973	(26,4)	10,58±9,16	Group 1-4

Mean:Mean SD; standard deviation *=p<0.001 Group 1; Spring, Group 2; Summer, Group 3; Autumn, Group 4; Winter

Table 3. Distribution of 25(OH)D₃ (ng/ml) levels by status and age groups

Status	n	(%)		
Severe deficiency group	<11	2224	(60,5)	
Deficiency group	11-20	939	(25,5)	
Inadequacy group	21-30	383	(10,4)	
Normal group	>30	133	(3,6)	
Age	n	(%)	(M.±SD)	p
18-39 age	1842	(50,1)	12,54±10,92	0,109
40-69 age	1452	(39,5)	12,16±8,64	
70 age	385	(10,5)	13,32±9,30	

M: Mean SD; standard deviation

Notes: Severe deficiency group (vitamin D level <11 ng/ml), II- Deficiency group (vitamin D level 11-20 ng/ml), III- Insufficiency group (vitamin D level 21-30 ng/ml) IV- normal group (with vitamin D level >30 ng/ml)

Table 4. Serum 25(OH)D₃ (ng/ml) level by month

Month	n	(%)	(M±SD)
January	300	(8,2)	10,79±9,21
February	380	(10,3)	9,45±8,20
March	300	(8,2)	11,09±10,32
April	299	(8,1)	10,31±6,51
May	325	(8,8)	11,04±7,69
June	275	(7,5)	14,44±8,45
July	301	(8,2)	13,07±11,91
August	312	(8,5)	13,55±8,88
September	281	(7,6)	14,65±13,60
October	246	(6,7)	18,11±10,83
November	366	(9,9)	13,30±9,39
December	294	(8,0)	11,83±10,08

M: Mean SD; standard deviation

4. Discussion

Vitamin D is a fat-soluble vitamin with a steroid character that plays a role in calcium homeostasis and bone mineralization. This vitamin is synthesized primarily from cholesterol in the skin and is also taken up in the diet at a low rate [16-18].

The findings of the present study revealed that the mean serum 25(OH)D₃ level (13.62 ± 11.53 ng/ml) in male patients was higher than that in female patients (12.14 ± 9.38 ng/ml). It was determined that there was a significant increase in the summer and autumn seasons compared to the winter and spring. There was no significant difference between age and serum 25(OH)D₃ concentration. 25(OH)D₃ status was shown to be 60.5% in the severe deficiency group. This study is the first to evaluate the differences in 25(OH)D₃ levels between age, gender, and seasons in and around Mardin province

Bolland et al. [19] stated that 25(OH)D₃ deficiency was present at a rate of 39% in men and 73% in women in a study conducted in 1,606 postmenopausal women and 378 elderly men. A study conducted by Vuceljic et al. [20] in Serbia found that the rate of 25(OH)D₃ deficiency in the winter season was higher than in the summer season, and the difference between them was significant in their study in the post-menopausal period. Van der Wielen et al., [21] in their study on 25(OH)D₃ levels in 824 elderly individuals during the winter season, reported that the deficiency was 47% in women and 36% in men.

In a study by Alayunt et al., in Siirt province, 25(OH)D₃ (19.20 ± 0.11 ng/ml) was higher in male patients than in female patients (15.96 ± 0.08 ng/ml) [22]. Taskiran et al. [23] in a study conducted with a 25(OH)D₃ cut-off value of 20 ng/ml, its deficiency was found to be 94.00%. In addition, this level was shown to be 9.6 ± 5.2 ng/ml in female patients and 14.6 ± 5.4 ng/ml in male patients [23]. Cubukcu et al. [24] demonstrated that 25(OH)D₃ concentration was 16.51 ± 11.04 ng/ml in female patients and 16.88 ± 10.19 ng/ml in male patients, and there was a significant difference between male and female patients in terms of season and age. In a study conducted in Elazig only in winter, it was found that the mean 25(OH)D₃ level was 16.81 ± 10.29 ng/ml in men and 14.61 ± 13.43 ng/ml in women. The rate of vitamin D (<20 ng/ml 25(OH)D₃), which was investigated as insufficient, was reported to be 73% in men and 78% in women [25].

In our study, 25(OH)D₃ concentration was found to be lower in female patients than in male patients. The results we obtained showed that they were compatible with the studies performed [22, 23]. The present study also revealed that a low level of vitamin D in women suggests that it is probably due to bone mineralization and local clothing.

Although the rate of sun exposure is higher in countries such as Italy, Spain, and Greece, it has been determined that vitamin D deficiency is lower than in Scandinavian countries. These authors also suggested that this level may be caused by excessive fish consumption and vitamin D supplementation. [25]. The fact that the average annual sunshine duration in Mardin is more than 3,000 hours and that the duration of sunshine is 8–9 hours throughout the year [26] has high potential in terms of endogenous synthesis of vitamin D. Another important result we evaluated in our study was the severe deficiency group, which was found to be 60.5%. The fact that this result is so high indicates that people do not go out in the sun during hot hours and that they are not aware that vitamin D can be synthesised endogenously.

In the study conducted in Van, no difference was found between age and 25(OH)D₃ concentration. Güzel et al., in their study conducted in Adana province in August and September in women with covered hands and faces, 25(OH)D₃ levels were reported to be 33.1 ng/ml 25(OH)D₃ in women with a deficit of 53.9 25(OH)D₃ ng/ml. In addition, it was stated that the summer season was significantly higher than the autumn and spring seasons in terms of seasonality [27]. Alayunt et al. [27]. showed that 25(OH)D₃ levels were lower in winter and spring than in summer and autumn, but vitamin D levels were

low in all four seasons. In a study conducted by Çolak et al., they reported that 25(OH)D₃ levels are close to each other in winter and autumn and that these values are higher in the spring and summer months [28].

In our study, it was shown that 25(OH)D₃ concentrations in the winter and spring seasons were significantly lower than in the autumn and summer seasons. 25(OH)D₃ concentration was observed with the lowest month in February, while October was observed to be the highest month in this respect. Alayunt et al. also found the highest value in terms of vitamin D in July and October. In our study, the fact that the amount of sunbathing time in the winter is less and the time spent inside the house is high suggests that a sedentary lifestyle may cause a deficiency in vitamin D metabolism.

Balahoroglu et al. [29] 25(OH)D₃ levels were 15.15 ± 9.01 ng/ml in the 18–39 age group, 15.7 ± 9.32 ng/ml in the 40–65 age group, and 16.25 ± 10.26 ng/ml in the 66 age group. In our study, 25(OH)D₃ levels were 12.54 ± 10.92 ng/ml in the 18–39 age group, 12.16 ± 8.64 ng/ml in the 40–69 age group, and 13.32 ± 9.30 ng/ml in the 70-age group. It was shown that there was a serious vitamin D deficiency when compared with the studies of other authors.

5. Conclusion

As a result, it has been shown that 25(OH)D₃ levels in female patients in Mardin province and its surroundings are lower than in male patients, and the prevalence of vitamin D deficiency is high in all seasons and in all age groups. In light of these findings, we think that in order to eliminate vitamin D deficiency, which plays an important role in the pathophysiology of diseases, consuming food sources rich in vitamin D and taking supplements and the importance of sunlight on vitamin D metabolism should be emphasized.

Ethical statement

The study was approved with the permission of the scientific researchers and Publication Ethics Committee of Mardin Artuklu University (11.08.2021 issue no: 7/6).

Conflict of interest: The author declares no conflict of interest.

Authors' Contributions

A. D: Conceptualization, Formal analysis, Funding acquisition, Investigation, Project administration, Supervision, Writing – review, and editing. The author reads and approved the final manuscript.

References

- [1] Holick, M.F., "Sunlight and vitamin D for bone health and prevention of autoimmune diseases cancers, and cardiovascular disease", *The American Journal of Clinical Nutrition*, 80(6), 1678-88, 2004. Doi: 10.1093/ajcn/80.6.1678S.
- [2] Holick, M.F., "Vitamin D: importance in the prevention of cancers, type 1 diabetes, heart disease, and osteoporosis", *The American Journal of Clinical Nutrition*, 79(3), 362–71, 2004. Doi: 10.1093/ajcn/79.3.362.
- [3] Holick, M.F., "Vitamin D deficiency", *The New England Journal of Medicine*, 357(3), 266–81, 2007. Doi: 10.1056/NEJMra070553.
- [4] Jenab, M., Bueno-de-Mesquita, H.B., Ferrari, P., van Duijnhoven, F.J., Norat, T., Pischon, T., Jansen, E.H., Slimani, N., Byrnes, G., Rinaldi, S., Tjønneland, A., Olsen, A., Overvad, K., Boutron-Ruault, M.C., Clavel-Chapelon, F., Morois, S., Kaaks, R., Linseisen, J., Boeing, H., Bergmann, M.M., Trichopoulou, A., Misirli, G., Trichopoulos, D., Berrino, F., Vineis, P., Panico,

- S., Palli, D., Tumino, R., Ros, M.M., van Gils, C.H., Peeters, P.H.M., Lund, E., Tormo, M.J., Ardanaz, E., Rodríguez, L., Sánchez, M.J., Dorronsoro, M., Gonzalez, C.A., Hallmans, G., Palmqvist, R., Roddam, A., Key, T.J., Khaw, K.T., Autier, P., Hainaut, P., Riboli, E., “Association between pre-diagnostic circulating vitamin D concentration and risk of colorectal cancer in European populations: a nested case–control study”, *British Medical Journal*, 340:b5500, 2010. Doi: 10.1016/j.maturitas.2009.12.013.
- [5] Parker, J., Hashmi, O., Dutton, D., Mavrodaris, A., Stranges, S., Kandala, N.B., Clarke, A., Franco, O.H., “Levels of vitamin D and cardiometabolic disorders: systematic review and meta-analysis”, *Maturitas*, 65(3), 225–36, 2010. Doi: 10.1016/j.maturitas.2009.12.013.
- [6] Munger, K.L., Levin, L.I., Hollis, B.W., Howard, N.S., Ascherio, A., “Serum 25-hydroxyvitamin D levels and risk of multiple sclerosis”, *The Journal of the American Medical Association*, 296(23), 2832–2838, 2006. Doi: 10.1001/jama.296.23.2832.
- [7] Newmark, H.L., Newmark, J., “Vitamin D and Parkinson’s disease a hypothesis”, *Movement Disorders*, 22(4), 461–468, 2007. Doi: 10.1002/mds.21317.
- [8] Trump, D.L., Deeb, K.K., Johnson, C.S., “Vitamin D: considerations in the continued development as an agent for cancer prevention and therapy”, *Cancer Journal*, 16(1), 1–9, 2010. Doi: 10.1097/PPO.0b013e3181c51ee6.
- [9] Ritterhouse, L.L., Lu, R., Shah, H.B., Robertson, J.M., Fife, D.A., Maecker, H.T., Du, H., Fathman, C.G., Chakravarty, E.F., Scofield, R.H., Kamen, D.L., Guthridge, J.M., James, J.A., “Vitamin D deficiency in a multi-ethnic healthy control cohort and altered immune response in vitamin D deficient European-American healthy controls”, *Plos One*, 9(4), e94500, 2014. Doi: 10.1371/journal.pone.0094500. eCollection 2014.
- [10] World Health Organization. “Vitamin and mineral requirements in human nutrition”, 2nd ed. Geneva, World Health Organization, 2005.
- [11] Ross, A.C., Taylor, C.L., Yaktine, A.L., Del Valle, H.B., editors. “Dietary Reference Intakes for calcium and vitamin. Committee to Review Dietary Reference Intakes for Vitamin D and Calcium”, *Institute of Medicine Washington*, DC: National Academies Press, 2010.
- [12] Misra, M., Pacaud, D., Petryk, A., Collett-Solberg, P.F., Kappy, M., Drug and therapeutics committee of the Lawson Wilkins pediatric endocrine society. “Vitamin D deficiency in children and its management: a review of current knowledge and recommendations”, *Pediatrics*, 122(2), 398e417, 2008. Doi: 10.1542/peds.2007-1894.
- [13] Adams, J.S., Hewison, M., “Update in vitamin D”, *The Journal of Clinical Endocrinology & Metabolism*, 5(2), 471-8, 2010. Doi: 10.1210/jc.2009-1773.
- [14] Christakos, S., Dhawan, P., Verstuyf, A., Verlinden, L., Carmeliet, G., “Vitamin D: metabolism, the molecular mechanism of action, and Pleiotropic Effects”, *Physiological Reviews*, 96(1), 365–408, 2016. Doi: 10.1152/physrev.00014.2015
- [15] Canadian Agency for Drugs and Technologies in Health. “Vitamin D Testing in the General Population: A Review of the Clinical and Cost-Effectiveness and Guidelines”, Ottawa (ON); 2015.
- [16] Deeb, K.K., Trump, D.L., Johnson, C., “Vitamin D signaling pathways in cancer: potential for anticancer therapeutics”, *Nature Reviews Cancer*, 7(9), 684–700, 2007. Doi: 10.1038/nrc2196.

- [17] Bouillon, R., Eelen, G., Verlinden, L., Mathieu, C., Carmeliet, G., Verstuyf, A., “Vitamin D and cancer”, *The Journal of Steroid Biochemistry and Molecular Biology*, 102(1-5), 156–62, 2006. Doi: [10.1016/j.jsbmb.2006.09.014](https://doi.org/10.1016/j.jsbmb.2006.09.014)
- [18] Prietl, B., Treiber, G., Pieber, T.R., Amrein, K., “Vitamin D and immune function”, *Nutrients*, 5(7), 2502–21, 2013. doi: [10.3390/nu5072502](https://doi.org/10.3390/nu5072502).
- [19] Bolland, M.J., Grey, A.B., Ames, R.W., Mason, B.H., Horne, A.M., Gamble, G.D., Reid, I.R.. The effects of seasonal variation of 25-hydroxyvitamin D and fat mass on a diagnosis of vitamin D sufficiency”, *The American Journal of Clinical Nutrition*, 86(4), 959-64, 2007. Doi: [10.1093/ajcn/86.4.959](https://doi.org/10.1093/ajcn/86.4.959).
- [20] Vuceljić, M., Ilić-Stojanović, O., Lazović, M., Grajić, M., “Vitamin D and parathyroid hormone in relation to bone mineral density in postmenopausal women”, *Vojnosanitetski pregled*, 69(3), 243-8, 2012. Doi: [10.2298/VSP1203243V](https://doi.org/10.2298/VSP1203243V)
- [21] Van der Wielen, R.P., Löwik, M.R., Van den Berg, H., de Groot, L.C., Haller, J., Moreiras, O., van Staveren, W.A., “Serum vitamin D concentrations among elderly people in Europe”, *Lancet*, 22, 346(8969), 207-10, 1995. Doi: [10.1016/s0140-6736\(95\)91266-5](https://doi.org/10.1016/s0140-6736(95)91266-5).
- [22] Alayunt, N.Ö., Özüdoğru, O., “Siirt bölgesinde D vitamini seviyesinin yaş, cinsiyet ve mevsimlere göre değişimi”, *Turk Journal Osteoporos*, 26(3), 160-164, 2020. Doi: [10.4274/tod.galenos.2020.37233](https://doi.org/10.4274/tod.galenos.2020.37233)
- [23] Taşkiran, B., Cansu, G.B., “Güneydoğu Bölgesinde erişkinlerde D vitamini eksikliği”, *Osmangazi Tıp Dergisi*, 39(1), 13-20, 2017. Doi: [10.20515/otd.52389](https://doi.org/10.20515/otd.52389)
- [24] Çubukçu, M., Acı, R., Müderrisoğlu, S., “Samsun İlinde D vitamini düzeylerinin yaş, cinsiyet ve mevsimsel özelliklere göre değerlendirilmesi”, *Ankara Medical Journal*, (4):769-75, 2019. Doi: [10.17098/amj.652002](https://doi.org/10.17098/amj.652002)
- [25] Telo, S., Kaman, D., Akgöl, G., “Elazığ İlinde D vitamini düzeylerinin yaş, cinsiyet ve mevsimlere göre değişimi”, *Fırat Tıp Dergisi*, 22(1), 29-33, 2017.
- [26] Mardin ilinin meteorolojik durumu, <https://www.mardintso.org.tr/mardin/cografyasi/>
- [27] Guzel, R., Kozanoglu, E., Guler-Uysal, F., Soyupak, S., Sarpel, T., “Vitamin D status and bone mineral density of veiled and unveiled Turkish women”, *Journal of Women's Health & Gender-Based Medicine*, 10(8), 765-70, 2001. Doi: [10.1089/15246090152636523](https://doi.org/10.1089/15246090152636523).
- [28] Çolak, A.A., Doğan, N., Bozkurt, Ü., Avcı, R., Karademirci, İ., “Vitamin D status in women in İzmir”, *Tepecik Eğitim ve Araştırma Hastanesi Dergisi*, 25(1), 38-42, 2015. Doi: [10.5222/terh.2015.038](https://doi.org/10.5222/terh.2015.038)
- [29] Balaharoglu, R., Cokluk, E., Alp, H.H., Üçler, R., Şekeroğlu, M.R., Huyut, Z., “Evaluation of seasonal relationship with vitamin D levels in Van region”, *Acta Medica Alanya*, 3(2), 124-128, 2019. Doi: [10.30565/medalanya.463904](https://doi.org/10.30565/medalanya.463904)



THE CHANGES IN HOFFBAUER AND SYNCYTIOTROPHOBLAST CELLS IN SERIOUS PREECLAMPSIA COMPLICATED WITH HELLP SYNDROME (ULTRASTRUCTURAL AND IMMUNOHISTOCHEMICAL STUDY)

Yusuf NERGİZ^{1*}  Şebnem NERGİZ²  Fırat AŞIR¹  Engin DEVECİ¹  Erdal SAK³ 
Sıddık EVSEN³  Selçuk TUNİK¹  Uğur ŞEKER¹ 

¹Department of Histology and Embryology, Faculty of Medicine, Dicle University, Diyarbakır, Turkey

²Department of Microbiology, Atatürk Health High School, Dicle University, Diyarbakır, Turkey

³Department of Obstetrics and Gynecology, Faculty of Medicine, Dicle University, Diyarbakır, Turkey

*Corresponding Author: email: yusufnergiz21@gmail.com

Abstract: HELLP syndrome is a syndrome characterized by hemolytic anemia, increased liver enzymes, and thrombopenia and can be seen in 1% of all pregnancies, 10-20% of pregnancies with pain, preeclampsia, and eclampsia. HELLP syndrome usually develops in the third trimester and its pathogenesis is not clear. Human placental villus stroma contains macrophages called Hoffbauer cells (HC), which are thought to be involved in many processes. HC is also called placental macrophage and has a role in many placental events. This study aimed to evaluate the immunohistochemistry and ultrastructural of syncytiotrophoblast and Hoffbauer cells in the placental villi of HELLP syndrome patients. In our study, placental tissues obtained from human normal and HELLP syndrome pregnancies were prepared for light and transmission electron microscopy (TEM) studies. Immunohistochemistry techniques were applied to placenta sections. HC localizations were determined with CD68 (Hoffbauer cell marker). Fine structure properties of HC and syncytiotrophoblasts were examined by TEM. When the HELLP group fetal placental sections were examined under the light microscope, intracytoplasmic edema in syncytiotrophoblast, degenerative vacuoles, and degenerative findings on cell surface membranes were observed. Moreover, villous edema was remarkable. The increase in the number of Hoffbauer cells per villus in the HELLP group was statistically significant ($p < 0.00$). Compared with the control group, there was a significant increase in the number of Hoffbauer cells and syncytiotrophoblast in HELLP group, and also degenerative changes were observed in the ultrastructural structure of these cells.

Keywords: HELLP, Hoffbauer cell, syncytiotrophoblast, immunohistochemistry, placenta.

Received: August 25, 2022

Accepted: November 22, 2022

1. Introduction

Since the middle of the 19th century, there have been many studies on the presence of large cells in the stroma of human placental chorionic villi. It was Kastschenko who pointed out the presence of these cells in the villous stroma. After 1885, researchers named Virchow, Chaletzky, and Neumann discovered large isolated cells with clear cytoplasm in hydatiform molar pregnancies. For this reason, these cells were called Chaletzky-Neumann cells in the past. Later, at the beginning of the 20th century, it was the researcher named Hoffbauer who best described the functional and morphological features of these cells in normal chorionic villi. For this reason, the term Hoffbauer cell has been widely used in the literature [1].

Hoffbauer cells in the villous stroma are round, pleomorphic, or star-shaped. They are 10-30 μm in diameter and are elongated cells. The prominent feature of these cells in early studies is that they have a vacuolated and granular cytoplasm [2]. Later, researchers reported that Hoffbauer cells have multiple membranes, electron-lucent vacuoles of varying size, dense granules with amorphous material, and short endoplasmic reticulum [3-4].

HELLP syndrome is generally considered to be a variant or complication of preeclampsia. It is a life-threatening obstetric complication [1]. The placenta plays a vital role in the nutritional transport between mother and fetus during pregnancy. The main cell type in the placenta is syncytiotrophoblast cells which are located in the intervillous space and in contact with maternal blood. Besides these cells, numerous fibroblast cells adjacent to the fetal capillaries, Hoffbauer cells, and tissue macrophages are also present [4]. There are two major cells in the placenta, trophoblast and Hoffbauer cells. Although there are many studies on trophoblasts surrounding chorionic villi, few studies are about Hoffbauer cells. Hoffbauer cells are fetal tissue macrophages in the chorionic villous stroma. These cells are located close to the trophoblast and fetal capillaries.

Hoffbauer cells express vascular endothelial growth factor [VEGF] that plays a role in the development of vasculogenesis and angiogenesis [5]. Hoffbauer cells in placental villi are located in the immediate vicinity of angiogenic cell cords and primitive vascular tubes [6]. Hoffbauer cells are placental macrophages present in the villi of the placenta during pregnancy. These cells are normally generated on the 18th day of pregnancy and function in the placenta until the end of pregnancy. The cellular origin of the Hoffbauer cells in the placenta varies during pregnancy. In the early stages of pregnancy, they originate from villi mesenchymal cells, but through the end of pregnancy derived by the transformation of fetal monocytes [7]. The role of Hoffbauer cells in the placenta has not been fully elucidated. However, an increase in Hoffbauer cells has been reported in various placental inflammation cases, particularly villitis. Syncytiotrophoblasts are formed by cellular fusion rather than by cellular division. They are continuous, acellular system and their boundaries are not clear [8]. The surface of these cells has irregular microvilli. The luminal cytoplasm contains vesicles surrounded by flat membranes. The remaining cytoplasm contains a large number of rough and smooth endoplasmic reticulum, a well-developed Golgi complex, and numerous mitochondria.

In this study, we aimed to investigate the immunohistochemistry and ultrastructural of the syncytiotrophoblast and Hoffbauer cells in the placental villi of pregnancies with HELLP syndrome.

2. Materials and Methods

The study was approved by the Dicle University Faculty of Medicine non-invasive clinical research ethics committee (record number: 456, date: 28.03.2012). This study was funded by the Dicle University Scientific Research Platform with grant number:13-TF-89. Twenty-five patients with HELLP syndrome and twenty-five healthy pregnant women, a total of 50 pregnant women, were included. Placental samples were obtained from the department of Obstetrics and Gynecology, Faculty of Medicine, Dicle University from women at 36 to 39 weeks of pregnancy. Criteria for HELLP syndrome were assigned as systolic/diastolic blood pressure (BP): 140/90 mmHg and proteinuria >300 mg in 24h.

2.1. Histologic technique

Placental tissue samples were fixed in 10% neutral formalin solution and a paraffin-embedding wax protocol was performed. 5 μm sections were taken for histological and for immunohistochemical staining. Sections were immunostained with Hoffbauer cell marker CD68 and two separate blinded researchers counted placental villi and Hoffbauer cells in the same areas. The mean number of Hoffbauer

cells per villi was determined. The data were analyzed by Student's t-test by the SPSS program, and the number of Hoffbauer cells was calculated in each group. Sections were evaluated by Zeiss imager A2 light microscope, and photomicrographs were taken.

2.2. Immunohistochemical technique

Placental samples were fixed in a 10% neutral formalin solution and processed for routine histological tissue processing. Sections were deparaffinized in xylene and brought to distilled water. To remove epitope blocking, samples were boiled in citrate buffer solution (pH:6.0) in a microwave oven at 700 W. 0.1% hydrogen peroxide was used to block endogenous peroxidase activity for 20 minutes. The blocking solution (Cat.No:85-9043, Invitrogen, USA) was done for 10 minutes. Sections were incubated at 4°C overnight with anti-CD68 (catalog no: ab125212, Abcam, 1:750). A secondary antibody (Invitrogen, USA) was applied for 20 minutes. Slides were then exposed to streptavidin peroxidase for 20 minutes. Diaminobenzidine (Invitrogen, USA) was used as chromogen. Sections were counterstained with hematoxylin and mounted with a mounting medium.

2.3. TEM technique

In order for the Transmission of an Electron Microscope (TEM), placental tissue samples were fixed in 2.5% buffered glutaraldehyde and then, in 1% osmium tetroxide for routine electron microscopic procedure. Semi-thin sections cut with Leica ultra-cut R ultramicrotome were stained with toluidine blue. Semi-thin sections on copper grids were counterstained by uranyl acetate-lead citrate. The grids were evaluated in Jeol 1010 transmission electron microscope, and micrographs were taken.

2.4. Statistical analysis

Statistical analysis was performed by using IBM SPSS version 25 software. Shapiro Wilk test was used for data contribution. Student's test-test and Mann-Whitney U test were used to compare the binary group averages. $P < 0.05$ was considered statistically significant.

3. Results

3.1. Immunohistochemical findings

In the sections stained with CD68 antibody, the positive Hoffbauer cell number per villus was 0.23 ± 0.02 in the control group (Fig.1A) and 0.83 ± 0.12 in the HELLP group (Fig.1B). The number of Hoffbauer cell counts per villi in HELLP group placentas (Fig.2) was statistically significant ($p < 0.001$).

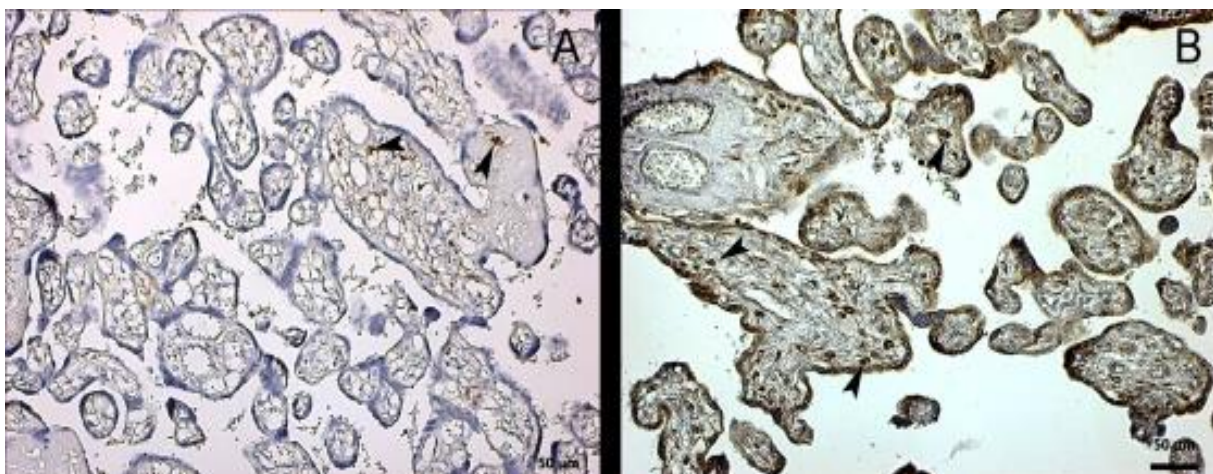


Figure 1. Compared to the control group, a significant increase in the number of CD 68 positive Hoffbauer cells per villus was observed in the placental villi of HELLP group. **A)** Control group, **B)** HELLP group (Staining: IHC CD 68, counterstaining with Hematoxylin, Bar: 50 μ m).

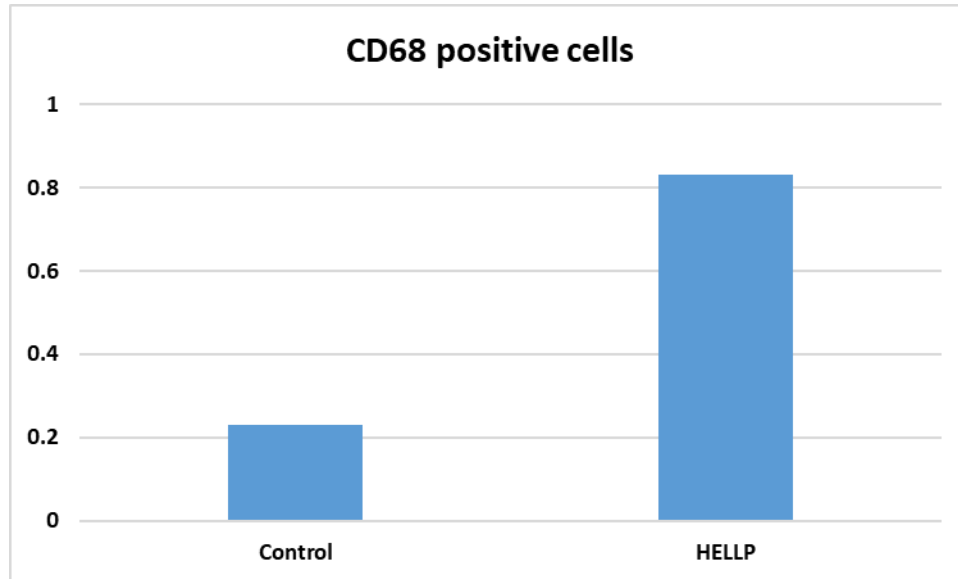


Figure 2. Graph showing the percentage of Hoffbauer cells per villus in control and HELLP group placentas.

3.2. Ultrastructural Findings

Syncytial nodes, syncytiotrophoblasts, Hoffbauer cells, and capillary endothelial structures were observed to have a normal histological structure in the control group of placental sections. Ultrastructural findings of cells in the placental villi of HELLP group. In the placental sections of the HELLP group, intracytoplasmic edema, degenerative vacuoles, and degenerative findings in cell surface membranes were observed in syncytiotrophoblasts. In addition, villous edema was prominent. In another placenta section of the same group, as well as intravascular coagulation, the presence of red blood cells in the extravascular areas due to endothelial degeneration, thinning of the capillary endothelium, villous edema, and degenerative vacuoles were observed (Figure 3).

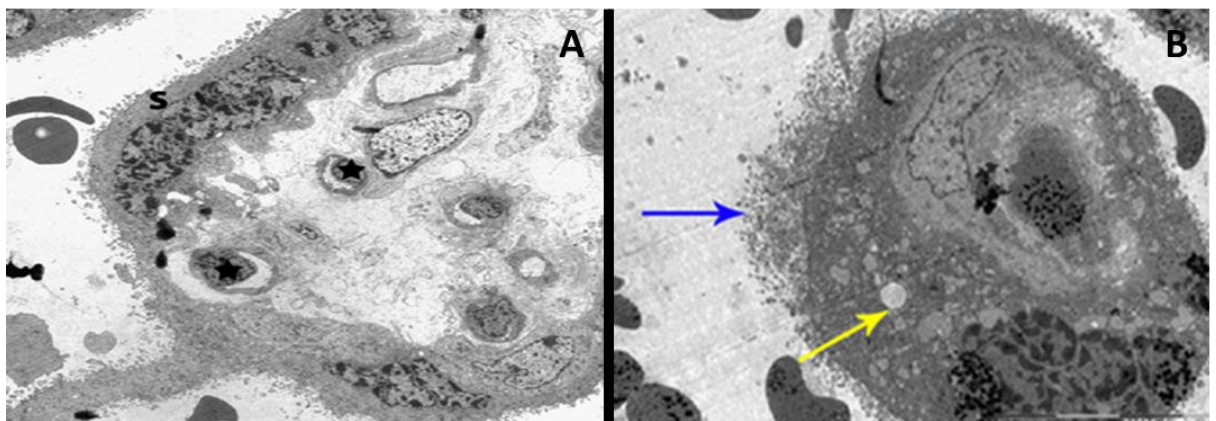


Figure 3. A) In the control group placental section, a structural histologic view to intensive microvilli on the surface of syncytiotrophoblasts, (S), and capillary endothelium cells (star) are seen. **B)** HELLP group placenta section. Degenerative structure (blue arrow) in cell surface membrane, intracytoplasmic edema, and degenerative vacuoles (yellow arrow) in syncytiotrophoblast (uranyl lead nitrate-uranyl acetate, Bar: 20000 nm)

4. Discussion

Preeclampsia is a clinical complication that starts in the 20th week of the pregnancy and continues until 4–6 weeks after birth. Preeclampsia is characterized by hypertension and proteinuria [11]. There are many risk factors that lead to preeclampsia such as abnormal trophoblastic invasion, endothelial dysfunction, impaired nitric oxide and lipid metabolism, and genetic and nutritional factors [12].

Immune tolerance at the feto-maternal junction of the placenta is a complex phenomenon. Although much is known about immune-capable macrophages in the maternal decidua, we know very little about Hoffbauer cells (HC) in fetal chorionic villi. In a study by Yang, no significant difference was found between the hypertensive and normotensive groups in terms of HC diameter. In the continuation of our study, CD14, CD68, and CD163 immunostaining were applied to placental sections and they emphasized that HC in the hypertensive group was weak in terms of immunostaining when compared to the control group [13].

In another study by Zhenghua et al., changes in the number and appearance of HC were reported to be associated with different pregnancy complications [14]. The results of our study are also supported by Demir et al and Kondi-Pafiti et al. These authors pointed out that there is a significant increase in the number of HC in pathological placentas such as gestational diabetes mellitus and intrauterine growth retardation [15-16].

Jones et al. [17] reported severe degenerative changes in the ultrastructural analysis of syncytial cell nuclei, such as pyknosis, peripheral chromatin condensation, and fusion of nuclear membranes. These morphological changes are similar to those of apoptosis, known as programmed cell death [18]. In similar studies, the increase in the number of apoptotic nuclei in trophoblasts of patients with preeclampsia has been pointed out [19-21]. Rath et al. [22] reported that trophoblastic basement membrane thickening was associated with preeclampsia and HELLP. Increased syncytiotrophoblasts in the HELLP placentas cause lesser absorption from the maternal blood as a result of a significant loss of microvilli, and thus the malnutrition of the fetus. In our study, we observed increasingly larger vacuoles and decreased pinocytotic vesicles in the cytoplasm of syncytiotrophoblast cells of the HELLP group, suggesting decreased transport characteristics of syncytiotrophoblasts. Dilatations in the rough endoplasmic reticulum [ER] cisternae, which are observed in these cases, and low electron density accumulation in them are responsible for the basement membrane thickening. Therefore, we emphasized that thickening basal membranes negatively affects the placental barrier function.

In a study by Brunoria et al. [23], they emphasized that smooth ER and rough ER cisterns are very dilated in syncytiotrophoblast cells of HELLP. This event is parallel to the results of our study. Especially in some chorion villi of HELLP placentas, we observed excessive proliferation of cytotrophoblasts and their invasion into stroma as common epithelial mass. Thus, since the stroma is confined in an extremely narrow central region, we thought of considerably reduced or even completely lost placental barrier function in these villi. HELLP syndrome is a systemic disease manifested by cytotrophoblast invasion deficiency or maternal endothelial dysfunction. Roberts et al. [24] showed that the most important factor in this disease is excessive maternal systemic inflammation or uteroplacental hypoxia against pregnancy.

The number of HC in the HELLP group of our study showed a significant increase compared to the control group, and this increase was statistically significant. These results of our study showed a

correlation with the results of the study conducted by Evsen et al. [25]. These researchers emphasized that the number of Hoffbauer cells in the placental villi of patients with HELLP syndrome showed a significant increase compared to the normotensive group. Evsen et al. indicated a significant increase in Hoffbauer cell count in HELLP syndrome. They suggested that this increase may be related to increased inflammation or adaptation mechanism in the fetal placenta. In the immunohistochemical results of our study, compared with the control group, we can say that there was a significant increase in Hoffbauer cell count in the HELLP group placentas. Hoffbauer cells are fetal tissue macrophages in the chorionic villus stroma of the human placenta. This cell population constitutes 40% of the villous stroma and continues to exist during pregnancy. Hoffbauer cells secrete prostaglandin E2 (PGE2) and thromboxane A2 (TXA2). There are publications indicating that the amount of PGE2 and TXA2 released by Hoffbauer cells in a low-oxygen culture medium is reduced [26].

In conclusion, a significant increase in placental Hoffbauer cells and syncytiotrophoblast cell counts as well as several ultrastructural changes were observed in the HELLP group compared to the control group.

Declarations

Ethical statement: Ethical approval was obtained from the Dicle University Faculty of Medicine non-invasive clinical research ethics committee with a record number:456. This study was performed in accordance with Helsinki Declarations. Financial support was funded by the Dicle University Scientific Research Platform (record number: 13-TF-89).

Conflict of interest:

The authors declare there is no conflict of interest.

Authors' Contributions:

Writing - Original draft preparation: Y.N., Ş.N., F.A.

Methodology: U.Ş., S.T.

Formal analysis: Y.N.

Writing: Y.N., Ş.N.

Conceptualization: Y.N., E.S.

Methodology: Y.N., S.E.

Investigation: S.T., F.A., E.D.

Resources: E.D.

Investigation: Y.N., F.A.

All authors read and approved the final manuscript.

References

- [1] C. Grigoriadis *et al.*, "Hofbauer cells morphology and density in placentas from normal and pathological gestations," (in eng), *Rev Bras Ginecol Obstet*, vol. 35, no. 9, pp. 407-12, Sep 2013, doi: 10.1590/s0100-72032013000900005.
- [2] M. T. Vinnars, E. Rindsjö, S. Ghazi, A. Sundberg, and N. Papadogiannakis, "The number of CD68(+) (Hofbauer) cells is decreased in placentas with chorioamnionitis and with advancing gestational age," (in eng), *Pediatr Dev Pathol*, vol. 13, no. 4, pp. 300-4, Jul-Aug 2010, doi: 10.2350/09-03-0632-0a.1.
- [3] A. Kondi-Pafiti, C. Grigoriadis, D. Samiotaki, A. Filippidou-Giannopoulou, C. Kleantithis, and D. Hassiakos, "Immunohistochemical study of inhibin A and B expression in placentas from normal and pathological gestations," (in eng), *Clin Exp Obstet Gynecol*, vol. 40, no. 1, pp. 109-12, 2013.

- [4] B. F. King, "Ultrastructural differentiation of stromal and vascular components in early macaque placental villi," (in eng), *Am J Anat*, vol. 178, no. 1, pp. 30-44, Jan 1987, doi: 10.1002/aja.1001780105.
- [5] E. Gokalp-Ozkorkmaz *et al.*, "Examination of Bcl-2 and Bax Protein Levels for Determining the Apoptotic Changes in Placentas with Gestational Diabetes and Preeclampsia," *Proceedings*, vol. 2, no. 25, p. 1548, 2018. [Online]. Available: <https://www.mdpi.com/2504-3900/2/25/1548>.
- [6] M. S. Suresh, "HELLP SYNDROME: An Anesthesiologist's Perspective," *Anesthesiology Clinics of North America*, vol. 16, no. 2, pp. 331-348, 1998/06/01/ 1998, doi: [https://doi.org/10.1016/S0889-8537\(05\)70025-0](https://doi.org/10.1016/S0889-8537(05)70025-0).
- [7] C. J. Jones, R. H. Choudhury, and J. D. Aplin, "Functional changes in Hofbauer cell glycobiology during human pregnancy," (in eng), *Placenta*, vol. 36, no. 10, pp. 1130-7, Oct 2015, doi: 10.1016/j.placenta.2015.07.131.
- [8] Y. Seval, E. T. Korgun, and R. Demir, "Hofbauer cells in early human placenta: possible implications in vasculogenesis and angiogenesis," (in eng), *Placenta*, vol. 28, no. 8-9, pp. 841-5, Aug-Sep 2007, doi: 10.1016/j.placenta.2007.01.010.
- [9] F. Asir, E. Deveci, E. G. Ozkorkmaz, F. Şahin, and I. S. Ermiş, "The Effect of Momordica charantia Ovarian Ischemia-Reperfusion," *JBM*, vol. 9, no. 12, pp. 8-14, 2021.
- [10] A. S. Laganà, A. Favilli, O. Triolo, R. Granese, and S. Gerli, "Early serum markers of preeclampsia: are we stepping forward?," (in eng), *J Matern Fetal Neonatal Med*, vol. 29, no. 18, pp. 3019-23, Sep 2016, doi: 10.3109/14767058.2015.1113522.
- [11] S. S. Karaşin and T. Çift, "The Role of Ischemia-modified Albumin as a Biomarker in Preeclampsia," (in eng), *Rev Bras Ginecol Obstet*, vol. 42, no. 3, pp. 133-139, Mar 2020, doi: 10.1055/s-0040-1709662.
- [12] S. W. Yang *et al.*, "DC-SIGN expression in Hofbauer cells may play an important role in immune tolerance in fetal chorionic villi during the development of preeclampsia," (in eng), *J Reprod Immunol*, vol. 124, pp. 30-37, Nov 2017, doi: 10.1016/j.jri.2017.09.012.
- [13] Z. Tang, V. M. Abrahams, G. Mor, and S. Guller, "Placental Hofbauer cells and complications of pregnancy," (in eng), *Ann N Y Acad Sci*, vol. 1221, pp. 103-8, Mar 2011, doi: 10.1111/j.1749-6632.2010.05932.x.
- [14] R. Demir and T. Erbençi, "Some new findings about Hofbauer cells in the chorionic villi of the human placenta," (in eng), *Acta Anat (Basel)*, vol. 119, no. 1, pp. 18-26, 1984, doi: 10.1159/000145857.
- [15] C. J. Jones and H. Fox, "Syncytial knots and intervillous bridges in the human placenta: an ultrastructural study," (in eng), *J Anat*, vol. 124, no. Pt 2, pp. 275-86, Nov 1977.
- [16] J. F. Kerr, A. H. Wyllie, and A. R. Currie, "Apoptosis: a basic biological phenomenon with wide-ranging implications in tissue kinetics," (in eng), *Br J Cancer*, vol. 26, no. 4, pp. 239-57, Aug 1972, doi: 10.1038/bjc.1972.33.
- [17] S. C. Smith, P. N. Baker, and E. M. Symonds, "Increased placental apoptosis in intrauterine growth restriction," (in eng), *Am J Obstet Gynecol*, vol. 177, no. 6, pp. 1395-401, Dec 1997, doi: 10.1016/s0002-9378(97)70081-4.

- [18] D. N. Leung, S. C. Smith, K. F. To, D. S. Sahota, and P. N. Baker, "Increased placental apoptosis in pregnancies complicated by preeclampsia," (in eng), *Am J Obstet Gynecol*, vol. 184, no. 6, pp. 1249-50, May 2001, doi: 10.1067/mob.2001.112906.
- [19] A. D. Allaire, K. A. Ballenger, S. R. Wells, M. J. McMahon, and B. A. Lessey, "Placental apoptosis in preeclampsia," (in eng), *Obstet Gynecol*, vol. 96, no. 2, pp. 271-6, Aug 2000, doi: 10.1016/s0029-7844(00)00895-4.
- [20] S. Sreenivasan and S. Khare, "The effects of passive smoking on the human placenta: A gross and microscopic study," *Journal of the Anatomical Society of India*, Original Article vol. 68, no. 1, pp. 34-38, January 1, 2019 2019, doi: 10.4103/jasi.Jasi_5_19.
- [21] I. de Luca Brunori *et al.*, "Placental barrier breakage in preeclampsia: ultrastructural evidence," (in eng), *Eur J Obstet Gynecol Reprod Biol*, vol. 118, no. 2, pp. 182-9, Feb 1 2005, doi: 10.1016/j.ejogrb.2004.04.024.
- [22] J. M. Roberts, R. N. Taylor, and A. Goldfien, "Clinical and biochemical evidence of endothelial cell dysfunction in the pregnancy syndrome preeclampsia," (in eng), *Am J Hypertens*, vol. 4, no. 8, pp. 700-8, Aug 1991, doi: 10.1093/ajh/4.8.700.
- [23] M. S. Evsen *et al.*, "Human placental macrophages (Hofbauer cells) in severe preeclampsia complicated by HELLP syndrome: immunohistochemistry of chorionic villi," (in eng), *Anal Quant Cytopathol Histopathol*, vol. 35, no. 5, pp. 283-8, Oct 2013.
- [24] B. Wetzka, D. E. Clark, D. S. Charnock-Jones, H. P. Zahradnik, and S. K. Smith, "Isolation of macrophages (Hofbauer cells) from human term placenta and their prostaglandin E2 and thromboxane production," (in eng), *Hum Reprod*, vol. 12, no. 4, pp. 847-52, Apr 1997, doi: 10.1093/humrep/12.4.847.

**MODIFICATION OF *ASPERGILLUS NIGER* ATCC 11414 GROWTH FOR THE ENHANCEMENT OF PROTEASE PRODUCTION BY THE EFFECT OF NATURAL MICROPARTICLES****Hasan Bugra COBAN^{1,2}** ¹Izmir International Biomedicine and Genome Institute, Dokuz Eylul University, Balçova, 35340, Izmir, Turkey²Izmir Health Technologies Development and Accelerator (BioIzmir), Dokuz Eylul University, Balçova, 35340, Izmir, Turkey*Corresponding author; bugra.coban@deu.edu.tr

Abstract: Even though fungal proteases are under interest, bulk fungal growth during production decreases the overall mass transfer and consequently the yield. In this study, instead of inorganic microparticles, various organic microparticles were used in the production medium to prevent bulky fungal growth and increase homogeneity. Results showed that all microparticle additions increased the maximum protease activity remarkably and also lowered the required time to reach the highest value. Among organic microparticle addition productions, the highest protease activity was reported as 100,76 U/mL in walnut shells added flasks, which was approximately 1,4 fold higher compared to the highest activity obtained in the control production. It was also reported that microparticle addition increased the homogeneity but also resulted in higher viscosity due to hyphae-type growth. Additionally, evaluation of various storage temperatures showed that produced enzyme lost only its 7% activity at 4°C at the end of 25 days.

Keywords: Fungal, protease, microparticle, productivity

Received: April 26, 2022

Accepted: September 25, 2022

1. Introduction

Proteases, which break down proteins into their subunits are produced by many organisms from viruses to prokaryotes and eukaryotes. Among them, microorganisms are the main commercial protease producers due to their biochemical diversity and being able to be modified with genetic modifications [1]. Even though *Bacillus* strains dominate the current protease production, interest in fungal proteases, especially in *Aspergillus* strains is increasing due to advantages in terms of high production levels, growth on waste solid materials, low cost, and ease of downstream process step [2,3].

In fungal productions, morphology is one of the most effective factors in yield and productivity. However, the tendency of fungal stains to create bulk growth in the production medium generally ends up with inefficient mass transfer and consequently low product formations. Therefore, preventing bulk fungal growth and the formation of a homogenized production medium is crucial to ensure stable, repeatable, and sustainable productions [4]. Various microparticles such as titanium oxide, aluminum oxide, and talcum were used in fungal productions to prevent bulky growth and aggregation and also to increase homogenization and production yield [5-11]. Even though this technique has many advantages such as low cost, ease of implementation, and not interfering with the fungal metabolism; waste management of these microparticles is a critical environmental problem. Due to the fact that they cannot

be biologically metabolized, disposal of these microparticles creates the necessity for extra costly process steps.

In this study, talcum and various organic microparticles such as walnut shells, pistachio shells, and coffee seeds were evaluated for their ability to enhance protease production with *Aspergillus niger* by controlling fungal growth in shake flask productions.

2. Materials and methods

2.1. Fungal strain and inoculum preparation

A. niger ATCC 11414 was kindly donated by Prof. Dr. Gülşad Uslu Şenel from Firat University, Department of Environmental Engineering, Turkey. The fungal strain was grown on potato dextrose agar (PDA) plates at 25°C for 6 days. The culture was transferred to sterile agar plates biweekly in order to maintain cellular viability. After the incubation, spores were collected by adding 8 mL of sterile 0,1% Tween 80. Suspension, which had approximately 10^8 spores/mL was used to inoculate the production media.

2.2. Shake flask productions

In this study, talcum, walnut shells, pistachio shells, and brewed coffee seeds were used as microparticles. Talcum was used without any pretreatment, whereas walnut shells, pistachio shells, and coffee seeds were first grinded in the coffee grinder and then sieved by using a 750 µm pore size sieve. Thereafter, grinded coffee seeds were brewed with an excessive amount of water to minimize extraction in the protease production medium. After that, all grinded organic microparticles were transferred into 75 mL of double distilled water in 250 mL flasks and autoclaved at 121°C for 15 minutes to minimize plant-originated extractions. Organic microparticles were then filtered and dried at 55°C for 8 hours before use. The chemical composition of the protease production medium consisted of 15 g glucose, 3 g meat extract, 2 g KH_2PO_4 , 10 g casein, 10 g peptone, and 10 g NaCl per liter of double distilled water. The prepared media was transferred into 250 mL shake flasks with 75 mL working volume and 5% (w/v) microparticles were added to the media. Thereafter, flasks were autoclaved at 121°C for 15 minutes and after cooling to room temperature, 3% (v/v) inoculum was added into each flask. Flasks were cultured at 25°C and 180 rpm for 6 days. Samples were collected every 24 hours to measure protease activity.

2.3. Protease activity measurement

Fungal protease activity was measured spectrophotometrically [12] with minor modifications. First, taken samples were centrifuged at 5500 rpm for 10 minutes and then 0.5 mL of supernatant was mixed with 2.5 mL of phosphate buffer (50 mM, pH: 7.0), which contained 0.6% (w/v) casein. After incubation at 25°C for 20 minutes, the reaction was finalized by the addition of 2.5 mL of 0.44 M trichloroacetic acid. The mixtures were settled for 10 minutes at room temperature and then centrifuged again at 5500 rpm for 10 minutes. From the supernatant, 0.25 mL liquid was first mixed with 1.25 mL of 0.5 M Na_2CO_3 and then 0.25 mL Folin-Ciocalteu phenol. The mixtures were stored at room temperature and dark for 30 minutes. The absorbance was measured at 600 nm using an uninoculated medium as blank. Enzymatic activity value was calculated using a pre-calculated tyrosine standard. One unit of enzyme unit (U) was defined as the amount of enzyme, which is required to release 1 µmol of tyrosine at 25°C per minute.

2.4. Stability of protease activity under various storage temperatures

Fungal protease, which was produced in walnut shell added flasks at the maximum level, was centrifuged at 5500 rpm for 10 minutes and then supernatants were transferred into the sterile microcentrifuge tubes. Thereafter, tubes were stored at -20, 4, and 25°C conditions, and samples were taken periodically to calculate the stability of activity.

3. Results and discussion

In this study, the effect of talcum and various organic microparticles on protease production by *A. niger* was evaluated. Fungal growth morphology, protease production yield, productivity, also enzyme stability under different temperature storage conditions were evaluated.

Viscosity is a key parameter to be considered in bioprocessing systems, which directly affects mass transfer, aeration and agitation efficiency, and power input [13]. Addition to production medium composition, fungal growth structure is also highly effective on medium rheology and viscosity. At 72 hours of the shake flask production, images were taken from the bottom of the flasks to make an evaluation of fungal growth morphologies (Figure 1). As it can be seen in Figure 1a, a heterogeneous fungal formation occurred in the flask, in which there was not any microparticle added. Lots of small sizes and also big bulk fungal growth structures were observed, which decreases the reliability of stability and repeatability of the productions. On the other hand, the production broth showed clear and not viscous characteristics in the control flask, which provides advantages during separation and purification steps. In all microparticle-added flasks, fungus performed only small or hyphae growth structures. Whereas talcum-added production flasks resulted in a very high viscous broth (Figure 1b), walnut shells added flask (Figure 1c) showed lower resistance to flow. Also, pistachio shells (Figure 1d) and coffee seed shells (Figure 1e) added flasks resulted in mild-level viscous broths.

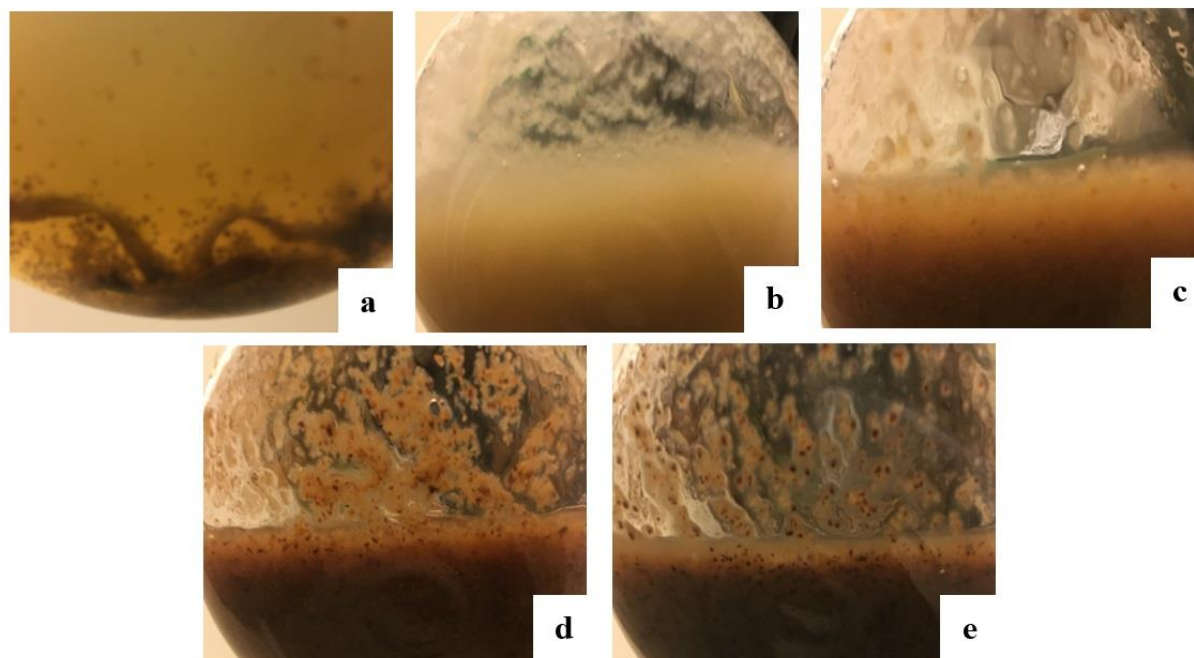


Figure 1. Fungal growth morphologies of *A. niger* with the effect of microparticles (a: Control, b: Talcum addition, c: Walnut shell addition, d: Pistachio shell addition, e: Coffee seed addition)

Fungal protease activities during the production were measured and graphed in Figure 2. It can be clearly seen from Figure 2 that, all microparticle-added flasks resulted in higher maximum protease activities compared to the control. The highest protease activity was calculated as 127,16 U/mL in talcum-added production and the lowest was in coffee seed-added production as 83,16 U/mL. Among organic microparticle-added productions, the maximum protease activity was calculated as 100,76 U/mL in walnut shells added flasks. However, the highest enzyme activity was computed as 73,26 U/mL in the control flask. It was also reported that the highest protease activities were obtained at 120 hours of production in all microparticle-added flasks. Nevertheless, the maximum protease activity was observed at 144 hours of production in the control. These results clearly state that microparticle addition both increased the maximum enzyme activity and also lowered the time to reach the top point, which resulted in higher productivity. Productivity values were calculated as 0,7, 1,74, 0,84, 0,9, and 0,97 U/mL/h for control, talcum added, walnut shell added, pistachio shell added, and coffee seed added productions, respectively. It was also noted that protease activities followed almost the same pattern till 24 h of the production, however lower enzyme activity was measured in coffee seed-added flasks compared to control at 48 h of the fermentation and then activity increased in the further sampling times. This can be explained by the potential negative effect of further released agrochemical byproducts such as phenolics and furans on microbial metabolism [14].

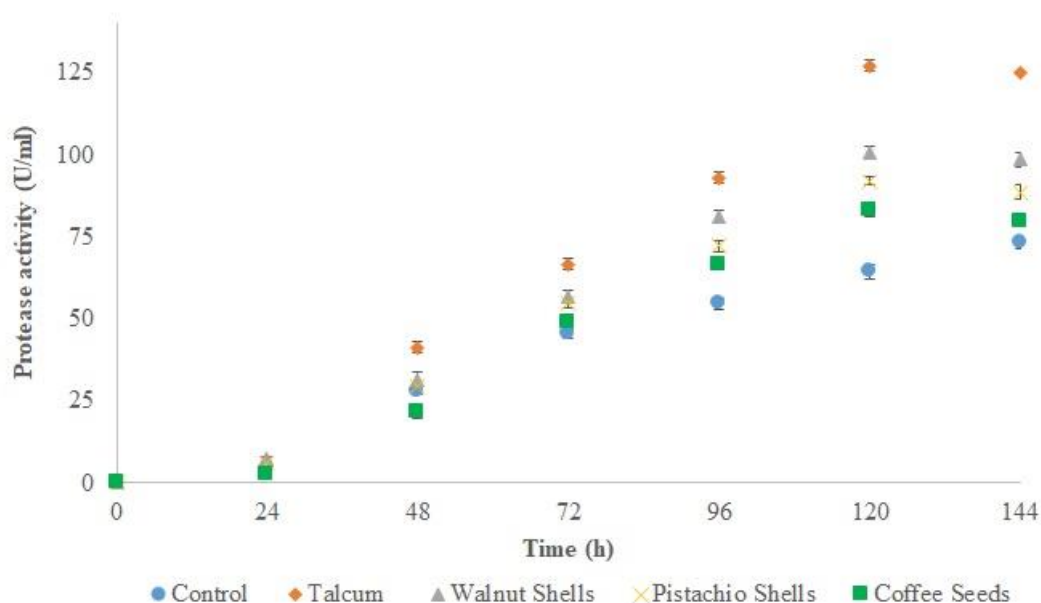


Figure 2. *A. niger* protease activity trends during the production under the effect of various microparticles.

The effect of microparticles on the enhancement of fungal protease production is further discussed and related to various physiochemical properties of the microparticles as shown in Table 1. A comparison of the densities of the microparticles showed that talcum is approximately 5 times heavier than other organic microparticles. Since all microparticles were added to the flasks based on weight per volume, small number of talcum microparticles were in the flask compared to others due to the higher density of talcum. Nevertheless, in comparison based on the particle size, talcum particles were 30 to 75 times smaller than organic microparticles, which potentially resulted in a higher number of talcum particles in the flasks compared to organic microparticles added flasks. Additionally, evaluation of the hardness of microparticles showed that talcum is the softest and coffee seed is the hardest microparticle used in this study. Hardness is an effective factor in fungal growth during especially a long period of

cultivation (144 h) in terms of fragility and preservation of the integrity of the particles. At least but not the less, talcum is not biologically available for fungi, and disposal of it causes serious environmental problems. However, organic microparticles can be disposed of environment without any side effects, and additionally, various nutrients such as sugars, which are released from plant-based wastes can be partially metabolized by the fungi during production [14].

Table 1. Various physicochemical properties of microparticles.

Property	Talcum	Walnut Shells	Pistachio Shells	Coffee Seeds
Density (g/cm ³)	2.58-2.83	0.48-0.52	0.45-0.50	0.56-0.75
Size (µm)	~10	~300-750	~300-750	~300-750
Hardness (Moh)	~1.0	~3.5	~3.5	~5.0
Biological degradation	No	Yes	Yes	Yes

After all, in order to make a more efficient comparison of the effect of organic and inorganic microparticles on fungal productions, optimization and standardization of mechanical, physical, and chemical properties of the particles are required.

Walnut shells added production broth was centrifuged and cell-free supernatants were transferred into the tubes and stored at -20, 4, and 25°C conditions. As seen in Figure 3, samples, which were stored at 4 and 25°C temperatures remained their activities at the end of the first day. However, freezing samples caused a sharp decrease (higher than 50%) in the protease activity even on the first day. This can be explained by the adverse effect of ice crystal occurrence on the protein structure of the enzyme [15]. Therefore, cryoprotectant addition to samples before freezing is highly recommended. After the first day, frozen samples almost kept their activity values the same till the end of 25 days. Activity differences between samples, which were kept at 4 and 25°C started to increase by the third day of storage. With the advantage of minimizing water activity, 4°C storage conditions resulted in better activity protection compared to 25°C. By the end of 25 days, protease activity losses were calculated as 7% and 25% for 4 and 25°C storage conditions, respectively.

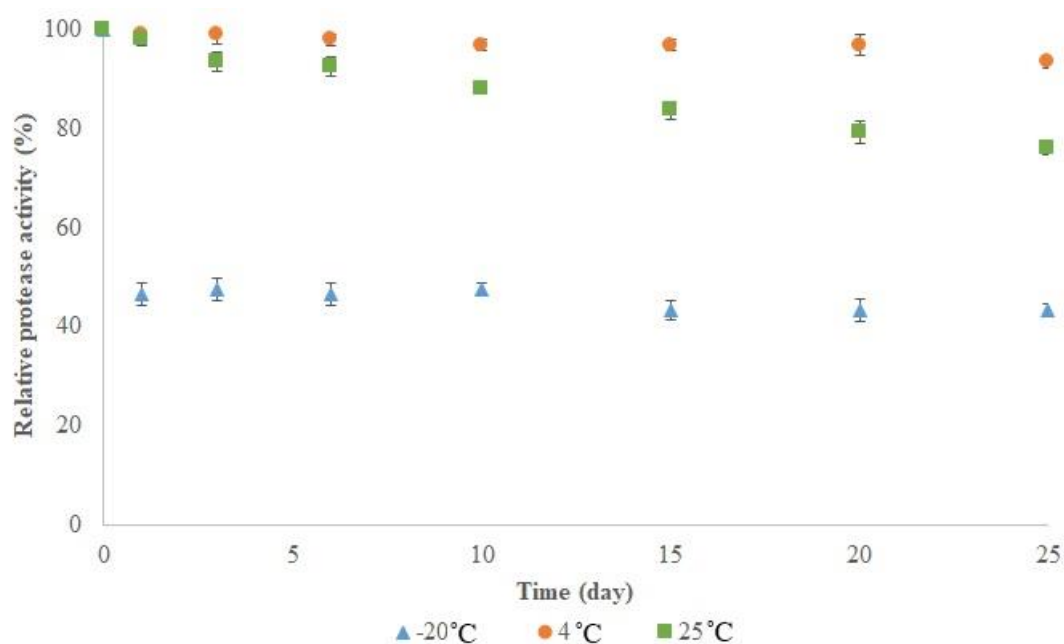


Figure 3. Effect of storage temperature on fungal protease activity

4. Conclusion

In this study, it was clearly shown that organic microparticles are strong substitute candidates for inorganic particles, which can be used for the enhancement of fungal production. The addition of organic microparticles can both increase the highest protease activity and also decrease the time, which is required to reach the maximum activity value. Additionally, it was shown that the mechanical and physicochemical properties of the microparticles should be further discussed and studied in order to provide a better understanding of the overall process. Furthermore, it was reported that produced enzyme can maintain its activity by 93% at the end of 25 days at 4°C storage conditions.

Acknowledgments

I thank Prof. Dr. Gülşad Uslu Şenel from Firat University, Department of Environmental Engineering for providing the fungal strain, which was used in this study, and also Ass. Prof. Dr. Hatice Güneş Özhan, who kindly shared her laboratory with me for my studies at Izmir Biomedicine and Genome Center.

Ethical statement

No ethical statement is needed for this study.

Conflict of interests

As the author, I declare no conflict of interest.

Author contributions

As the single author in this study, I fully contributed to the study conception and design (% 100).

The author read and approved the final manuscript.

References

- [1] Purushothaman, K., Bhat, S.K., Singh, S.A., Marathe, G.K., Rao, A.R.G.A., “Aspartic protease from *Aspergillus niger*: Molecular characterization and interaction with pepstatin A”, *International Journal of Biological Macromolecules*, 139, 199-212, 2019. Doi: 10.1016/j.ijbiomac.2019.07.133
- [2] Siala, R., Frikha, F., Mhamdi, S., Nasri, M., Kamoun, A.S., “Optimization of acid protease production by *Aspergillus niger* I1 on shrimp peptone using statistical experimental design”, *The Scientific World Journal*, 2012. Doi: 10.1100/2012/564932
- [3] Yin, L.J., Hsu, T.H., Jiang, S.T., “Characterization of acidic protease from *Aspergillus niger* BCRC 32720”, *Journal of Agricultural and Food Chemistry*, 61(3), 662-666, 2013. Doi: 10.1021/jf3041726
- [4] Karahalil, E., Coban, H.B., Turhan, I. “A current approach to the control of filamentous fungal growth in media: microparticle enhanced cultivation technique”, *Critical Reviews in Biotechnology*, 39(2), 192-201, 2019. Doi: 10.1080/07388551.2018.1531821
- [5] Coban, H.B, Demirci, A., “Enhancement and modeling of microparticle-added *Rhizopus oryzae* lactic acid production”, *Bioprocess and Biosystems Engineering*, 39(2), 323-330, 2016. Doi: 10.1007/s00449-015-1518-0
- [6] Coban, H.B., Demirci, A., Turhan, I., “Microparticle-enhanced *Aspergillus ficuum* phytase production and evaluation of fungal morphology in submerged fermentation”, *Bioprocess and Biosystems Engineering*, 38(6):1075-1080, 2015. Doi: 10.1007/s00449-014-1349-4

- [7] Coban, H.B., Demirci, A., Turhan, I., “Enhanced *Aspergillus ficuum* phytase production in fed-batch and continuous fermentations in the presence of talcum microparticles”, *Bioprocess and Biosystems Engineering*, 38(8), 1431-1436, 2015. Doi: 10.1007/s00449-015-1384-9
- [8] Kaup, J.A., Ehrich, K., Pescheck, M., Schrader, J., “Microparticle-enhanced cultivation of filamentous microorganisms: Increased chloroperoxidase formation by *Caldariomyces fumago* as an example”, *Biotechnology and Bioengineering*, 99(3):491-498, 2008. Doi: 10.1002/bit.21713
- [9] Driouch, H., Hansch, R., Wucherpennig, T., Krull, R., Wittmann, C., “Improved enzyme production by bio-pellets of *Aspergillus niger*: Targeted morphology engineering using titanate microparticles”, *Biotechnology and Bioengineering*, 109(2), 462-471, 2012. Doi: 10.1002/bit.23313
- [10] Walisko, R., Krull, R., Schrader, J., Wittmann, C., “Microparticle based morphology engineering of filamentous microorganisms for industrial bio-production”, *Biotechnology Letters*, 34(11), 1975-1982, 2012. Doi: 10.1007/s10529-012-0997-1
- [11] Driouch, H., Roth, A., Dersch, P., Wittmann, C., “Filamentous fungi in good shape: Microparticles for tailor-made fungal morphology and enhanced enzyme production”, *Bioengineered Bugs*, 2(2), 100-104, 2011. Doi:10.4161/bbug.2.2.13757
- [12] Vaithanomsat, P., Malapant, T., Apiwattanapiwat, W., “Silk degumming solution as substrate for microbial protease production”, *Kasetsart Journal - Natural Science*, 42, 543-551, 2008, Doi:10.1016/j.jbiotec.2008.07.1967
- [13] de Jesus, S.S., Neto, J.M., Maciel, R., “Hydrodynamics and mass transfer in bubble column, conventional airlift, stirred airlift and stirred tank bioreactors, using viscous fluid: A comparative study”, *Biochemical Engineering Journal*, 118, 70-81, 2017. Doi: 10.1016/j.bej.2016.11.019
- [14] Demirel, F., Germec, M., Coban, H.B., Turhan, I., “Optimization of dilute acid pretreatment of barley husk and oat husk and determination of their chemical composition”, *Cellulose*, 25(11), 6377-6393, 2018. Doi:10.1007/s10570-018-2022-x
- [15] Cao, E.H., Chen, Y.H., Cui, Z.F., Foster, P.R., “Effect of freezing and thawing rates on denaturation of proteins in aqueous solutions”, *Biotechnology and Bioengineering*, 82(6), 684-690, 2003. Doi:10.1002/bit.10612

**DYNAMIC SUBSTANCE RESEARCH IN DOMESTIC AND IMPORTED BLACK TEA SOLD IN TURKEY****Kasım TAKIM¹** , **Mehmet Emin AYDEMİR^{2*}** ¹Harran University, Faculty of Veterinary, Department of Basic Sciences, Şanlıurfa, Turkey²Harran University, Faculty of Veterinary, Department of Veterinary Food Hygiene and Technology, Şanlıurfa, Turkey

*Corresponding author: aydemiremin23@gmail.com

Abstract: Tea is a popular product known worldwide with health benefits for consumers. For centuries, it has been considered a safe and healthy beverage. Although the tea plant has many beneficial effects on human health, the chemicals that can be found in the tea plant can cause negative effects on health. Recently, the use of dyes in teas comes to the fore among imitations or adulterations made in foods recently. These substances pose a health risk. The purpose of this study; sold in the province in Turkey's Southeast Anatolia and Eastern Anatolia regions and to assess the presence of dye in domestic and imported tea. In the study (Mardin; 7, Şırnak; 3, Van; 15, Diyarbakir; 13, Siirt; 9, Batman; 4, Gaziantep; 14, Kilis; 4 and Şanlıurfa; 10) Iran, Sri Lanka, India and originating in Turkey A total of 79 samples were taken from the black teas and a wool yarn dyeing analysis with (GMMAY S: 94-107) method was performed to look for dyes. The analyzes were carried out in an advanced private laboratory with European Union accreditation. According to the analysis results, no dye was detected in any of the tea samples. According to these results, it was concluded that no dyestuff is used in the harvesting, processing, drying, and packaging stages of local and imported teas sold in the Southeastern Anatolia and Eastern Anatolia regions. Turkey determined to make the presence of dyes in general in the domestic and imported tea in other regions such analysis is required.

Keywords: Black tea, Dyestuff, Iranian tea, Sri Lanka tea, Turkish tea.

Received: July 8, 2021

Accepted: September 16, 2022

1. Introduction

Tea is an aromatic beverage prepared by pouring hot or boiling water over the dried leaves of the plant known as *Camellia sinensis*. With a history of 5000 years, tea is among the most consumed beverages all over the world after water [1-3]. In the world, the tea plant is grown from about 42 degrees of latitude in the northern hemisphere, where the precipitation is abundant and the climate is warm, to 27 degrees of latitude in the southern hemisphere. China, India, Sri Lanka, Kenya, Vietnam, Indonesia, SSBC, Japan, Myanmar, Turkey, Bangladesh, Iran, Argentina, Uganda, Tanzania, Malawi, Thailand, Nepal, Rwanda, Burundi, and Ethiopia are from countries where tea plants are grown general [4]. 80% of tea production is made in India, China, Sri Lanka, Indonesia, Kenya, Turkey, and Japan [5-6]. The phenolic compounds found in the tea plant have many beneficial effects on human health such as antioxidant, antimicrobial, anticancer, anti-inflammatory, antiviral, lowering cholesterol, lowering blood pressure, reducing the risk of cardiovascular disease, and reducing the risk of osteoporotic fractures elderly [7-10]. However, the presence of harmful pollutants such as heavy metals, mycotoxins, and pesticide residues in the tea plant can have negative effects on health [11-12]. In addition to these

harmful substances, it is also claimed that dyes are used as food additives in order to make the color of the tea plant look beautiful when it is put into water, obtain standard color, and produce faster color. The Ministry of Agriculture and Forestry also reported in the official gazette on 13.01.2020 that dyestuff, which is a food additive, was detected in 11 tea brands [13].

Food additive refers to substances that are not consumed as food alone but are expected to be a component of that food either directly or indirectly, as a result of being added to food during technological production stages such as production, treatment, processing, preparation, and packing. Food dyes, which are among food additives, are of special importance today. Food dyes are substances that give or restore color to foods, that are not consumed as food in general, and aren't used as a specialty component of food [14]. The reasons for adding dyes to foods; are to protect the color naturally found in food, to create a technological standard color in food, to give different color tones to the food, and to hide low qualities in food [15].

As a result of the widespread use of food dyes in foods and their legalization with legislation, many methods have been developed to detect these substances in foods. In the analysis of water-soluble synthetic organic dyes used in foods; methods such as wool thread dyeing method, paper chromatography (PC), thin layer chromatography (TLC), column chromatography (CC), gas chromatography (GC), high-pressure liquid chromatography (HPLC) are used [16].

When coloring agents are required to be used in foods, the doses determined by Joint Expert Committee in Food Additives and Contaminants (JECFA) and Codex Alimentarius must be followed. Many harmful effects on health occur when these doses are not followed or when exposed to dyes for a long time. Dyestuffs have genotoxic, carcinogenic, and neurotoxic effects on the body. In addition, it causes, allergic reactions, skin rashes, and asthma. It is reported to cause hyperactivity in children [17-22] As stated in the Turkish Food Codex Regulation on Food Additives, it is not allowed to use any coloring substance in tea. Therefore, before the tea is offered for consumption, imitation or adulteration is made when coloring substances are added consciously, provided that they create a standard color in the product technologically and do not hide their low quality. The purpose of this study, Located in Turkey's Southeast Anatolia and Eastern Anatolia regions that are sold provinces in domestic and imported teas, is to determine whether there is a dye and whether there is any imitation and adulteration. and adulteration.

2. Materials and Methods

2.1. Collection of samples

Within the scope of the study, Mardin; 7, Şırnak; 3, Van; 15, Diyarbakir; 13, Siirt; 9, Batman; 4, Gaziantep; 14, Kilis; 4, and Şanlıurfa; 10 to be a total of 79 black tea samples, were collected (Figure 1). Collected teas from Iran, Sri Lanka, and India and originated in Turkey. Tea samples were taken from city markets and coffee shops in sterile sample bags and brought to the laboratory. Samples were kept in a dry and cool environment until analysis.

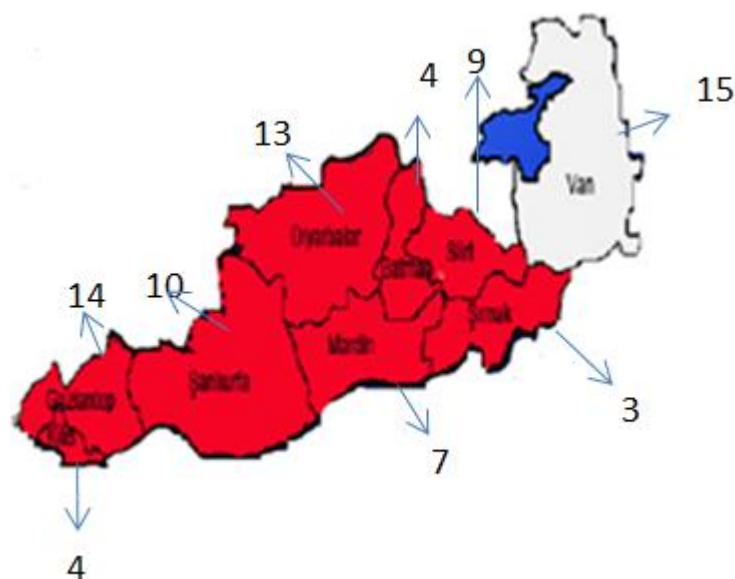


Figure 1. Cities and number of samples

2.2. Analyzing samples

Analyzes were carried out in an advanced private laboratory accredited by the European Union (Environmental Food and Industrial Laboratories Group). In this laboratory, wool yarn dyeing analysis was carried out according to the (GMMAY S: 94-107) method for the determination of dyestuff in teas.

Dyeing wool yarns method

This method is based on the principle that acidic dyes in aqueous acetic acid solution and basic dyes in ammonia solution dye degreased white wool. The method is based on two principles. one.; Synthetic dyes are mostly hydrophobic and adhere insolubly to wool, so they cannot be removed by washing in water. 2. Natural dyes found in foods are mostly hydrophilic because they are phenolic derivative compounds and because they can dissolve in water, they leave the wool during washing. These two different behavior patterns are used in the process of distinguishing natural and synthetic dyes from each other.

2.2.1 Preparation of wool yarns

In order to degrease the raw wool yarns, it was extracted with petroleum ether in a soxhlet device. The woolen threads were left to dry. After drying, 5% NH_3 solution was added and kept in a water bath at 80°C for 1 hour. Then the woolen threads were washed generously with pure water and left to dry. The dried wool threads were kept in a glass container for use [16].

2.2.2 Dyeing of wool yarns

The tea sample was dissolved in distilled water in a beaker. 10% KHSO_4 solution was dropped until the solution was pH 2. Then, some degreased wool threads were placed in the environment. In order for the dyes in the environment to be absorbed by the wool yarns, each was placed in a 60°C water bath and kept for half an hour. Then the woolen threads taken in the beaker were washed with distilled water. As a result of the washing process, if the dyes were not retained by the woolen yarns, the dye was considered present. If the paint flows and leaves the wool, it is considered as no paint [23]. As a result of washing, the wool threads that did not run off dye were placed in a beaker and 10 ml of 5% NH_3 solution was added and heated in a water bath for 30 minutes. If the dye does not separate from the

woolen yarns, it was accepted as a natural dye. If the dye was separated from the woolen threads, it was accepted as a synthetic dye [16].

3. Results and Discussion

As a result of the analyzes, dyes were not detected in any of the 79 tea samples as shown in Table 1.

Table 1. Dyes results in tea samples

City of Sample Taken	Number of Samples	Colorant	Analysis Method
Mardin	7	(N.D. *)	GMMAY S:94-107
Şırnak	3	(N.D.)	GMMAY S:94-107
Van	15	(N.D.)	GMMAY S:94-107
Diyarbakır	13	(N.D.)	GMMAY S:94-107
Siirt	9	(N.D.)	GMMAY S:94-107
Batman	4	(N.D.)	GMMAY S:94-107
Gaziantep	14	(N.D.)	GMMAY S:94-107
Kilis	4	(N.D.)	GMMAY S:94-107
Şanlıurfa	10	(N.D.)	GMMAY S:94-107

(*No Detected)

Food dyes, which are a group of food additives, are defined by the International Food Codex Commission (The Codex Alimentarius) as "a substance added to color or add color to foods". However, although the codex prohibits some dyes and the use of dyestuffs for some foods, these prohibitions are abused and used for imitation and adulteration in foods. Despite these properties, they are considered to be health risks due to their possible carcinogenic and teratogenic effects. In earlier Turkey and other countries the tea, associated with the dye residue wasn't observed in a scientific study. As a result of this study consumed in Turkey's domestic and imported tea, it has been no detected dye residue. In contrast to the results of this study, teas imported into Turkey It is claimed that artificial dye was added. It is claimed that this dye is aniline, the dye obtained by distilling hard coal. It is said that aniline is not distinguished in tea. Because it oxidizes and turns brown when exposed to oxygen and because it has a pleasant odor [24]. Without any analysis, it has been understood that this information, which was told only on estimation, had no scientific basis, but was speculation. In addition, the Ministry of Agriculture and Forestry reported in the official gazette on 13.01.2020 that dyestuffs were detected in 11 tea brands [13]. Since this date is later than this study, we could not analyze the teas belonging to the relevant companies. We chose the most preferred companies in the tea originating in Turkey. No paint residue was found in these. The list announced by the Ministry was in line with the results of this study.

4. Conclusion

The results of this study express a clear finding that imported teas do not contain dyes. The fact that tea brands with dyestuffs announced by the Turkey Ministry of Agriculture and Forestry are completely domestic production and the results of our study on imported teas, It has put an end to the speculation that there are dyes in imported teas until now. In fact, the most important point that causes such speculation is the fact that imported teas, known as illegal tea, give a lot of color during the brewing process. The fact that imported tea has eaten a smuggled label and gives almost twice as much brew during brewing than domestic teas has raised suspicion about whether dyes are added to these teas. Of

course, it is quite possible for such a suspicion to occur. But, it is interesting that no formal answer to this question has been given to this day. This work we have done puts an end to speculation. We think that the reason why imported teas are brewed more is related to the extraction rates and sludge coefficient of these tea types and we recommend that a further study be conducted on this subject.

Acknowledgments

This work was financially supported by Harran University Scientific Research Projects Unit (Project Number: HUBAP- 19016). A small part of the data in this study was presented at the "International Tea Congress, 2022" event.

Compliance to the Research and Publication Ethics

This study was carried out in accordance with the rules of research and publication ethics.

Conflict of Interest

The authors declare no conflict of interest.

Author's Contributions

Kasım TAKİM: Conceptualization, Data curation, Investigation, Project administration, Resources, Supervision, Writing – original draft, Writing– review & editing.

Mehmet Emin AYDEMİR: Formal analysis, Conceptualization, Data curation, Investigation, Methodology, Software, Writing– original draft.

References

- [1] L. Diby, J. Kahia, C. Kouamé, and E. Aynekulu, "Tea, Coffee, and Cocoa," *Encycl. Appl. Plant Sci.*, 3, 420–425, 2016, doi: 10.1016/B978-0-12-394807-6.00179-9.
- [2] B. Schwarz, H. P. Bischof, and M. Kunze, "Coffee, tea, and lifestyle," *Prev. Med. (Baltim.)*, 23(3), 377–384, 1994, doi: 10.1006/pmed.1994.1052.
- [3] D. L. McKay and J. B. Blumberg, "The Role of Tea in Human Health: An Update," *J. Am. Coll. Nutr.*, 21(1), 1–13, 2002, doi: 10.1080/07315724.2002.10719187.
- [4] H. K. Kurt, G., Hacıoğlu, "Dünya ülkeleri ile türkiye'nin çay üretiminin istatistiklerle incelenmesi," in *Doğu Karadeniz Kalkınma Ajansı II. Rize Kalkınma Sempozyumu*, 2013, pp. 39–63.
- [5] M. Amirahmadi, S. Shoeibi, M. Abdollahi, H. Rastegar, R. Khosrokhavar, and M. P. Hamedani, "Monitoring of some pesticides residue in consumed tea in Tehran market," *Iran. J. Environ. Heal. Sci. Eng.*, 10(1), 1-6, 2013, doi: 10.1186/1735-2746-10-9.
- [6] H. Cihan, Endemic agricultural products in Blacksea Area: Production, marketing and consumption of nut, tea, kiwi, Master thesis, Karadeniz Teknik University, Trabzon, Turkey, 2014.
- [7] L. Zhang, Z. zhu Zhang, Y. bin Zhou, T. jun Ling, and X. Chun Wan, "Chinese dark teas: Postfermentation, chemistry and biological activities," *Food Research International*, 53(2) 600–607, 2013, doi: 10.1016/j.foodres.2013.01.016.
- [8] N. Khan and H. Mukhtar, "Tea polyphenols for health promotion," *Life Sciences*, 81(7) 519–533, 2007, doi: 10.1016/j.lfs.2007.06.011.
- [9] C. L. Shen, M. C. Chyu, and J. S. Wang, "Tea and bone health: Steps forward in translational nutrition1-5," *Am. J. Clin. Nutr.*, 98(6), 1694-1699, 2013, doi: 10.3945/ajcn.113.058255.

- [10] Y. Isono, *et al.*, "Black tea decreases postprandial blood glucose levels in healthy humans and contains high-molecular-weight polyphenols that inhibit α -glucosidase and α -amylase in vitro: a randomized, double-blind, placebo-controlled, crossover trial," *Functional Foods in Health and Disease*, 11(5), 222-236, 2021, doi: [10.31989/ffhd.v11i5.791](https://doi.org/10.31989/ffhd.v11i5.791).
- [11] A. M. Abd El-Aty, J. H. Choi, M. M. Rahman, S. W. Kim, A. Tosun, and J. H. Shim, "Residues and contaminants in tea and tea infusions: a review," *Food Addit. Contam. - Part A Chem. Anal. Control. Expo. Risk Assess.*, 31(11), 1794–1804, 2014, doi: [10.1080/19440049.2014.958575](https://doi.org/10.1080/19440049.2014.958575).
- [12] K. Takım, and M. E. Aydemir, "Şanlıurfa İlinde Tüketilen Kaçak Çaylarda LC-MS ve GC-MS ile Pestisit Analizi," *Kahramanmaraş Sütçü İmam Üniversitesi Tarım ve Doğa Dergisi*, 21(5), 650-664, 2018, doi:[10.18016/ksudobil.402273](https://doi.org/10.18016/ksudobil.402273).
- [13] Anonymous 2020(a), "Tarım Orman Bakanlığının Kamuoyuna Duyurusu," 2020. <https://www.tarimorman.gov.tr/Lists/Duyuru/Attachments/1102/:2020-1.pdf>.
- [14] Anonymous, "Gıda katkı maddeleri yönetmeliği", *Türk Gıda Kodeksi*, 2013.
- [15] D. Başkan, Developing a new reversed-phase high-performance liquid chromatography (RP-HPLC) for determination of some of food colorants substances, Master thesis, Karadeniz Teknik University, Trabzon, Turkey, 2015.
- [16] H. Keskin, *Besin Kimyası Cilt II*. İstanbul: İstanbul Üniversitesi Yayınları, 1982.
- [17] Y. F. Sasaki *et al.*, "The comet assay with 8 mouse organs: Results with 39 currently used food additives," *Mutat. Res. - Genet. Toxicol. Environ. Mutagen.*, 519(1–2), 103–119, 2002, doi: [10.1016/S1383-5718\(02\)00128-6](https://doi.org/10.1016/S1383-5718(02)00128-6).
- [18] B. Atlı, Food dyes, Master thesis, Namik Kemal University, Tekirdağ, Turkey, 2010.
- [19] Ayper, B. and Binokay, S. "Gıda katkı maddeleri ve sağlığımıza etkileri" *Arşiv Kaynak Tarama Dergisi*, 19(3), 141-154, 2010.
- [20] Büyükdere, Y. and Ayaz, A, "Gıdalarda kullanılan renklendiricilerin sağlık yönü: dikkat eksikliği hiperaktivite bozukluğu", *Beslenme ve Diyet Dergisi*, 44(2), 169-177, 2016.
- [21] S. Şen, H. Aksoy, and S. Yılmaz, "Genotoxic, carcinogenic potential of food additives and their other effects on human health Gıda katkı maddelerinin genotoksik, karsinojenik potansiyeli ve insan sağlığı üzerindeki diğer etkileri," *J. Hum. Sci.*, 14(4), 3093-3108, 2017, doi: [10.14687/jhs.v14i4.4700](https://doi.org/10.14687/jhs.v14i4.4700).
- [22] I. S. Khan, *et al.*, "Genotoxic effect of two commonly used food dyes metanil yellow and carmoisine using *Allium cepa* L. as indicator," *Toxicology reports*, 7, 370-375, 2020, doi:[10.1016/j.toxrep.2020.02.009](https://doi.org/10.1016/j.toxrep.2020.02.009)
- [23] M. Prochazka, "Modern Food Analysis," *J. AOAC Int.*, 54(6), 1456–1456, 1971, doi: [10.1093/jaoac/54.6.1456b](https://doi.org/10.1093/jaoac/54.6.1456b).
- [24] Anonymous. 2020 (b), "Kaçak çaya kömürün damıtılmasıyla elde edilen boya katılıyor," Apr. 07, 2020. <https://www.sabah.com.tr/yasam/2018/03/19/kacak-caya-komurun-damitilmasiyla-elde-edilen-boya-katiliyor>.



Research Article

SOLUTION FOR STEKLOV BOUNDARY VALUE PROBLEM INVOLVING THE $p(x)$ -LAPLACIAN OPERATORS

Zehra YÜCEDAĞ^{*1}  Vahup MURAD² 

¹ Dicle University, Department of Mathematics, 21280, Diyarbakir, Turkey

² Dicle University, Department of Mathematics, 21280, Diyarbakir, Turkey

* Corresponding author; zyucedag@dicle.edu.tr

Abstract: In this paper, we are concerned with Steklov boundary value problem involving $p(x)$ -Laplacian operator. By means of the Mountain Pass theorem together with Ambrosetti- Rabinowitz condition, we prove the existence of a nontrivial weak solution in Sobolev spaces with variable exponent under appropriate conditions $f(x, u)$.

Keywords: Variable exponent Lebesgue-Sobolev spaces, variational methods, Ambrosetti- Rabinowitz condition.

Received: January 25, 2022

Accepted: September 24, 2022

1. Introduction

In this article, we study the following Steklov boundary value problem involving $p(x)$ -Laplacian operator

$$\begin{cases} \operatorname{div}(a(x, \nabla u)) = 0, & x \in \Omega, \\ a(x, \nabla u) \frac{\partial u}{\partial \nu} = \lambda f(x, u), & x \in \partial\Omega, \end{cases} \quad (\mathbf{P})$$

where $\Omega \subset \mathbb{R}^N$ ($N \geq 2$) is a bounded with smooth boundary, $p \in C(\overline{\Omega})$, $f: \partial\Omega \times \mathbb{R} \rightarrow \mathbb{R}$ is a Carathéodory function, λ is a positive parameter, $\frac{\partial u}{\partial \nu}$ is the outer unit normal derivative on $\partial\Omega$,

$a(x, \varepsilon): \overline{\Omega} \times \mathbb{R}^N \rightarrow \mathbb{R}^N$ is the continuous derivative with respect to ε the mapping $A(x, \varepsilon): \overline{\Omega} \times \mathbb{R}^N \rightarrow \mathbb{R}^N$, and $\operatorname{div}(a(x, \nabla u))$ is $p(x)$ -Laplacian type operator.

The operator $\operatorname{div}(a(x, \nabla u))$, which appears in (\mathbf{P}) , is a more general operator than the $p(x)$ -Laplacian operator

$$\Delta_{p(x)} u := \operatorname{div} \left(|\nabla u|^{p(x)-2} \nabla u \right).$$

In this study, we assume that A , a and f satisfy the following conditions:

(A1) The following inequality holds:

$$|a(x, \varepsilon)| \leq c \left(1 + |\varepsilon|^{p(x)-1} \right), \text{ for all } x \in \overline{\Omega} \text{ and all } \varepsilon \in \mathbb{R}^N.$$

(A2) $A(x, 0) = 0$, for all $x \in \overline{\Omega}$.

(A3) The monotonicity condition holds:

$$(a(x, \varepsilon) - a(x, \eta))(\varepsilon - \eta) \geq 0,$$

for all $x \in \overline{\Omega}$ and all $\varepsilon, \eta \in R^N$ with equality if and only if $\varepsilon = \eta$.

(A4) The following inequality holds:

$$|\varepsilon|^{p(x)} \leq a(x, \varepsilon)\varepsilon \leq p(x)A(x, \varepsilon),$$

for all $x \in \overline{\Omega}$ and all $\varepsilon \in R^N$.

(A5) A is $p(x)$ -uniformly convex: There exists a constant $m > 0$ such that

$$A\left(x, \frac{\xi + \zeta}{2}\right) \leq \frac{1}{2}A(x, \xi) + \frac{1}{2}A(x, \zeta) - m\|\xi - \zeta\|^{p(x)},$$

for all $x \in \overline{\Omega}$ and all $\xi, \zeta \in R^N$.

(f1) $f : \partial\Omega \times R \rightarrow R$ is a Carathéodory condition such that

$$f(x, t) \leq c + c_1|t|^{q(x)-1}$$

where c and c_1 are positive constants and $q(x) \in C(\partial\Omega)$ such that $p^+ < q^- \leq q(x) < p^\circ(x)$.

(f2) $f(x, t) = o(|t|^{p^+-1})$ as $t \rightarrow 0$, for all $x \in \partial\Omega$ and $p^+ < q^-$.

(AR) Ambrosetti-Rabinowitz's condition: there exist $t^* > 0$ and $p^+ < \theta$ such that

$$0 < \theta F(x, t) \leq f(x, t)t, \quad |t| \geq |t|^*, \quad \text{for all } x \in \partial\Omega.$$

Moreover, throughout this paper, we define

$$p^*(x) = \begin{cases} \frac{Np(x)}{N-p(x)}, & \text{if } N > p(x) \\ \infty, & \text{if } N \leq p(x) \end{cases} \quad \text{and} \quad p^\circ(x) = \begin{cases} \frac{(N-1)p(x)}{N-p(x)}, & \text{if } N > p(x) \\ \infty, & \text{if } N \leq p(x). \end{cases}$$

In recent years, the study of variational problems in the variable exponent Lebesgue-Sobolev spaces is an interesting topic of research due to its significant role in many fields of mathematics. These types of problems have been interesting topics like electrorheological fluids, elastic mechanics, stationary thermo-rheological viscous flows of non-Newtonian fluids, and image processing [2,5,12,13,18].

Recently, many authors have intensively studied the nonlinear boundary value problems involving $p(x)$ -Laplacian operator [1,4,7,8,14,15,17]. For example, in [3], the author studied the existence and multiplicity of solutions by using a variation of the Mountain Pass for the following Steklov problem standard growth condition,

$$\begin{cases} \Delta_{p(x)} u = |u|^{p(x)-2} u, & x \in \Omega, \\ |\nabla u|^{p(x)-2} \frac{\partial u}{\partial \nu} = f(x, u), & x \in \partial\Omega \end{cases}$$

where f is not satisfy the Ambrosetti-Rabinowitz type condition.

In [9], the authors constrained the existence and multiplicity of solutions by using the Mountain Pass theorem and Ricceri's three critical points theorem under the appropriate conditions for the following Steklov problem standard growth condition,

$$\begin{cases} \operatorname{div}(a(x, \nabla u)) = 0, & x \in \Omega, \\ a(x, \nabla u)\nu = f(x, u), & x \in \partial\Omega, \end{cases}$$

Motivated by the above paper, we get some existing results of weak solutions to the problem (P). This paper is organized as follows. In Section 2, we recall the definition of the variable exponent Lebesgue - Sobolev spaces. In Section 3, we give the main results.

2. Preliminaries

We state some definitions and basic properties of variable exponent Lebesgue-Sobolev spaces $L^{p(x)}(\Omega)$, $W^{1,p(x)}(\Omega)$ and $W_0^{1,p(x)}(\Omega)$ [8,10,13,16].

Set

$$C_+(\bar{\Omega}) = \{p: p(x) \in C(\bar{\Omega}), \inf p(x) > 1, \text{ for all } x \in \bar{\Omega}\}$$

For any $p(x) \in C_+(\bar{\Omega})$, we write

$$1 < p^- := \inf_{x \in \Omega} p(x) \text{ and } p^+ := \sup_{x \in \Omega} p(x) < \infty$$

Define the variable exponent Lebesgue space by

$$L^{p(x)}(\Omega) = \left\{ u \mid u: \Omega \rightarrow \mathbb{R} \text{ is measurable such that } \int_{\Omega} |u(x)|^{p(x)} dx < \infty \right\},$$

with the norm

$$\|u\|_{p(x)} := \inf \left\{ \beta > 0 : \int_{\Omega} \left| \frac{u(x)}{\beta} \right|^{p(x)} dx \leq 1 \right\},$$

and $(L^{p(x)}(\partial\Omega), \|u\|_{p(x)})$ becomes a Banach space.

Similarly, we can define for $p(x) \in C_+(\partial\Omega)$,

$$L^{p(x)}(\partial\Omega) = \left\{ u \mid u: \partial\Omega \rightarrow \mathbb{R} \text{ is measurable such that } \int_{\partial\Omega} |u(x)|^{p(x)} d\sigma < \infty \right\}$$

with the norm

$$\|u\|_{L^{p(x)}(\partial\Omega)} := \inf \left\{ \zeta > 0 : \int_{\partial\Omega} \left| \frac{u(x)}{\zeta} \right|^{p(x)} d\sigma \leq 1 \right\},$$

where $d\sigma$ is the measure on the boundary. $(L^{p(x)}(\partial\Omega), \|u\|_{p(x)})$ becomes a Banach space.

The variable exponent Sobolev space $W^{1,p(x)}(\Omega)$ is defined by

$$W^{1,p(x)}(\Omega) = \left\{ u \in L^{p(x)}(\Omega) : |\nabla u| \in L^{p(x)}(\Omega) \right\},$$

and equipped with the norm,

$$\|u\|_{1,p(x)} = \|u\|_{p(x)} + \|\nabla u\|_{p(x)}, \quad \forall u \in W^{1,p(x)}(\Omega)$$

The space $W_0^{1,p(x)}(\Omega)$ is denoted as the closure of $C_0^\infty(\Omega)$ in $W^{1,p(x)}(\Omega)$ with respect to the norm $\|u\|_{1,p(x)}$. For $u \in W_0^{1,p(x)}(\Omega)$, we can define an equivalent norm $\|u\| = \|\nabla u\|$.

Proposition 2.1. [3,6,12] $L^{p'(x)}(\Omega)$ is the conjugate space of $L^{p(x)}(\Omega)$, where $\frac{1}{p(x)} + \frac{1}{p'(x)} = 1$.

Then, we write Hölder-Type inequality

$$\left| \int_{\Omega} uv dx \right| \leq \left(\frac{1}{p^-} + \frac{1}{p^+} \right) \|u\|_{p(x)} \|v\|_{p'(x)},$$

for any $u \in L^{p(x)}(\Omega)$ and $v \in L^{p(x)}(\Omega)$.

The modular of the $L^{p(x)}(\Omega)$ space, which is the mapping $\rho_{p(x)}(u): L^{p(x)}(\Omega) \rightarrow \mathbb{R}$ defined by

$$\rho_{p(x)}(u) = \int_{\Omega} |u(x)|^{p(x)} dx, \quad \forall u \in L^{p(x)}(\Omega).$$

Proposition 2.2. [6,10,16] If $u, u_n \in L^{p(x)}(\Omega)$ ($n = 1, 2, \dots$) and $p^+ < \infty$, we denote

- (i) $|u|_{p(x)} = 1$ ($< 1, > 1$) $\Leftrightarrow \rho_{p(x)}(u) = 1$ ($< 1, > 1$),
- (ii) $\min\left(|u|_{p(x)}^{p^-}, |u|_{p(x)}^{p^+}\right) \leq \rho_{p(x)}(u) \leq \max\left(|u|_{p(x)}^{p^-}, |u|_{p(x)}^{p^+}\right)$,
- (iii) $|u_n|_{p(x)} \rightarrow 0$ ($\rightarrow \infty$) $\Leftrightarrow \rho_{p(x)}(u_n) \rightarrow 0$ ($\rightarrow \infty$),
- (iv) $|u_n - u|_{p(x)} \rightarrow 0$ ($\rightarrow \infty$) $\Leftrightarrow \rho_{p(x)}(u_n - u) \rightarrow 0$ ($\rightarrow \infty$).

Proposition 2.3. [14,15,17] We define $\varphi_{p(x)}(u) = \int_{\partial\Omega} |u|^{p(x)} d\sigma$, $\forall u \in L^{p(x)}(\partial\Omega)$. Then

- (i) $|u|_{L^{p(x)}(\partial\Omega)} \geq 1 \Rightarrow |u|_{L^{p(x)}(\partial\Omega)}^{p^-} \leq \varphi_{p(x)}(u) \leq |u|_{L^{p(x)}(\partial\Omega)}^{p^+}$
- (ii) $|u|_{L^{p(x)}(\partial\Omega)} < 1 \Rightarrow |u|_{L^{p(x)}(\partial\Omega)}^{p^+} \leq \varphi_{p(x)}(u) \leq |u|_{L^{p(x)}(\partial\Omega)}^{p^-}$.

Proposition 2.4. [10,15]

- (i) If $1 < p^- \leq p^+ < \infty$ then the spaces $L^{p(x)}(\Omega)$, $W^{1,p(x)}(\Omega)$ and $W_0^{1,p(x)}(\Omega)$ are separable, reflexive and uniformly convex Banach spaces,
- (ii) If $q(x) \in C_+(\overline{\Omega})$ and $1 \leq q(x) < p^*(x)$ for all $x \in \overline{\Omega}$, then the embedding $W^{1,p(x)}(\Omega) \rightarrow L^{q(x)}(\Omega)$ is compact and continuous,
- (iii) If $q(x) \in C_+(\partial\Omega)$ and $1 \leq q(x) < p^\circ(x)$ for all $x \in \partial\Omega$, then the trace embedding $W^{1,p(x)}(\Omega) \rightarrow L^{q(x)}(\partial\Omega)$ is compact and continuous,
- (iii) Poincaré inequality, i.e. there exists a positive constant $C > 0$ such that

$$\|u\| \leq C |u|_{p(x)}, \quad \text{for all } u \in W_0^{1,p(x)}(\Omega).$$

Definition 2.5. [16] Let X be a Banach space and the function $I \in C^1(X, \mathbb{R})$. We say that I satisfies the Palais-Smale condition (PS) in X if any sequence $\{u_n\}$ in X such that $I(u_n)$ is bounded and $I'(u_n) \rightarrow 0$ as $n \rightarrow \infty$ has a convergent subsequence. $I \in C^1(X, \mathbb{R})$

Lemma 2.6. (Mountain Pass Theorem) [16] Let X be a Banach space and the function $I \in C^1(X, \mathbb{R})$ satisfies the Palais-Smale condition. Assume that $I(0) = 0$, and the following conditions hold.

- (i) There exists two positive real numbers τ and r such that $I(u) \geq \tau$ with $\|u\| = r$,
- (ii) There exists $u_1 \in X$ such that $\|u_1\| > r$ and $I(u_1) < 0$.

Put $G = \{g \in C([0,1], X) : g(0) = 0 \text{ and } g(1) = u_1\}$. Set $\beta = \inf \{ \max I(g) : g \in G \}$. Then $\beta \geq \tau$ and β is a critical value of I .

3. Main Results

Let X denote the variable exponent Sobolev space $W_0^{1,p(x)}(\Omega)$. The main results of the present paper is:

Theorem 3.1. If (A1) - (A5), (f1), (f2), and (AR) hold, then problem (P) has a nontrivial weak solution for any $\lambda \in (0, \infty)$.

We say that $u \in X$ is a weak solution of (P) if

$$\int_{\Omega} a(x, \nabla u) \nabla v \, dx - \lambda \int_{\partial\Omega} f(x, u) v \, d\sigma = 0$$

for all $v \in X$.

The energy functional corresponding to the problem (P) is defined as $I : X \rightarrow R$

$$I(u) = \int_{\Omega} A(x, \nabla u) \, dx - \lambda \int_{\partial\Omega} F(x, u) \, d\sigma = \Lambda(u) - \lambda J(u),$$

where $\Lambda(u) = \int_{\Omega} A(x, \nabla u) \, dx$ and $J(u) = \int_{\partial\Omega} F(x, u) \, d\sigma$.

Proposition 3.2. [3,9] Let $f : \partial\Omega \times R \rightarrow R$ is a Carathéodory function satisfying (f1). For each $u \in X$ set $J(u) = \int_{\partial\Omega} F(x, u) \, d\sigma$. Then, $J(u) \in C^1(X, R)$ and

$$\langle J'(u), v \rangle = \int_{\partial\Omega} f(x, u) v \, d\sigma,$$

for all $v \in X$. Moreover, the operator $J' : X \rightarrow X^*$ is compact.

Lemma 3.3. [9, 11]

- (i) A verifies the growth condition: for all $x \in \overline{\Omega}$ and all $\varepsilon \in R^N$,

$$|A(x, \varepsilon)| \leq c_1 \left(|\varepsilon| + |\varepsilon|^{p(x)} \right),$$
- (ii) A is $p(x)$ -homogeneous: for all $z \geq 1$, $x \in \overline{\Omega}$ and $\varepsilon \in R^N$,

$$\varepsilon \in R^N \quad A(x, z\varepsilon) \leq A(x, \varepsilon) z^{p(x)}.$$

Lemma 3.4. [6, 9, 11, 14]

- (i) The functional $\Lambda(u)$ is well-defined on X .
- (ii) The functional $\Lambda(u)$ is of class $C^1(X, R)$ and

$$\langle \Lambda'(u), v \rangle = \int_{\Omega} a(x, \nabla u) \nabla v \, dx, \text{ for all } u, v \in X.$$

- (iii) The functional $\Lambda(u)$ is weakly lower semi-continuous on X .

- (iv) I is weakly lower semi-continuous on X .
- (v) I is well-defined on X .
- (vi) For all $u, v \in X$

$$\Lambda(u) - \Lambda(v) \geq \langle \Lambda'(v), u - v \rangle$$

- (vii) For all $u, v \in X$ and $m > 0$ is a constant

$$\Lambda\left(\frac{u+v}{2}\right) \leq \frac{1}{2}\Lambda(u) + \frac{1}{2}\Lambda(v) - m\|u-v\|^{p^-}.$$

Therefore, from Proposition 2.3, Proposition 3.1, and Lemma 3.3, it is easy to see that $I(u) \in C^1(X, R)$ the critical points I are weak solutions of **(P)**. Moreover, the derivate of I is the mapping $I : X \rightarrow R$

$$\langle I'(u), v \rangle = \int_{\Omega} a(x, \nabla u) \nabla v \, dx - \lambda \int_{\partial\Omega} f(x, u) v \, d\sigma,$$

for any $u, v \in X$ [8,15,17].

Lemma 3.5. Assume that the conditions **(A1)** - **(A4)**, **(f1)**, **(f2)**, and **(AR)** hold. Then the following statements hold:

- (i) There exist two positive real numbers τ and r such that $I(u) \geq r > 0$ with $\|u\| = \tau$,
- (ii) There exists $u_1 \in X$ such that $\|u_1\| > \tau$ and $I(u_1) < 0$.

Proof (i): For $\|u\| < 1$, from **(f1)** and **(f2)**, we have

$$|F(x, u)| \leq \varepsilon |u|^{p^+} + c_{\varepsilon} |u|^{q(x)}, \text{ for all } (x, u) \in \partial\Omega \times R. \quad (1.1)$$

Then, using the above inequality **(1.1)** and **(A4)**, we write

$$\begin{aligned} I(u) &= \int_{\Omega} A(x, \nabla u) \, dx - \lambda \int_{\partial\Omega} F(x, u) \, d\sigma \\ &\geq \int_{\Omega} \frac{1}{p(x)} |u|^{p(x)} \, dx - \lambda \int_{\partial\Omega} \left(\varepsilon |t|^{p^+} + c_{\varepsilon} |t|^{q(x)} \right) \, d\sigma \end{aligned}$$

On the other hand, by Proposition 2.4 (iii), we can write

$$X \rightarrow L^{p^+}(\Omega) \text{ and } X \rightarrow L^{q^+}(\partial\Omega) \rightarrow L^{q^-}(\partial\Omega)$$

Thus, there exist constants $c_2, c_3, c_4 > 0$ for all $u \in X$,

$$\int_{\Omega} |u|^{p^+} \, dx \leq c_2 \|u\|^{p^+}, \int_{\partial\Omega} |u|^{q^+} \, d\sigma \leq c_3 \|u\|^{q^+} \text{ and } \int_{\partial\Omega} |u|^{q^-} \, d\sigma \leq c_4 \|u\|^{q^-}, \quad (1.2)$$

Moreover, using Proposition 2.1, Proposition 2.2, Proposition 2.3, **(A4)**, the inequalities (1.1) and (1.2), we obtain

$$I(u) \geq \frac{c_5}{p^+} \|u\|^{p^+} - \lambda \left(c_6 \varepsilon \|u\|^{p^+} + c_{\varepsilon} c_7 \|u\|^{q^-} \right)$$

Choose $\varepsilon > 0$ small enough such that $\lambda c_6 \varepsilon < \frac{c_5}{2p^+}$, we obtain

$$I(u) \geq \|u\|^{p^+} \left(\frac{c_5}{2p^+} - \lambda c_7 c_\varepsilon \|u\|^{q^- - p^+} \right).$$

Let us define the function $\eta : [0,1] \rightarrow R$ by

$$\eta(t) = \frac{c_5}{2p^+} - \lambda c_7 c_\varepsilon t^{q^- - p^+},$$

where c_5, c_6 and c_7 are positive constants. Since $p^+ < q^-$ the function η is strictly positive in a neighborhood of zero.

(ii) Let $\omega \in X \setminus \{0\}$ and $t > 1$. From (AR), we obtain $|F(x, t)| \geq c_8 |t|^\theta$ for all $(x, t) \in \partial\Omega \times R$ and c_8 is a positive constant. Then, by Lemma 3.3 (ii), we get

$$\begin{aligned} I(t\omega) &= \int_{\Omega} A(x, \nabla t\omega) dx - \lambda \int_{\partial\Omega} F(x, t\omega) d\sigma \\ &\leq \frac{c_9 t^{p^-}}{p^-} \int_{\Omega} A(x, \nabla \omega) dx - \frac{\lambda c_8 t^{q^-}}{q^+} \int_{\partial\Omega} |\omega|^{q(x)} d\sigma \end{aligned}$$

where c_8 is constant. Since $q^- > p^-$ we conclude that $I(t\omega) < 0$ as $t \rightarrow \infty$. There exists $u_1 = t\omega \in X$ such that $\|u_1\| > \tau$ and $I(u_1) < 0$. The proof is completed.

Lemma 3.6. Suppose that the conditions (A1) - (A5), (f1), (f2) and (AR) hold. Then I satisfies the (PS) condition.

Proof; Suppose that $\{u_n\} \subset X$ is a (PS)-sequence that satisfy the properties:

$$I(u_n) \rightarrow c_{10} \text{ and } I'(u_n) \rightarrow 0 \text{ in } X^* \text{ as } n \rightarrow \infty, \tag{1.3}$$

where X^* is dual space of X and c_{10} is a positive constant.

We prove that $\{u_n\}$ possesses a convergent subsequence. Firstly, we show that $\{u_n\}$ is bounded in X . We do the proof by contradiction. That is, we show that $\|u_n\| \rightarrow \infty$ as $n \rightarrow \infty$.

By using the condition (A4), we can write

$$\int_{\Omega} |\nabla u_n|^{p(x)} \leq \int_{\Omega} a(x, \nabla u_n) \nabla u_n dx \leq p^+ \int_{\Omega} A(x, \nabla u_n) dx. \tag{1.4}$$

Moreover, using (1.3), (1.4), (AR), and Proposition 2.2 and considering $\|u_n\| > 1$ for n large enough, we have

$$\begin{aligned} 1 + c_{10} &\geq I(u_n) - \frac{1}{\theta} \langle I'(u_n), u_n \rangle \\ &= \int_{\Omega} A(x, \nabla u_n) dx - \lambda \int_{\partial\Omega} F(x, u_n) d\sigma - \frac{1}{\theta} \int_{\Omega} a(x, \nabla u_n) \nabla u_n dx + \frac{\lambda}{\theta} \int_{\partial\Omega} f(x, u_n) u_n d\sigma \\ &\geq \left(\frac{1}{p^+} - \frac{1}{\theta} \right) \|u_n\|^{p^-}. \end{aligned}$$

Since $\theta > p^+$, we obtain that $\{u_n\}$ is bounded in X and $u \in X$ such that $u_n \rightarrow u$ (weak convergent) in X . Now, we prove that $\{u_n\}$ strongly convergent to u in X .

By relation (1.3), we obtain the following $\langle I'(u_n), u_n - u \rangle \rightarrow 0$ as $n \rightarrow \infty$.

That is,

$$\begin{aligned} & \langle I'(u_n), u_n - u \rangle \\ &= \int_{\Omega} a(x, \nabla u_n)(\nabla u_n - \nabla u) dx - \lambda \int_{\partial\Omega} f(x, u_n)(u_n - u) d\sigma \rightarrow 0. \end{aligned}$$

From (f1) and Proposition 2.1, we write

$$\begin{aligned} & \left| \int_{\partial\Omega} f(x, u_n)(u_n - u) d\sigma \right| \leq \left| \int_{\partial\Omega} (c + c_1 |u_n|^{q(x)-1})(u_n - u) d\sigma \right| \\ & \leq c_{11} \|u_n - u\|_{q(x)} + c_{12} \left\| |u_n|^{q(x)-1} \right\|_{q'(x)} \|u_n - u\|_{q(x)}. \end{aligned}$$

Moreover, thanks to the compact embedding $X \rightarrow L^{q(x)}(\partial\Omega)$, we have

$$u_n \rightarrow u \text{ (strongly convergent) in } L^{q(x)}(\partial\Omega). \quad (1.5)$$

By Proposition 2.2 and relation (1.5), we get

$$\int_{\partial\Omega} f(x, u_n)(u_n - u) d\sigma \rightarrow 0 \text{ as } n \rightarrow \infty.$$

Taking into account the above inequality, we have

$$\int_{\Omega} a(x, \nabla u_n)(\nabla u_n - \nabla u) dx \rightarrow 0 \text{ as } n \rightarrow \infty.$$

That is,

$$\lim_{n \rightarrow \infty} \langle \Lambda'(u_n), u_n - u \rangle = 0.$$

Then, from Lemma 3.4 (vi), we can write

$$0 = \lim_{n \rightarrow \infty} \langle \Lambda'(u_n), u_n - u \rangle \leq \lim_{n \rightarrow \infty} (\Lambda(u) - \Lambda(u_n)) = \Lambda(u) - \lim_{n \rightarrow \infty} \Lambda(u_n)$$

or

$$\lim_{n \rightarrow \infty} \Lambda(u_n) \leq \Lambda(u)$$

and from Lemma 3.4 (iii), we obtain

$$\lim_{n \rightarrow \infty} \Lambda(u_n) = \Lambda(u).$$

Now, we assume by contradiction that $\{u_n\}$ does not converge strongly to u in X . Then, there exists $\xi > 0$ and a subsequence $\{u_{n_k}\}$ of $\{u_n\}$ such that $\|u_{n_k} - u\| \geq \xi$. Moreover, by Lemma 3.4(vii), we can write the following inequality

$$\frac{1}{2} \Lambda(u) + \frac{1}{2} \Lambda(u_{n_k}) - \Lambda\left(\frac{u + u_{n_k}}{2}\right) \geq m \|u - u_{n_k}\|^{p^-} \geq m \xi^{p^-}.$$

Letting $k \rightarrow \infty$ in the above inequality, we have

$$\limsup_{n \rightarrow \infty} \Lambda\left(\frac{u + u_{n_k}}{2}\right) \leq \Lambda(u) - m \xi^{p^-}.$$

We also have $\left\{\frac{u + u_{n_k}}{2}\right\}$ converges weakly to u in X . On the other hand, using Lemma 3.4 (iii), we obtain

$$\Lambda(u) \leq \liminf_{n \rightarrow \infty} \Lambda\left(\frac{u + u_{n_k}}{2}\right),$$

and this is a contradiction. Hence, it follows that $\{u_n\}$ converges strongly to u in X . The proof of Lemma 3.6 is complete.

Proof of Theorem 3.1. from Lemma 3.5, Lemma 3.6, and $I(0) = 0$ from (A2), I satisfies all statements of Lemma 2.6. Thus, I has a nontrivial critical point, i.e., problem (P) has a nontrivial weak solution.

4. Conclusion

Through this paper, we have studied the existence of a nontrivial weak solution of the nonlinear Steklov boundary value problem in variable exponent Sobolev spaces and using the variational method under appropriate conditions on f and a .

Conflict of interest

The authors declare no conflict of interest.

Authors' Contributions

Z.Y.: Conceptualization, Methodology, Formal analysis, Writing - Original draft preparation (%50)

V. M.: Conceptualization, Methodology, Resources, Investigation (%50).

All authors read and approved the final manuscript.

Ethical Statement

The authors declare that this document does not require ethics committee approval or any special permission. Our study does not cause any harm to the environment.

References

- [1] Allaoui, M., "Continuous spectrum of Steklov nonhomogeneous elliptic problem", *Opuscula Math.* 37(6), 853–866, 2005.
- [2] Antontsev, S. N. and Shmarev S. I., "A model porous medium equation with variable exponent of nonlinearity: existence, uniqueness and localization properties of solutions", *Nonlinear Anal.* 6, 515-545, 2005.
- [3] Ayoujil, A., "On the superlinear Steklov problem involving the $p(x)$ -Laplacian", *EJQTDE.*, 38, 1–13, 2014.
- [4] Ben Ali K., Ghanmi, A. and Kefi, K., "On the Steklov problem involving the $p(x)$ -Laplacian with indefinite weight", *Opuscula Math.* 37(6),779–794, 2017.
- [5] Chen, Y., Levine, S. and Rao, M., "Variable exponent, linear growth functionals in image processing", *SIAM J Appl Math.* 66, 1383–1406, 2006.
- [6] Fan, X., Zhang, Q. and Zhao, D., "Eigenvalues of $p(x)$ -Laplacian Dirichlet problem", *J. Math. Anal. Appl.* 302, 306–317, 2015.
- [7] Deng, SG., "Eigenvalues of the (x) -Laplacian Steklov problem", *J. Math Anal Appl.* 339, 925–937, 2008.
- [8] Ourraoui A., "Existence and uniqueness of solutions for Steklov problem with variable exponent, Adv. in the Theory of Nonlinear", *Anal. and its Appl.*, 1 (5), 158-166, 2021.
- [9] Karim, B., Zerouali, A., and Chakrone O., "Existence and multiplicity of a -harmonic solutions for a Steklov problem with variable exponents", *Bol. Soc. Paran. Mat.*, 32(2), 125-136, 2018.

- [10] Kováčik, O. and Rákosník J., “On spaces $L^{p(x)}$ and $W^{k,p(x)}$ ”, *Czechoslovak Math. J.* 41(4), 592-618, 1991.
- [11] Mashiyev, R. A., Cekic, B., Avci, M. and Yucedag, Z., “Existence and multiplicity of weak solutions for nonuniformly elliptic equations with nonstandard growth condition”, *Complex Variables and Elliptic Equations*, 57(5), 579-595, 2012.
- [12] Mihăilescu, M. and Rădulescu, V., “A multiplicity result for a nonlinear degenerate problem arising in the theory of electrorheological fluids”, *Proceedings of the Royal Society A.*, 462, 2625-2641, 2006.
- [13] Ruzicka, M., *Electro-rheological fluids: modeling and mathematical theory*. Lecture notes in mathematics, vol. 1784. Berlin: Springer-Verlag; 2000.
- [14] Yucedag, Z., “Existence results for Steklov problem with nonlinear boundary condition”, *Middle East Journal of Science.*, 5(2), 146 – 154, 2019.
- [15] Wei, Z. and Chen, Z., “Existence results for the $p(x)$ -Laplacian with nonlinear boundary condition”, *Applied Math.*, Vol.2012, 2012. doi:10.5402/2012/727398.
- [16] Willem, M., *Minimax Theorems*, Birkhauser, Basel, 1996.
- [17] Zerouali A., Chakrone O. and Anano A., “Existence and multiplicity solutions results for elliptic problem with nonlinear conditions and variable exponents”, *Bol. Soc. Paran. Mat.*, 2 (33), 121-131, 2015.
- [18] Zhikov, VV., “Averaging of functionals of the calculus of variations and elasticity theory”, *Math. USSR. Izv.*, 29, 33–66, 1987.



DETERMINATION OF BIOACTIVITIES OF *Convallaria Majalis* L. (LILY OF THE VALLEY), ISOLATING PHARMACEUTICAL ACTIVE INGREDIENTS AND INVESTIGATION ITS INDUSTRIAL USAGE

Nazan DEMİR^{*1}  Sıla Nezahat DAŞDEMİR¹  Alevcan KAPLAN²  Yaşar DEMİR¹ 

¹ Muğla Sıtkı Koçman University, Cosmetic Products Application and Research Center, Muğla / Turkey

¹ Muğla Sıtkı Koçman University, Cosmetic Products Application and Research Center, Muğla / Turkey

¹ Muğla Sıtkı Koçman University, Cosmetic Products Application and Research Center, Muğla / Turkey

² Batman University, Department of Crop and Animal Production, Sason Vocational School, Batman/Turkey

*Corresponding author's e-mail: nazdemir@mu.edu.tr

Abstract: In this study, some biological activities of *Convallaria majalis* L. (Asparagaceae), which attracts attention with its pleasant smell, were determined, and the isolation of drug active substances and industrial usability were investigated. For this purpose, the protease enzyme that catalyzes the hydrolysis of proteins, which is one of the most important enzyme groups in both industrial and biochemical applications, into peptides and amino acids was purified from *C. majalis*. The protease enzyme was purified using Three phase partitioning (TPP) method. Optimum pH and temperature for the enzyme, K_m , and V_{max} values for casein, azocasein, gelatin, hemoglobin, and azoalbumin substrates were determined. Sodium dodecyl sulfate-poly acrylamide gel electrophoresis (SDS-PAGE) was used to check the purity of the purified protease enzyme. The molecular weight of the enzyme was calculated as 54.347 kDa using gel filtration chromatography. The effects of SDS (Sodium dodecyl sulfate), EDTA (Ethylenediaminetetraacetic acid), β -mercaptoethanol compounds and Mg^{2+} , Ca^{2+} , Mn^{2+} , Ni^{2+} , Hg^{2+} , Fe^{2+} , and Fe^{3+} cations (10 mM, 1 mM, and 0.1 mM) concentrations on enzyme activity were investigated. Volatile and aromatic components analyzed with Headspace gas chromatography/mass spectroscopy (GC/MSD). It was determined that *C. majalis* flowers contain volatile organic compounds, citronellol (9.6 %), geraniol (8.4 %), benzyl alcohol (35 %), phenylacetone (3.0 %), farnesol (1.9 %), 2,3-dihydrofarnesol (0.88 %), green grassy notes; (Z)-3-hexen-1-ol (11 %), and (Z)-3-hexenyl acetate (7.8 %). As a result of the work, it was determined that the aromatic of *C. majalis* can be used as an active ingredient and it has been concluded that there is industrial use.

Keywords: Asparagaceae, *Convallaria majalis*, Muğla, Protease Enzyme, Volatile and Aromatic Components

Received: October 31, 2022

Accepted: December 26, 2022

1. Introduction

Medicines are used by all healthcare professionals today to improve health and treat diseases. The use of drugs began in BC when it was realized that some parts of plants and animals healed diseases or healed injured people. Many countries around the world such as Egypt, India, Iran, and China have been developing traditional medicines and medical practices for hundreds of years [1]. Even today, where technology is developing rapidly, herbal medicines are still an important part of the pharmaceutical market [2]. However, this plant richness cannot be utilized sufficiently. The reason for this is that even a single plant has a wide variety of phytochemicals and the effect of using a whole plant as a medicine

is often not known precisely, and the therapeutic efficacy of herbal medicines is due to the assembled efficacy of different biological active substances in the plant raw material. [2-3]. The properties of plants that are important for human health have been investigated in laboratories since 1926 [4].

Considering these studies, Turkey is a natural laboratory with its rich flora and many medicinal and aromatic plants. The *Asparagaceae* family (*Puschkinia* Adams, *Chionodoxa* Boiss., *Scilla* L., *Prospero* Salisb., *Muscari* Mill., *Bellevalia* Lapeyr. and *Convallaria* L.), which contains many medicinal and aromatic plants, plants have been researched recently. Turkey is the “diversity center” of these breeds. These genus, which are discussed under the *Liliaceae* family in the 8th volume of Flora of Turkey and the East Aegean Islands [5], are currently evaluated under the *Asparagaceae* family [6]. The *Asparagaceae* family includes 128 genera and 2929 species that are naturally distributed in temperate, subtropical, and tropical regions around the world. In Turkey, this family is represented by 182 species belonging to 19 genus [7-8-9]. The genus *Convallaria* L. is represented in Turkey by the taxa *C. majalis* L. var. *transcaucasica* (Utkin ex Grossh.) Knorr. and *C. majalis* L. var. *majalis* L. [5]. *C. majalis* has many uses in pharmaceutical fields. It is collected in the spring and dried in the shade. Drog is odorless and has a very bitter taste. In its composition, saponins and glycosides (convallatoxin) carries. It has diuretic and heart-strengthening effects of fresh flowers effects are greater. It is used successfully in mild heart weakening [10]. Again, according to the literature data of the study of Chushenko et al. [11], the dry air parts of the plant contain between 0.1 % and 0.5 % CG (cardiac glycosides). The primary glycosides of the remarkably varied group it contains are convalloside (from 4 % to 24 %), convallatoxinol (from 10 % to 20 %), convallatoxin (from 4% to 40%), lokundjoxide (from 1 % to 25 %) and desglucocheirotxin (from 3 % to 15 %) [12]. The raw material of the plant has been used for a long period and a number of drugs have been improved on its basis, one of which is the drug “Corglycon” produced by LLC “Pilot” [2].

To the best of our knowledge, as in this study, there is no study in which the parameters presented in the study of *C. majalis* are combined. Therefore, in this study, it was aimed to purify and characterize the protease enzyme and to investigate the potential of this flower to be used in the cosmetic, food, and pharmaceutical industries.

2. Materials and Methods

2.1. Chemicals and Reagents

Casein, azocasein, azoalbumin, hemoglobin, standard serum albumin, ethanol, gelatin, methanol, ammonium persulfate, acrylamide, N, N'-methylene bisacrylamide, bromphenol blue, glycine, N, N, N', N' tetramethyl ethylene diamine, *n*-butanol, hydrochloric acid, sodium hydroxide, sodium dodecyl sulfate, acetic acid, glycerine, sodium chloride, sodium acetate, sodium phosphate, phosphoric acid, sulfuric acid, Coomassie brilliant blue G- 250, Coomassie brilliant blue R-250, protein standards, *t*-butanol, hexane, trichloro acetic acid (TCA) chemicals were obtained from Sigma-Aldrich Chemia GmbH Steinheim Germany.

2.2. Plant Material

C. majalis was harvested from Akyaka, Muğla, and its surroundings during the maximum flowering period (in April and May 2017). The plant was identified by one of the authors (Dr. Alevcan Kaplan from Batman University) and given a voucher specimens Muğla/2016/02 before being deposited at the Muğla Sıtkı Koçman University. *C. majalis* flowers were kept in deep freezing at -80 °C until used in the experiments

2.3. Purification of Protease Enzyme from *C. majalis* Flowers (TPP method)

2.3.1 Preparation of Homogenate

C. majalis flower (10 g) was weighed, crushed in a mortar until the surface area was thoroughly reduced, and homogenized by adding 150 mL of PBS (sodium phosphate buffer; pH 7, 0.05 M). It was placed in a -80 °C cooler in a suitable beaker, and thereafter a few hours it was removed and left to dissolve at room temperature. This process was performed three times. The homogenate, which was removed from -80 °C and dissolved at room temperature was filtered and kept for 25 min centrifuged at 6,000 rpm. Protein content determination was made in the supernatant after centrifugation of the homogenate [13].

2.4. Determination of Protease Enzyme Activity

The PA (proteolytic activity) of the protease enzyme purified from the lily of the valley was determined by the casein digestion method in the presence of 1 % casein. 1 g of casein was dissolved in 95 mL of 0.05 M phosphate buffer (pH 7) and the volume was made up to 100 mL with the same buffer. The prepared solution was kept in a 95 °C water bath for 30 min and was ready to be used. In the proteolytic activity measurement, 1 mL of casein, and 0.5 mL of enzyme solution were added and the total volume was completed to 2.5 mL with buffer solution. Enzyme-added tubes were incubated in a water bath at 40 °C for 20 min. Thereafter, 3 mL of 5 % TCA (trichloroacetic acid) was added to the reaction stopped. It was incubated for 30 min for complete precipitation to occur and after this time it was centrifuged at 6,000 rpm for 20 min. After the supernatant was filtered, the amount of fragmented products in the supernatant was assigned by the Bradford method. The PA was calculated as µg protein/mL that the enzyme breaks down per min [14].

2.5. SDS-PAGE analysis of Enzyme

It was controlled whether the protease enzyme purified by Laemmli was purified and subunit by SDS-PAGE [15].

2.6. Kinetic Studies on Protease Enzyme Purified from *C. majalis*

2.6.1 Assignment of Optimum pH

To define the optimum pH of the protease enzyme purified from *C. majalis* flower, its PA against casein was used. To define the optimum pH, acetate buffer was used for pH 4-5, phosphate buffer was used for pH 6-7, Tris-HCl buffer was used for pH 8-9, and borate buffer was used for pH 10. The pH of the buffer solutions was adjusted using 1 M HCl and 1 M NaOH solutions. 1 mL of casein solution, 500 µL of enzyme solution, and 1 mL of buffer solution at appropriate pH were added to each sample tube. 1 blank solution was prepared for all samples as blank; buffer was used in lieu of enzyme in blank solution.

2.6.2 Assignment of Optimum Temperature

In order to define the optimum temperature of the protease enzyme purified from *C. majalis* flower, the activity was defined by increasing 10 °C in the range of 0 to - 90 °C. For each temperature experiment, 2 tubes, 1 blank, and 1 sample were prepared. 1 mL of casein solution and 500 µL of enzyme solution were added to the sample tubes and the final volume was made up to 2.5 mL with buffer solution. Blind, tube, and sample; It was incubated for 20 min at 10 to - 90 °C. Then, the reaction was stopped by adding 3 mL of 5 % TCA. It was incubated for 30 min for complete precipitation to occur

and after this time it was centrifuged at 6.000 rpm for 15 min. After the supernatant was filtered, the amount of fragmented products in the supernatant was defined by the Bradford Method [16].

2.6.3 Molecular Mass Determination of Protease Enzyme Purified from *C. bmajalis* by Gel Filtration Chromatography Method

After purifying the protease enzyme from *C. majalis* flower, its molecular mass was defined using GFC (gel filtration chromatography) method. Suspension Sepharose 4B (140 mL) was dissolved in distilled water and allowed to swell overnight at room temperature. The gel (1x30) was then loaded onto the column. Equilibration was performed with 0.05 M Na_3PO_4 /1 mM DTT buffer until no absorbance was observed in the column at 280 nm. BSA (66 kDa), Albumin EGG (45 kDa), β -Amylase (200 kDa), β -lactalbumin (18.4 kDa), and Lysozyme (14.3 kDa) solutions to be 0.2 mg/mL after column equilibration loaded and eluted with 0.05 M Na_3PO_4 /1 mM DTT buffer and a standard graph was created. After the column was re-equilibrated, the purified protease enzyme was loaded onto the column and eluted from the column using the same buffer. The flow rate of the column was adjusted to 20 mL/h with the help of a peristaltic pump. Eluates were collected at 4 mL in each tube. The molecular mass of the enzyme was defined with the help of the standard graph created.

2.6.4 Assignment of Kinetic Parameters (V_{\max} and K_m values) of Protease Enzyme Purified from *C. majalis*

The PA of the enzyme was used to define the V_{\max} and K_m values of the protease enzyme purified from the *C. majalis* flower. 100 μL , 200 μL , 400 μL , 600 μL , and 800 μL were added to all the tubes from the solution containing 1 g casein in 100 mL. 500 μL of enzyme solution and buffer solution were added to the tubes with a final volume of 2.5 mL. The tubes were incubated at 40 °C for 20 min, after which 3 mL of 5 % TCA solution was added to the tubes. After 30 min, the precipitated proteins were centrifuged at 6.000 rpm for 15 min and then filtered and the amount of protein in the supernatant was defined by the Bradford method. Blanks were prepared at the same substrate concentrations without the enzyme, buffer solution was used instead of the enzyme. $1/V$ versus $1/[S]$ Lineweaver Burk plotted. Kinetic parameters (V_{\max} and K_m values) were calculated from the results we obtained.

2.7. Assignment of Substrate Specificity of Protease Enzyme Purified from *C. majalis*

The substrate specificity of the protease enzyme purified from *C. majalis* flower against casein, hemoglobin, gelatin, azoalbumin, azocasein substrates was determined by utilizing the proteolytic activity of the enzyme. In order to determine the enzyme's activity, 100 μL , 200 μL , 400 μL , 600 μL , and 800 μL of 1 % hemoglobin, gelatin, azoalbumin, and azocasein solutions were taken and the volume was completed to 1 mL using distilled water. 0.5 mL of enzyme solution was added to each prepared tube, and buffer solution was added so that the final volume was 2.5 mL. It was incubated at 40 °C for 20 min. Then, the reaction was stopped by adding 3 mL of 5 % TCA. It was incubated for 30 min for complete precipitation to occur and after this time it was centrifuged at 6.000 rpm for 15 min. After the supernatant was filtered, the number of fragmented products in the supernatant was defined by the Bradford Method [16]. The PA for the enzyme breaks down μg protein/mL. calculated in min.

2.8. Assignment of the Effect of Some Cations on Protease Enzyme Activity Purified from *C. majalis*

To determine the effect of some cations on protease enzyme activity purified from *C. majalis*, a concentration of 10 mM; HgCl₂, CaCl₂, FeCl₂, and MgCl₂ solutions were prepared. 100 µL, 200 µL, 300 µL, 400 µL, and 500 µL were taken from these solutions with final concentrations of 0.4 mM, 0.8 mM, 1.2 mM, 1.6 mM, and 2 mM. Concentration of 0.1 mM; HgCl₂, CaCl₂, FeCl₂, MgCl₂ solutions were prepared. 100 µL, 200 µL, 300 µL, 400 µL, and 500 µL were taken from these solutions with final concentrations of 0.004 mM, 0.008 mM, 0.012 mM, 0.016 mM, and 0.02 mM, and their effect on the purified protease enzyme was determined. Proteolytic activity was determined by the casein digestion method in the presence of 1 % casein. 1000 µL of the substrate (1 % casein), 500 µL of enzyme solution, 100 µL, 200 µL, 300 µL, 400 µL, and 500 µL of 10 mM, 1 mM, and 0.1 mM cation solutions were added to each tube and the final volume was 2, made up to 5 mL. After mixing, the tubes were incubated in a water bath at 40 °C for 20 min. After 20 min, 3 mL of 5 % TCA solution was added to each tube and left to stand for 30 min. It was centrifuged at 6.000 rpm for 15 min and the supernatant was filtered. The amount of disintegrated product in the supernatant was defined by the Bradford method [16].

2.9. Assignment of the Effect of Some Chemicals on the Protease Enzyme Activity Purified from *C. majalis*

The effects of SDS, EDTA and β-mercapto ethanol on the protease enzyme activity purified from *C. majalis* flower was investigated. For this, the proteolytic activity of the purified enzyme against the casein substrate was used. 100 µL, 200 µL, 300 µL, 400 µL, and 500 µL were taken from 0.1 mM, 1 mM and 10 mM prepared SDS, EDTA, and β-mercaptoethanol solutions, 1 mL of 1 % casein solution and 0, 5 mL of enzyme solution was added. The volume was made up to 2.5 mL using a buffer solution. The amount of protein that the enzyme breaks down per min was calculated by the Bradford Method [16].

2.10. Assignment of Aromatic Volatile Organic Compounds of *C. majalis* Flowers by Headspace GC/MSD

The fresh *C. majalis* flower, which was cut into pieces, was weighed as 5.00 g into a 20 mL headspace vial. Then, anhydrous MgSO₄ was added to it and it was mixed completely with the magnetic. The vial was placed in the headspace sampler and the extraction process was started, which will take 30 min at 90 °C. After 30 min, the volatile components at the top of the vial were transferred with helium gas for 1 min by the headspace sampler with a GC Split/Splitless inlet transferline. Headspace GC/MSD instrument analysis parameters are given in Table 1.

Table 1. Headspace GC/MSD instrument analysis parameters

Device Parameters	
Balancing Time	2 min
Maximum Temperature	300 °C
Device Program	60 °C for 1min for 10 °C /min; 100 °C for 1 min 10 °C/min; 260 °C for 8 min
Operation time	30 min
MMI Input Parameters	
Method	Divide
Heater	250 °C

Table 1. Continued.

Thermal Aux (Transfer Line)	
Heater	On
Temperature	250 °C
Column	
Name	Agilent J&W 19091S-431UI HP-5MS UI (15µm×250µm×0.25µm)
Pressure	21.801 psi
Flow	1.8 mL/min
MS Acquire Parameter	
Acquisition Mode	View
EM voltage	1200
Low mass	35.0
High mass	400.0
Threshold	150
MS Source	230 °C max 250 °C
MS quadrupole	150 °C max 200 °C
GC-MSD Parameters	
Device Temperature	95 °C
Cycle Temperature	110 °C
Transfer Line Temperature	120 °C
Bottle Balance	30 min
Injection Time	1 min
GC Turnover Time	40 min
Bottle Size	20 mL
Fill Mode and Pressure	Pressure / 14psi
Cooldown	0.5 min
Extraction Method	Multiple extractions

3. Results and Discussion

In recent years, scientists have been increasingly interested in natural compounds that can act as therapeutics or preventatives against diseases [17]. It has been stated by the World Health Organization that 21,000 plant species are suitable for the preparation of medicines [18]. In industrial production processes, it is possible to use environmentally friendly biological methods by using plants instead of chemical methods. The environmental friendliness of many industrial processes is increased by using enzymes. Processes using enzymes are cleaner, safer, and often more economical. New products developed with biotechnological methods have less negative effects on the environment [19]. And, it is known that proteolytic enzymes obtained from plants are very interesting because they can be active in a wide temperature and pH range [20]. Here, we isolated and purified the protease from *C. majalis* flowers and performed enzyme kinetics study and industrial usability potential was revealed.

In the first step of the study, the protease enzyme was purified by the TPP method, which is a practical and usually one-step process that can be used quite successfully and widely in recent years, especially in the separation of enzymes and proteins [1]. The choice of organic solvent and phase-forming salt is a very important step in the TPP system. Ammonium sulfate, which is an effective cosmotropic agent, was preferred as the phase-forming salt, and t-butanol, which is a cosmotropic and clumping agent at room temperature, was preferred as the organic solvent. In this process, while the ammonium sulfate saturation was 30 % (w/v) and the homogenate: the t-butanol ratio was 1:1.5, the enzyme preferred to stay in the middle phase predominantly. Thus, characterization processes were

performed using these ratios. The results are depicted in Table 2. As seen in Table 2, it was observed that the activity and protein amount were higher with the TPP method, a purification fold of 1.04, and a yield of 77.7 % was obtained. The purity and subunit of the protease enzyme purified by SDS-PAGE developed by Laemmli [15] were checked (Figure 1). There are many studies reporting a significant increase in enzyme activity and yield with the TPP method [21-22]. Uçkaya [23] found the protease enzyme from the *C. sinensis* plant at 40 % (w/v) ammonium sulfate saturation and 1:1.5 (v/v) homogenate:t-butanol ratio with an activity yield of 677.51 % and a purification fold of 9.04 and purified from the middle phase of the TPP system with a purification fold. Gul et al. [24] bromelain protease enzyme from the crown waste of pineapple by TPP method (1.0:0.5) with a crude ratio of 70 % $(\text{NH}_4)_2\text{SO}_4$ saturation t-butanol extract at pH 7.0, with purification fold of 3.4 with a recovery of 244 %. We can suggest that TPP is an effective non-chromatographic method for the extraction of proteases from crude extracts and that the method can be developed and used commercially in implementation in different industrial sectors such as food and medicine.

Table 2. Purification results of protease enzyme purified from homogenate obtained from *C. majalis* flower by TPP method

Samples	Volume (mL)	Activity (EU/mL)	Total activity (U)	Total protein (mg)	Specific activity (U/mg)	Purification (folds)	Yield (%)
Homogenate	100	0.894	89.4	107.75	0.82	1	100
Medium phase	100	0.695	69.5	82.87	0.84	1.024	77.7

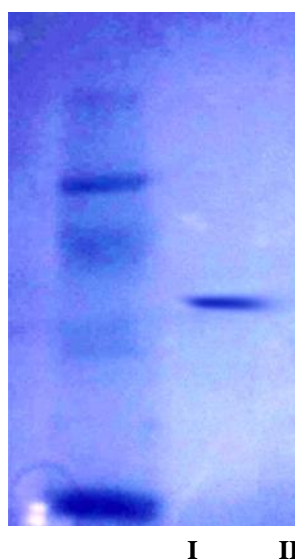


Figure 1. SDS-PAGE image of the purified protease enzyme (I, standard protein mix: BSA (66 kDa), Albumin EGG (45 kDa), β -Amylase (200 kDa), β -lactalbumin (18.4 kDa), Lysozyme (14.3 kDa); II, Protease enzyme purified from *C. majalis* flower)

To define the optimum pH value of protease enzyme purified from *C. majalis* flowers, activity measurements were made at a pH 4-5, phosphate buffer for pH 6-7, Tris-HCl buffer for pH 8-9, and borate buffer for pH 10 and the activity-pH graph was plotted. The amount of PA versus pH change is shown in Figure 2. It was defined that the optimum pH of the enzyme was 5 and it showed activity in the pH 4-9 range. The skin pH is between 4.0 and 6.0. Considering this result, it is thought that the use of *C. majalis* in cosmetic products and perfumes may be suitable for skin health. Moreover, the fact that the enzyme remains active in a wide temperature and pH range indicates that it can be used in different

areas of industrial processes. Similarly, similar, or different findings have been reported in various studies on different plant proteases [25-26-24]. The difference in the findings may be due to the different plant materials. And, in order to define the optimum temperature of the *C. majalis* purified protease enzyme, the activity was defined by increasing 10°C in the range of 0 to -90 °C. The amount of PA versus temperature change is shown in Figure 3. It was defined that the optimum temperature of the enzyme was 30 °C and the enzyme demonstrated activity in the range of 20 to -60 °C. The optimum temperature of the protease enzyme that purifies from the *C. majalis* flower is at the appropriate temperature for enzymes. This shows that the enzyme will not lose its activity under room conditions in cosmetic products. Gul et al. [24] reported the optimum temperature of bromelain protease as 35 °C. Many studies reporting different or similar optimum temperatures have been reported by different researchers [27-28-29-30].

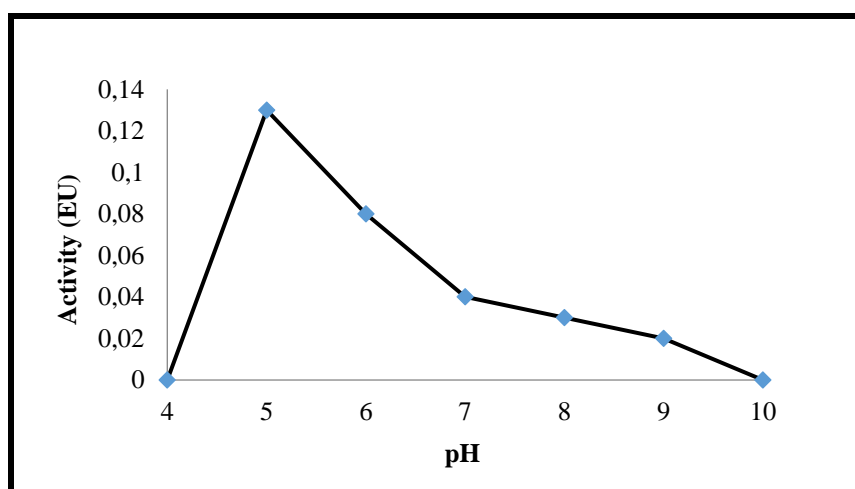


Figure 2. The efficacy of pH on the activity of protease enzyme purified from *C. majalis* flowers

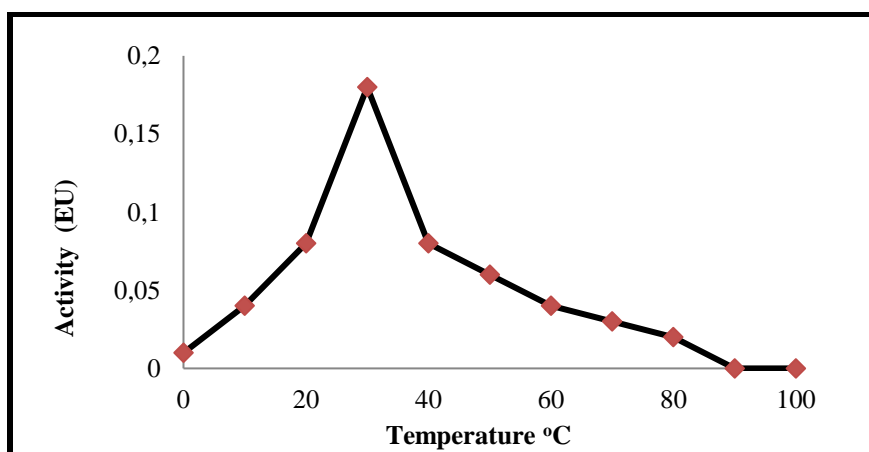


Figure 3. The efficacy of temperature on the activity of protease enzyme purified from *C. majalis* flowers

Afterward, the molecular mass of protease enzyme purified from *C. majalis* flower was determined by GFC method. The molecular mass of the protease enzyme purified from the *C. majalis* was defined as 54.347 kDa by GFC method. The standard graph prepared for molecular weight determination is given in Figure 4 and the calculations for the standard protein graph are given in Table 3. The absorbance graph prepared for the molecular weight determination of the protease enzyme from

C. majalis flowers by gel filtration chromatography is shown in Figure 4, and the calculations for the molecular weight determination are shown in Table 4. Banik et al. [31] obtained purified of the protease having a molecular mass of 51 kDa. Khan et al. [32] calculated the molecular weight of a new cysteine protease enzyme purified from *Juglans regia* L. as 11.2 kDa. Demir et al. [27], calculated the molecular weight of cysteine protease isolated from *Capparis spinosa* L. capsules as 46 kDa. In the other literature research, *Viola odorata* L. 25 kDa [33], *Pinus brutia* Ten. 28.2 kDa [34], *Chrysanthemum coronarium* L. 33.2 kDa [35], *Lilium candidum* L. 29.2 kDa [36], *Citrus limon* (L.) Burm.F. 12 kDa, *Citrus sinensis* (L.) Osbeck 30 kDa [23], *Fragaria* × *ananassa* (Duchesne ex Weston) Duchesne ex Rozier [37] protease enzyme as a result of gel filtration chromatography molecular weights were determined. It was observed that the molecular weight of *C. majalis* was twice that of other plants.

Table 3. Calculations for the standard protein chart

Standard protein mixture	MW(Dalton)	Tube sequence	Ve/Vo	LnMW
Lysozyme	14300	44	13.681	9.568
β-Lactoglobuline	18400	35	10.882	9.820
Albumin, EGG	45000	23	7.151	10.714
Albumin, Bovine	66000	18	5.597	11.097
β- Amylase	200000	13	4.042	12.206

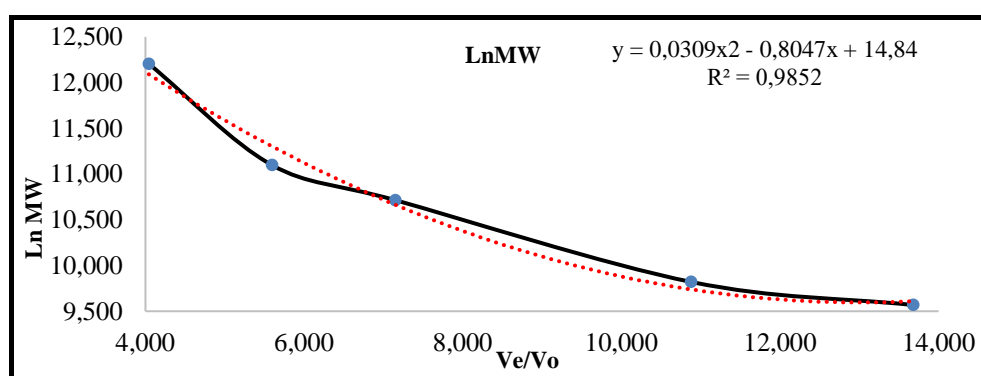


Figure 4. Gel filtration chromatography standard curve

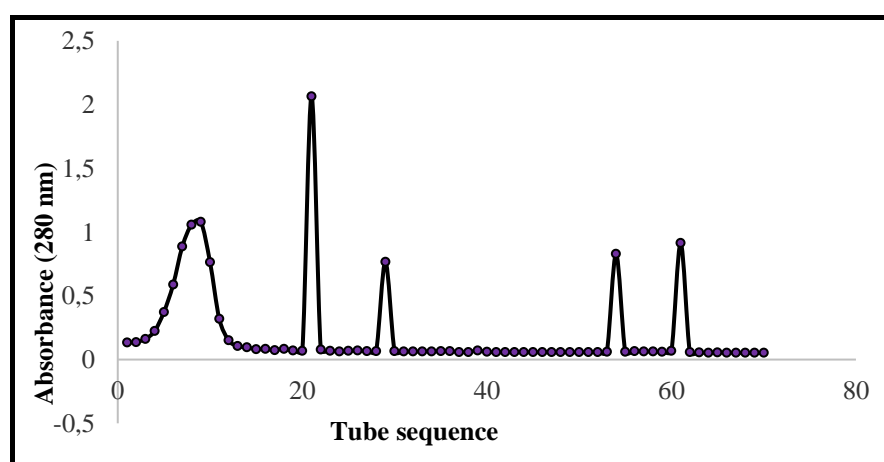


Figure 4. Absorbance graph prepared for molecular mass determination of protease enzyme from *C. majalis* flowers by CFG method

Table 4. Calculations for molecular mass determination of protease enzyme purified from *C. majalis* flowers by CFG method

Proteins	MW (Dalton)	Tube sequence	Ve/Vo	LnMW
1. Protein	373304	9	2.798	12.830
2. Protein	54347	21	6.529	10.903
3. Protein	24256	29	9.017	10.096
4. Protein	22924	54	16.790	10.040
5. Protein	44057	61	18.966	10.693

In order to define the substrate specificity of the protease enzyme purified from *C. majalis* flowers, proteolytic activity measurements were made against hemoglobin, gelatin, azoalbumin, azocasein substrates, and Lineweaver-Burk plots were drawn. By using these graphs, K_m and V_{max} values were determined for each substrate and shown in Table 5. As shown in Table 5 the most interest was against the casein (K_m and V_{max} values; 1.20 μ M and 1.295 μ g/mL.min, respectively), and no activity in azocasein substrate. Demir et al. [27] reported that cysteine protease from *Capparis spinosa* showed an exhibited the greatest protease activity with gelatin (K_m and V_{max} values; 0,96 mg/L and 2.17 mg/L · min) and no activity toward hemoglobin and azoalbumin. Demir et al. [29] calculated the K_m and V_{max} values of white oleander, pink oleander, and red oleander plants against casein substrate, 1.187 μ M and 1.303 μ g/mL.min; 1.230 μ M and 1.315 μ g/mL.min; 1.229 μ M and 1.309 μ g/mL.min, respectively. Banik et al. [31] noted that the K_m and V_{max} values of the protease enzyme isolated from the leaves of *Moringa oleifera* Lam. as 5.47 mg/mL and V_{max} as 588.23 μ M/min. Yıldırım Çelik [38] determined the K_m and V_{max} values of the protease enzyme purified from *Crocus biflorus* Mill. tubers as 0.9 g/L and 47 mg/L.min, respectively. Additionally, they noted that the enzyme has also been found to break down hemoglobin, albumin, and gelatin. Alicı [37] tried to define the substrate specificity by comparing the activity values of pure strawberry protease in the presence of azocasein-modified substrate and natural protein substrates such as casein, BSA, gelatin, and hemoglobin. It was determined that the enzyme replied with all tested substrates, showing the highest specificity against hemoglobin and the lowest specificity against casein.

Table 5. Substrate specificity results of protease enzyme purified from *C. majalis* flowers

Substrate	K_m (μ M)	V_{max} (μ g/mL.min)
Casein	1.20	1.295
Hemoglobin	2.24	1.441
Azoalbumin	1.84	0.705
Gelatin	2.88	1.041
Azocasein	nd*	nd*

*nd: not determined

The effect of Hg^{2+} , Mn^{2+} , Ca^{2+} , Fe^{2+} , Fe^{3+} , Ni^{2+} , Mg^{2+} (10 mM, 1 mM, 0.1 mM) cations on the activity of the protease enzyme purified from *C. majalis* flowers was also defined. Chlorinated salts of all cations were used. Results are demonstrated in Table 6. It was determined that Mg^{2+} , Fe^{2+} , Fe^{3+} and Ca^{2+} ions activate the enzyme and Hg^{2+} , Mn^{2+} , and Ni^{2+} cations inhibited the enzyme. Demir et al. [27] reported that all Hg^{2+} concentrations on the enzyme (cysteine protease from *Capparis spinosa*) activity of metal ions inhibited the protease activity, Ca^{2+} , Mg^{2+} , and Zn^{2+} activate the enzyme, especially at low concentrations, while Co^{2+} inhibited the enzyme, albeit less than Hg^{2+} , at high concentrations. Yıldırım

Çelik [38] reported that upon the activity of the protease enzyme purified from *Crocus* tubers, Ca^{2+} and Mg^{2+} metal ions with concentrations of 10^{-1} and 10^{-2} M increased the activity of the enzyme in both concentrations, Fe^{3+} completely inhibits the enzyme at 0.1 M concentration, Fe^{3+} ions increased the activity of the enzyme at 0.01 M concentration, while Zn^{2+} ions did not affect it at both concentrations. Alici [37] as a result of the study, examining the efficacy of metal ions on the enzyme activity (protease enzyme purified from strawberries) shows that all metal ions, except Co^{2+} ions, inhibit the enzyme. Especially Cu^{2+} , Hg^{2+} , Cd^{2+} , and Mn^{2+} ions caused the strawberry protease enzyme to lose most of its activity and even Cu^{2+} and Mn^{2+} ions (5 mM) completely inhibited the enzyme. The activation effect of Co^{2+} ions on strawberry protease is extremely impressive. When Co^{2+} ions were used at the level of 2 mM, it increased the enzyme activity by 172 %, and when used at the level of 5 mM, it increased by 237%.

Table 6. Results of the effect of some cations on protease enzyme activity purified from *C. majalis* flowers

Chemicals	Concentrations (mM)	Proteolytic activity (%)
Control	-	100
MgCl_2	0.1	107.28
	1	103.8
	10	70.15
MnCl_2	0.1	98.70
	1	95.18
	10	88.43
FeCl_2	0.1	108.31
	1	96.92
	10	72.06
NiCl_2	0.1	98.71
	1	87.05
	10	61.83
FeCl_3	0.1	113.34
	1	112.26
	10	104.21
CaCl_2	0.1	103.19
	1	98.20
	10	91.19
HgCl_2	0.1	99.03
	1	94.33
	10	80.26

The effects of SDS (Sodium dodecyl sulfate), EDTA (Ethylene diamine tetra acetic acid), and β -mercaptoethanol on the protease enzyme activity purified from *C. majalis* flower were investigated. For this, the proteolytic activity of the purified enzyme against the casein substrate was used. Results are depicted in Table 7. In the experiments, it was determined that the activity of the enzyme was partially inhibited at low concentrations of SDS and EDTA (known as active site-directed inhibitors) and that all chemicals used completely inhibited the enzyme at high concentrations. Inhibition of the enzyme in the presence of SDS indicates that it has more than one subunit. The decrease in activity in the presence of β -mercaptoethanol indicates the presence of disulfide bonds in the purified enzyme. By breaking the β -mercaptoethanol disulfide bonds, it changes the three-dimensional structure of the enzyme and causes it to lose its activity [39]. The decrease in activity in the presence of EDTA indicates that there is a metal

ion in the center of the enzyme as a cofactor. According to Demir et al. [27] reported that they observed that all compounds (PMSF, DIPP, β -mercaptoethanol, SDS, Phenanthroline, EDTA, and Iodoacetamide) tested on the activity of the enzyme (cysteine protease from *Capparis spinosa*) showed an inhibitory effect and that it was difficult to classify according to the catalytic type of this protease. Yıldırım Çelik [38] determined that SDS completely inhibited the enzyme at a concentration of 0.1 M, while β -mercaptoethanol did not affect the activity of the enzyme at a concentration of 0.01 M, but increased the activity at a concentration of 0.1 M.

Table 7. The results of the determination of the effect of some chemicals on the protease enzyme activity purified from *C. majalis* flowers

Chemicals	Concentrations (mM)	Proteolytic activity (%)
Control	-	100
EDTA	0.1	21.89
	1	9.40
	10	3.17
SDS	0.1	57.81
	1	32.25
	10	5.50
β -mercaptoethanol	0.1	12.40
	1	7.28
	10	0.52

Aroma substances of *C. majalis* flowers were determined using Headspace GC/MSD (Table 8). It was observed that the amount of benzyl alcohol (35%), *Z*-3-hexen-1-ol (11%), citronellol (9.6%), and geraniol (8.4%) were high. Compounds with high protective properties are those that give off a nice smell. Generally considered a safe and effective solvent, benzyl alcohol is widely used in paints, adhesives, and curing inks. In addition, while it is widely used as a perfume as a floral fragrance, it is also preferred as a stabilizer and preservative in the food, cosmetic and pharmaceutical industries due to its antimicrobial activity [40]. *Z*-3-hexen-1-ol (syn: *cis*-3-hexen-1-ol) can also play a decisive role in the grassy scent of green tea as "raw" due to its extremely strong and pungent green flavor. It is also a significantly important active ingredient found in vegetables such as grapes, passion fruit, and *Toona sinensis* (Juss.) M.Roem. [41]. Citronellol has some pharmacological effects such as antibacterial, antifungal, antispasmodic, hypotensive, vasorelaxant, and anticonvulsant activities [42]. In the literature review of Geraniol, this phytochemical has anti-diabetic, cardioprotective, *in vivo* and *in vitro* antitumor activity; It is seen that it has antidepressant effect, insecticidal and/or repellent activity, antifungal, antioxidant, anti-inflammatory and antibacterial activity [43]. The inclusion of valuable flavoring substances leads us to a conclusion that is integrated with the other findings detected in the study. It is clearly seen that the *C. majalis* protease enzyme can be used effectively and healthily in various business fields such as cosmetics, textiles, and pharmaceutical industries. This study is also very valuable in terms of providing information to these sectors.

Table 8. Percentages of aroma components identified in *C. majalis* flowers

No	Name of Component	Percentage (%)
1	Benzyl Alcohol	35
2	Z)-3-hexene-1-ol	11
3	Citronellol	9.6
4	Geraniol	8.4
5	(Z)-3-hexenyl acetate	7.8
6	Geranyl acetate	3.3
7	(Z)-3-hexene-1-ol	3.0
8	Phenylacetonitrile	3.0
9	Famesol	1.9
10	Nerol	1.3
11	Geranial + benzyl acetate	0.96
12	2,3-dihydrofarnesol	0.88
13	Phenethyl alcohol	0.78
14	(E)-2-hexenal	0.18
15	Octanol	0.15
16	Nonanal	0.1
17	Decanal	0.07
18	Neral	0.02

4. Conclusion

As a result, each step of the purification, characterization, and investigation of different application areas of the protease enzyme from the *C. majalis* plant has been carried out successfully. *C. majalis* was used for the first time in our study as a source of protease enzyme. There are many ethnobotanical applications of the *C. majalis* plant, and it has been revealed in this study that it is important to integrate these data into ethnopharmacological use and to bring it into the scientific world as a source of protease enzymes for many industrial sectors such as cosmetics, textiles, and food.

Acknowledgment

Sıla Nezahat Daşdemir's master thesis is a part of this study. This research subject was supported by the Scientific Research Projects Coordination Unit of Muğla Sıtkı Koçman University with the project numbered 15/236. The authors thank Muğla Sıtkı Koçman University Scientific Research Projects Coordination Unit for their support.

The Declaration of Ethics Committee Approval

The author declares that this document does not require ethics committee approval or any special permission. Our study does not cause any harm to the environment.

The Declaration of Conflict of Interest/ Common Interest

No conflict of interest or common interest has been declared by the author.

Authors' Contributions

N. D: Conceptualization, Methodology, Formal analysis, Writing - Original draft preparation

S. N.D: Conceptualization, Methodology, Resources, Investigation

A.K: Methodology, Formal analysis, Writing - Original draft preparation

Y.D: Conceptualization, Methodology, Formal analysis, Writing - Original draft preparation

All authors read and approved the final manuscript.

References

- [1] Daşdemir, S.N., “Müge Çiçeğinin (*Convallaria majalis*) Bazı Biyoaktivitelerinin Belirlenmesi Ve Diğer Bazı Çiçeklerle Birlikte Parfüm Tasarımında Kullanılabilirliğinin Araştırılması”, Yüksek Lisans Tezi, Muğla Sıtkı Koçman Üniversitesi, Fen Bilimleri Enstitüsü, Muğla, (2017).
- [2] Khanin, V.A., Moiseev, O.O., Babkina, A.Y., Kotenko, O.M., Kotov, A.G., “Development of the New Approach to Quality Control of Extracts of the Plant Raw Material on the Example of *Convallaria majalis*”, *News of Pharmacy*, 2,86,2016.
- [3] Godswill, A.C., “Medicinal Plants: The Medical, Food, and Nutritional Biochemistry and uses”, *International Journal of Advanced Academic Research | Sciences, Technology and Engineering*, 5, 11,220-241, 2019.
- [4] Faydaoğlu, E., Sürücüoğlu, M., “Geçmişten Günümüze Tıbbi ve Aromatik Bitkilerin Kullanılması ve Ekonomik Önemi”, *Kastamonu Üniversitesi Orman Fakültesi Dergisi*, 11,1, 52-67, 2011.
- [5] Davis, P.H., “*Flora of Turkey and the East Aegean Islands*”, Vol.8, Edinburgh at the University Press, pp.84, 1984.
- [6] Yıldırım, H., “*Asparagaceae* Familyası Altında Yer Alan Bazı Cinslere (*Scilla*, *Puschkinia*, *Chionodoxa*, *Prospero*, *Muscari* ve *Bellevalia*) Yönelik Sistematik Bir Yaklaşım”, *Herbarium Turcicum*, 1, 1-14, 2022.
- [7] Davis, P.H., Mill, R.R., Tan, K., “*Flora of Turkey and the east Aegean islands (Supplement)*”, Edinburgh Univ. Press, Edinburgh, 1988.
- [8] Güner, A., Aslan, S., (eds.) “*Türkiye bitkileri listesi:(damarlı bitkiler)*”, Nezahat Gökyiğit Botanik Bahçesi Yayınları, 2012.
- [9] İlçim, A., Karataş, H., Karahan, F., “Bazı *Muscari* Mill. (*Asparagaceae*) Türleri Üzerine Karşılaştırmalı Morfolojik, Anatomik ve Palinolojik Çalışmalar”, *Iğdır Üniversitesi Fen Bilimleri Enstitüsü Dergisi*, 10(2) 846-854, 2020.
- [10] Baytop, T., “*Türkiye’de Bitkiler ile Tedavi*”, Baskı II, Nobel Tıp Kitabevleri LTD., İstanbul, s. 234, 1999.
- [11] Chushenko, V.N., Vinnik, E.V., Komissarenko, N.F., Stupakova, E.P., Petukhova, T.V., Zinchenko, V.V., “Carbohydrates of the flowers of *Convallaria majalis* and *C. keiskei*”, *Chemistry of Natural Compounds*, 28, 242-243,1992.
- [12] Kopp, B., Kubelka, W., “New cardenolides from *Convallaria majalis*”, *Planta Medica*, 45,195-202, 1982.
- [13] Rawdkuen, S., Chaiwut, P., Pintathang, P., Benjakul, S., “Three-phase partitioning of protease from *Calotropis procera* latex”, *Biochemical Engineering Journal*, 50, 145-149,2010.
- [14] Fadiloğlu, S., “Immobilization and characterization of ficin”, *Nahrung/Food*, 45 (2), 143-146, 2001.
- [15] Laemmli, U.K., "Cleavage of structural proteins during the assembly of the head of bacteriophage T4". *Nature*, 227(5259), 680-685, 1970.

- [16] Bradford, M. M., "A rapid and sensitive method for the quantitation of microgram quantities of protein utilizing the principle of protein-dye binding", *Analytical Biochemistry*, 72, 248-254, 1976.
- [17] Leaman, D. J., "Sustainable Wild Collection of Medicinal and Aromatic Plants, Development of an International Standard", *Medicinal and Aromatic Plants*, chapter 7, 97-107, 2006.
- [18] Ersöz, T., "Bitkisel Tedaviye Bilimsel Bakış: Doğrular ve Yanlışlar". *Journal of Pediatric Infection*, 5, 217-222, 2011.
- [19] Özgen, Ö., Emiroğlu, H., Yıldız, M., Tag, A.S., Puruçcuoğlu, E., "Tüketiciler ve Modern Biyoteknoloji: Model Yaklaşımlar", Ankara Üniversitesi Biyoteknoloji Enstitüsü Yayınları No,1, Ankara,4, 2007.
- [20] González-Rábade, N., Badillo-Corona, J.A., Aranda-Barradas, J.S., Oliver Salvador, M.C., "Production of plant proteases *in vivo* and *in vitro* -A review. *Biotechnology Advances*, 29, 983-996, 2011.
- [21] Narayan, A.V., Madhusudhan, M.C., Raghavarao, K.S.M.S., "Extraction and purification of ipomoea peroxidase employing three-phase partitioning", *Applied Biochemistry and Biotechnology*, 151, 263-272, 2008.
- [22] Singh, R.K., Gourinath, S., Sharma, S., Roy, I., Gupta, M.N., Betzel, C., Srinivasan, A., Singh, T. P., "Enhancement of enzyme activity through three-phase partitioning: Crystal structure of a modified serine proteinase at 1.5 Å resolution", *Protein Engineering*, 14, 307-313,2001.
- [23] Uçkaya, F., "*Citrus sinensis* (L.) Osbeck (Portakal) ve *Citrus limon* (L.) Burm.F. (Limon) Çiçeklerinden Proteaz ve Peroksidaz Enzimlerinin Saflaştırılması ve Endüstride Kullanımlarının Araştırılması", Doktora Tezi, Muğla Sıtkı Koçman Üniversitesi, Fen Bilimleri Enstitüsü, Muğla, 2015.
- [24] Gul, A., Khan, S., Arain, H., Khan, H., Ishrat, U., Siddiqui, M., "Three-phase partitioning as an efficient one-step method for the extraction and purification of bromelain from pineapple crown waste", *Journal of Food Processing and Preservation*, 00,1-9, 2022.
- [25] Huan, XW., Chen, L.J., Luo, Y.B., Guo, H.Y., Ren, F.Z., "Purification, characterization, and milk coagulating properties of ginger proteases", *Journal of Dairy Science*, 94, 2259-2269,2011.
- [26] Nafi, A., Ling, F, H., Bakar, J., Ghazali, H.M., "Partial characterization of an enzymatic extract from Bentong ginger (*Zingiber officinale* var. *Bentong*)", *Molecules*, 19, 12336-12348, 2014.
- [27] Demir, Y., Güngör, A.A., Duran, E.D., Demir, N., "Cysteine Protease (Capparin) from Capsules of Caper (*Capparis spinosa*)", *Food Technology and Biotechnology*, 46 (3), 286-291,2008.
- [28] Demir, N., Taşgın, E., "Hindiba (*Cichorium intybus* L.) Bitkisinden Myrosinaz Enziminin Saflaştırılması, Karakterize Edilmesi ve Kozmetik Alanında Kullanılabilirliğinin İncelenmesi", *Süleyman Demirel Üniversitesi Fen Bilimleri Enstitüsü Dergisi*, 16, 307-314, 2012.
- [29] Demir, N., Daşdemir, S.N., Can, Z., "Purification and Characterization of Protease Enzyme from Oleander (*Nerium oleander*) Flowers of Different Colors", *International Journal of Innovative Research and Reviews*,1(1), 21-26, 2017.
- [30] Febriani, K., Wahyuni, I., Setiasih, S., Hudiyono, S., "Comparative study of two methods of fractionation bromelain from pineapple core extract (*Ananas comosus*)", In AIP Conference Proceedings, 1862 (1), 030095, AIP Publishing LLC, 2017.

- [31] Banik, S., Biswas, S., Karmakar, S., “Extraction, purification, and activity of protease from the leaves of *Moringa oleifera* [version 1; referees: 2 approved, 1 approved with reservations]” *F1000Research*, 7, 1151, 2018.
- [32] Khan, A.A., Fazili, A.B.A., Bhat, S.A., Bhat, W.F., Asghar, M.N., Khan, M.S., Bano, B., “Purification, characterization and studies of a novel cysteine protease inhibitor from *Juglans regia*: Implications as a potential biopesticide”, *Journal of King Saud University – Science*, 34, 101829, 2022.
- [33] Demiray, A., “Kozmetik Amaçlı Kullanım İçin Kır Menekşesinde (*Viola odorata*) Bazı Biyokimyasal Aktivitelerin Aranması ve Tanımlanması”, Yüksek Lisans Tezi, Muğla Sıtkı Koçman Üniversitesi, Fen Bilimleri Enstitüsü, Muğla, 2013.
- [34] Akçay, O., “Kızılcım Kabuğundan (*Pinus brutia*) Etken Madde İzolasyonu ve Değişik Enzim Aktiviteleri Üzerindeki Etkilerinin İncelenmesi”, Yüksek Lisans Tezi, Muğla Sıtkı Koçman Üniversitesi, Fen Bilimleri Enstitüsü, Muğla, 2014.
- [35] Demirkent, B.P., “Datça Papatyasının (*Chrysanthemum coronarium*) Bazı Biyoaktif Bileşenlerinin Belirlenmesi; İlaç ve Kozmetik Endüstrisinde Hammadde Olarak Kullanılabilirliğinin Araştırılması”, Yüksek Lisans Tezi, Muğla Sıtkı Koçman Üniversitesi, Fen Bilimleri Enstitüsü, Muğla, 2015.
- [36] Işık, C., “Mis Zambağının (*Lilium candidum*) Biyokimyasal Aktivitelerinin Belirlenmesi ve endüstriyel Amaçlı Kullanılabilirliğinin Araştırılması”, Yüksek Lisans Tezi, Muğla Sıtkı Koçman Üniversitesi, Fen Bilimleri Enstitüsü, Muğla, 2014.
- [37] Yıldırım Çelik, S., “Çiğdem (*Crocus biflorus*) Yumrularından Proteaz Enziminin Saflaştırılması ve Saflaştırılan Enzimin Kazeinin Koagülasyonunda Kullanılabilirliğinin Araştırılması”, *Gıda*, 43 (2), 231-239, 2018.
- [38] Alıcı, E.A., “Çilek Meyvesinden Proteaz Enziminin Saflaştırılması, Karakterizasyonu ve Uygulama Alanlarının Araştırılması”, Doktora Tezi, Sakarya Üniversitesi, Fen Bilimleri Enstitüsü, Sakarya, 2019.
- [39] Lehninger, A. L., “*Principles of biochemistry*”, Worth Publishers Inc., New York, pp, 1152, 2013.
- [40] Liu, L., Zhu, Y., Chen, Y., Chen, H., Fan, C., Mo, Q., Yuan, J., “One-Pot Cascad Biotransformation for Efficient Synthesis of Benzyl Alcohol and Its Analogs”, *Chemistry-An Asian Journal*, 15, 101, 2020.
- [41] Nie, C., Xiao Du, Y.G., Bian, J.L., Li H., Zhang, X., Wang, C.M., Li, S.Y., “Characterization of the effect of cis-3-hexen-1-ol on green tea aroma”, *Scientific Reports*. 10, 15506, 2020.
- [42] Brito, R.G., Guimarães, A.G., Quintans, J.S.S., Santos, M.R.V., De Sousa, D.P, Jr Badaue-Passos, D., de Lucca Jr, W., Brito, F.A., Barreto, E.O., Oliveira, A.P., Quintans, L.J., “Citronellol, a monoterpene alcohol, reduces nociceptive and inflammatory activities in rodents”, *Journal of Natural Medicines*, 66, 637-644, 2012.
- [43] Pereira de Lira, M.H., de Andrade Júnior, F.P., Queiroga Moraes, G.F., da Silva Macenac, G., de Oliveira Pereira F., Lima, I.O., “Antimicrobial activity of geraniol: an integrative review”, *Journal of Essential Oil Research*, 32 (3), 187-197, 2020.



SOME NOVEL SCHIFF BASE DERIVATIVES AS PROMISING CHOLINESTERASE INHIBITORS WITH ANTIOXIDANT ACTIVITY AGAINST ALZHEIMER'S DISEASE: SYNTHESIS, CHARACTERIZATION AND BIOLOGICAL EVALUATION

Ercan ÇINAR^{*,1}  Mehmet BOĞA²  Giray TOPAL³  Reşit ÇAKMAK⁴ 

¹Department of Nursing, School of Health Sciences, Batman University, Batman, Turkey

²Department of Analytical Chemistry, Faculty of Pharmacy, Dicle University, Diyarbakır, Turkey

³Ziya Gökalp Faculty of Education, Department of Chemistry, Dicle University, Diyarbakır, Türkiye

⁴Medical Laboratory Techniques Program, Vocational School of Health Services, Batman Uni., Batman, Turkey

* Corresponding author; ercan.cinar@batman.edu.tr

Abstract: In this study, five novel Schiff base derivatives (6-10) except for 9 were synthesized for the first time, characterized, and tested for their inhibition activities against acetylcholinesterase (AChE) and butyrylcholinesterase (BChE). Also, the Antioxidant activities of these molecules were examined by DPPH and ABTS assays. Their molecular structures were characterized by three spectroscopic techniques. In AChE assay, compound 6 (95.87±1.59 % inhibition) inhibited this enzyme better than galanthamine (76.98±0.42 % inhibition). In BChE assay, compound 10 with an 87.92±1.08% inhibition value in the series indicated the highest activity compared to galanthamine (76.30±0.28 % inhibition). In ABTS radical scavenging assay, compounds 7, 8, and 9 except for 6 and 10 indicated higher antioxidant activities compared to butylated hydroxytoluene (BHT). It is believed that these results may contribute to the design and synthesis of novel antioxidant agents, AChE, and BChE inhibitors.

Keywords: Schiff base, Antioxidant agent, Cholinesterase inhibitor, Alzheimer's disease.

Received: November 14, 2022

Accepted: December 28, 2022

1. Introduction

Alzheimer's disease (AD), which is a fatal neurodegenerative disease, is the most common cause of dementia in the aged population [1-3]. It is a nervous system disorder in which damage occurs in neurons in the brain, which manifests itself with progressive loss of cognitive functions such as attention, speech, and decision-making ability, especially memory loss [4, 5]. The pathology of progressive and cognitive dysfunction associated with aging in AD remains unclear, and therefore there is still no definitive radical treatment for AD [6]. Today, approximately 35 million people worldwide are affected by AD, and it is presumed that this number will reach approximately 65 billion in 2030 and 115 million in 2050. [7]. These data demonstrate the importance of developing an efficacious therapy.

The most significant pathological features of AD are β -amyloid extracellular plaques, intracellular neurofibrillary tangles formed by excessive phosphorylation of tau protein, loss of cholinergic neurons in the basal forebrain, and oxidative stress [8, 9]. Inadequate cholinergic transmission plays a significant role in the emergence of cognitive, functional, and behavioral symptoms in AD. Therefore, cholinesterase inhibitors (ChEIs) are used to increase the decreased amount of acetylcholine (ACh) in the brain in the cholinergic hypothesis [10, 11]. This hypothesis is the only currently accepted hypothesis

to explain the nature of this disease [12, 13]. The mechanisms of drugs currently employed in the therapy of this disease are based on this hypothesis [14, 15]. The treatments are usually planned to increase the function of the cholinergic system with either receptor agonists or ChEIs [16, 17]. Until now, ChEIs such as tacrine, donepezil, rivastigmine, and galanthamine has been approved by the US Food and Drug Administration (FDA) for use as AChE inhibitors [18].

In order to fully elucidate the etiology of this disease, other hypotheses such as the amyloid hypothesis, the tau hypothesis, and the oxidative stress hypothesis have been proposed, in addition to the cholinergic hypothesis [19]. In the oxidative stress hypothesis, it has been suggested that AD occurs as a result of degeneration and death in neurons due to increased oxidative stress [20]. In the treatment process of AD, the prevention of oxidative stress, which causes neuron degeneration and subsequent neuron death, is significant in terms of the therapy approach. Antioxidants are known to reduce oxidative stress [21, 22]. Therefore, the antioxidant activities of the designed compounds for this research were also investigated.

Nitrogen-containing heterocycles are found in the structure of many drug molecules and pharmaceutically active natural and synthetic molecules [23]. 4-Aminoantipyrine (4-AAP) and its derivatives constitute a significant class of nitrogen-containing heterocyclic compounds. They are known to display a wide range of various biological properties [24-30].

Encouraged by the aforementioned findings, herein we aimed to research the inhibition potency of novel Schiff bases against AChE and BChE. Also, the antioxidant activities of these compounds were evaluated by ABTS and DPPH assays. The inhibition activity results and antioxidant potencies of new Schiff bases were compared with standard molecules. Galanthamine as the standard compound for these enzymes was utilized. The inhibition activity results were given as % inhibition at 200 μM . Antioxidant activity values were given as IC_{50} (μM) for these assays. BHT, butylated hydroxyanisole (BHA), and α -Tocopherol (α -TOC) as the standard antioxidants in these assays were utilized. The molecular structures of new molecules were characterized by FT-IR, ^1H NMR, and ^{13}C NMR.

2. Materials and Methods

2.1. Chemistry and analysis

All chemicals employed in this manuscript were provided by commercial suppliers. A digital melting point instrument was used for the determination of the melting points of the target molecules. NMR (the Bruker AVANCE III 500 MHz spectrometer) and FT-IR spectra (the Perkin-Elmer spectrophotometer) for the characterization of target molecules were used, respectively.

2.2. The synthesis of aryl Sulfonates

Aryl sulfonate derivatives (**1-5**) were obtained and characterized in one of our previous studies. The synthesis procedure is given in detail in that study [31].

2.3. The preparation of Schiff bases

The synthesis procedure of novel compounds (**6-10**) was given in our previous study [25, 28].

2.3.1 2-(((Antipyrine-4-yl)imino)methyl)-5-(diethylamino)phenyl 4-chlorobenzenesulfonate (**6**)

Light yellow solid, yield: 80%, m.p. 174-175°C. FT-IR (cm^{-1}) ν_{max} : 3073, 2977 (C-H arom.), 2932, 2874 (C-H aliph.), 1646 (C=O), 1590 (C=N), 1348 (SO_2 asym.), 1190 (SO_2 sym.). ^1H NMR (CDCl_3): δ 9.32 (s, 1H, $-\text{CH}=\text{N}$), 7.91 – 7.80 (m, 3H, Ar-H), 7.54 – 7.40 (m, 4H, Ar-H), 7.37 – 7.24 (m, 3H, Ar-H), 6.61 – 6.52 (m, 2H, Ar-H), 3.37 (q, $J = 7.1$ Hz, 4H, $-\text{N}(\text{CH}_2\text{CH}_3)_2$), 3.09 (s, 3H, $-\text{N}-\text{CH}_3$),

2.38 (s, 3H, =C-CH₃), 1.18 (t, *J* = 7.2 Hz, 6H, -N(CH₂CH₃)₂) ppm. ¹³C NMR (CDCl₃): δ 160.78 (C=O), 151.56 (C=N), 150.82, 150.44, 150.06, 140.41, 135.19, 133.49, 130.56, 129.30, 129.16, 127.75, 126.62, 124.15, 119.23, 117.51, 110.51, 105.41 (Ar-C and Pyr-C), 44.70 (-N(CH₂CH₃)₂), 36.15 (-N-CH₃), 12.53 (-N(CH₂CH₃)₂), 10.05 (=C-CH₃) ppm.

2.3.2 3-(((Antipyrine-4-yl)imino)methyl)phenyl 4-chlorobenzenesulfonate (7)

Yellow solid, yield: 81%, m.p. 162-163 °C. FT-IR (cm⁻¹) ν_{\max} : 3085, 3012 (C-H arom.), 2982, 2930 (C-H aliph.), 1653 (C=O), 1573 (C=N), 1374 (SO₂ asym.), 1184 (SO₂ sym.). ¹H NMR (CDCl₃): δ 9.63 (s, 1H, -CH=N), 7.81 – 7.74 (m, 2H, Ar-H), 7.65 (dt, *J* = 7.8, 1.2 Hz, 1H, Ar-H), 7.54 – 7.43 (m, 5H, Ar-H), 7.41 – 7.26 (m, 4H, Ar-H), 7.03 – 7.01 (m, 1H, Ar-H), 3.17 (s, 3H, -N-CH₃), 2.44 (s, 3H, =C-CH₃) ppm. ¹³C NMR (CDCl₃): δ 160.52 (C=O), 154.48 (C=N), 152.22, 149.88, 140.99, 140.18, 134.55, 133.86, 129.96, 129.86, 129.54, 129.24, 127.16, 127.15, 124.59, 123.55, 120.08, 117.9 (Ar-C and Pyr-C), 35.61 (-N-CH₃), 9.98 (=C-CH₃) ppm.

2.3.3 2-(((Antipyrine-4-yl)imino)methyl)-6-methoxyphenyl 4-chlorobenzenesulfonate (8)

Yellow solid, yield: 88%, m.p. 235-236 °C. FT-IR (cm⁻¹) ν_{\max} : 3090, 3008 (C-H arom.), 2935, 2841 (C-H aliph.), 1649 (C=O), 1567 (C=N), 1375 (SO₂ asym.), 1191 (SO₂ sym.). ¹H NMR (CDCl₃): δ 9.42 (s, 1H, -CH=N), 7.89 – 7.83 (m, 2H, Ar-H), 7.63 (dd, *J* = 7.9, 1.2 Hz, 1H, Ar-H), 7.48 (t, *J* = 7.8 Hz, 2H, Ar-H), 7.43 – 7.36 (m, 4H, Ar-H), 7.32 (t, *J* = 7.3 Hz, 1H), 7.29 – 7.21 (m, 1H, Ar-H), 6.98 (dd, *J* = 8.2, 1.3 Hz, 1H, Ar-H), 3.79 (s, 3H, -OCH₃), 3.15 (s, 3H, -N-CH₃), 2.43 (s, 3H, =C-CH₃) ppm. ¹³C NMR (CDCl₃): δ 160.03 (C=O), 152.39 (C=N), 152.93, 150.77, 140.20, 138.37, 134.77, 134.74, 132.80, 130.24, 129.25, 129.20, 127.44, 126.89, 124.40, 118.48, 118.40, 113.92 (Ar-C and Pyr-C), 56.12 (-OCH₃), 35.77 (-N-CH₃), 10.03 (=C-CH₃) ppm.

2.3.4 5-(((Antipyrine-4-yl)imino)methyl)-2-methoxyphenyl 4-chlorobenzenesulfonate (9)

Light yellow solid, yield: 79%, m.p. 232-233 °C. FT-IR (cm⁻¹) ν_{\max} : 3055, 2973 (C-H arom.), 2930, 2838 (C-H aliph.), 1646 (C=O), 1582 (C=N), 1365 (SO₂ asym.), 1182 (SO₂ sym.). ¹H NMR (CDCl₃): δ 9.62 (s, 1H, -CH=N), 7.86 – 7.78 (m, 2H, Ar-H), 7.72 (d, *J* = 1.9 Hz, 1H, Ar-H), 7.56 (dd, *J* = 8.4, 1.9 Hz, 1H, Ar-H), 7.53 – 7.43 (m, 3H, Ar-H), 7.42 – 7.35 (m, 2H, Ar-H), 7.35 – 7.24 (m, 1H, Ar-H), 6.86 (d, *J* = 8.5 Hz, 1H, Ar-H), 3.61 (s, 3H, -OCH₃), 3.14 (s, 3H, -N-CH₃), 2.44 (s, 3H, =C-CH₃) ppm. ¹³C NMR (CDCl₃): δ 160.78 (C=O), 151.95 (C=N), 154.67, 153.07, 140.62, 138.65, 134.74, 134.72, 131.55, 130.09, 129.19, 129.08, 128.92, 126.94, 124.41, 121.61, 118.32, 112.26 (Ar-C and Pyr-C), 55.71 (-OCH₃), 35.79 (-N-CH₃), 10.03 (=C-CH₃) ppm.

2.3.5 1-(((Antipyrine-4-yl)imino)methyl)naphthalen-2-yl 4-chlorobenzenesulfonate (10)

Yellow solid, yield: 89%, m.p. 214 °C. FT-IR (cm⁻¹) ν_{\max} : 3105, 3061 (C-H arom.), 2971, 2926 (C-H aliph.), 1640 (C=O), 1581 (C=N), 1344 (SO₂ asym.), 1165 (SO₂ sym.). ¹H NMR (CDCl₃): δ 9.90 (s, 1H, -CH=N), 9.12 (d, *J* = 9.6 Hz, 1H, Np-H), 7.91 – 7.77 (m, 4H, Ar-H and Np-H), 7.58 – 7.48 (m, 5H, Ar-H and Np-H), 7.46 (dd, *J* = 8.5, 1.2 Hz, 2H, Ar-H), 7.41 – 7.33 (m, 1H, Ar-H), 7.32 – 7.22 (m, 2H, Ar-H), 3.22 (s, 3H, -N-CH₃), 2.44 (s, 3H, =C-CH₃) ppm. ¹³C NMR (CDCl₃): δ 160.03 (C=O), 152.60 (C=N), 152.23, 147.38, 140.44, 134.74, 133.62, 132.67, 131.45, 131.31, 130.49, 129.37, 129.22, 128.27, 127.60, 127.14, 126.81, 126.39, 125.65, 124.48, 122.13, 118.41 (Ar-C, Np-C and Pyr-C), 35.73 (-N-CH₃), 10.11 (=C-CH₃) ppm.

2.4. General procedure for determining the anticholinesterase activities of the target molecules

In this research, the inhibitory performance of new compounds towards cholinesterases was determined, respectively [32]. The method used in the present study was explained in detail in our previous studies [27, 29, 31, 33].

2.5. General procedure for determining the antioxidant activities of the target molecules

The antioxidant potential of new molecules in DPPH and ABTS assays was determined according to the methods of Blois et al. [34] and Re et al. [35], respectively. These two antioxidant activity assays have been given in detail in the previous studies of our group [27, 29, 31].

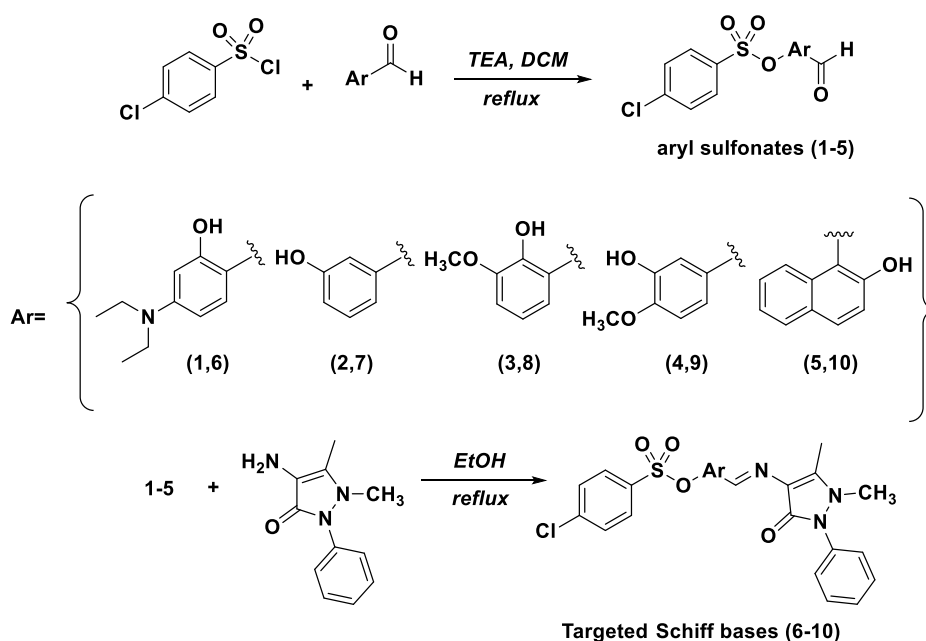
2.6. Statistical Analysis

Anticholinesterase and antioxidant and activity results of the target molecules in this research are stated as the mean \pm SD of three parallel measurements. The statistical significance was forecasted employing a Student's t-test, where $p < .05$ was considered important.

3. Results

3.1. Chemistry

The designed Schiff base derivatives (**6-10**) for this study were obtained by two steps as outlined in Scheme 1. In the first synthesis step to acquire sulfonates (**1-5**), the *O*-sulfonylation of the phenolic aldehydes with 4-CBSC was carried out under reflux for 5. In the final step to obtain novel Schiff bases as the target molecules, compounds **1-5** were successfully reacted with 4-AAP in an ethanol medium for 2 h under reflux. In a literature search, we determined that the target molecules **6, 7, 8** ve **10** except for **9** were synthesized for the first time. On the other hand, the intermediates (**1-5**) used in this research to obtain the target compounds were obtained and characterized in one of our previous studies [31]. In that study, the anticholinesterase and antioxidant activities of the intermediates were investigated.



Scheme 1. The synthesis procedure of Schiff base derivatives (**6-10**)

In this research, all newly obtained compounds were absolutely characterized. FT-IR spectra of novel Schiff base derivatives observed that the two important bands, C=N group and C=O group stretching bands at 1567-1590 cm^{-1} at 1640-1653 cm^{-1} respectively. Respectively, the asymmetric and symmetric SO_2 group stretching bands were also determined at 1344-1375 and 1165-1191 cm^{-1} . On the other hand, ^1H NMR spectra of the newly obtained compounds, -CH=N proton signal were observed at 9.32-9.90 ppm. The protons of -N- CH_3 and =C- CH_3 were observed as a singlet at 3.09-3.22 ppm and 2.38-2.44 ppm, respectively. Respectively, ^{13}C NMR spectra of compounds, the carbons of -N- CH_3 and =C- CH_3 resonated at 35.61-36.15 and 9.98-10.11 ppm. The signal of the C=O carbon was determined to resonate at 160.03-160.78 ppm. The signal of CH=N was detected at 151.56-154.48 ppm [25, 28].

3.2. Biological activity results

3.2.1. The inhibition activity results

Nowadays, due to the predicted increases in the number of Alzheimer's patients, the increase in treatment costs, and the long treatment process, great importance is given to the development of novel drugs in the therapy of AD worldwide [1-5, 16-18]. In this research, we determined the inhibition activities of some new heterocyclic molecules (**6-10**) as the target molecules against AChE and BChE (Table 1).

Table 1. The inhibitory activity results of Schiff bases

The target molecules	AChE	BChE
6	95.87±1.59	67.72±1.22
7	75.21±1.01	66.03±1.08
8	66.65±0.42	37.92±0.43
9	63.77±1.96	34.88±0.80
10	80.23±0.14	87.92±1.08
Galanthamine	76.98±0.42	76.30±0.28

(i) In AChE assay, the results of our study displayed that all tested compounds had varying % inhibition values. Among them, compounds **6** (95.87±1.59 % inhibition) and **10** (80.23±0.14% inhibition) were determined to inhibit AChE more than galanthamine (76.98±0.42% inhibition). Compound **6**, a Schiff base derivative based on 4-(diethylamino)salicylaldehyde, showed the highest activity towards this enzyme. Other than this, compound **9** (63.77±1.96% inhibition), a Schiff base derivative based on 3-hydroxy-4-methoxybenzaldehyde, exhibited the weakest activity against this enzyme.

(ii) In BChE assay, we found that the compound **10** (87.92±1.08% inhibition), a Schiff base derivative based on 2-hydroxy-1-naphthaldehyde in this series showed the highest activity against BChE. Apart from this compound, compounds **6** (67.72±1.22% inhibition) and **7** (66.03±1.08% inhibition) showed the closest activities to galanthamine (76.30±0.28% inhibition). On the other hand, compound **9** (34.88±0.80% inhibition), a Schiff base derivative based on 3-hydroxy-4-methoxybenzaldehyde, demonstrated the weakest activity against BChE

3.2.1 The activity results of antioxidant agents

In the current research, the antioxidant activity results of all Schiff base derivatives were given in Table 2.

Table 2. The results of DPPH and ABTS assays

IC ₅₀ values (μM)	DPPH	ABTS
The target molecules		
6	532.79±2.61	64.82±1.05
7	283.24±2.02	25.67±0.93
8	478.78±3.25	37.79±0.37
9	476.09±4.49	24.88±0.75
10	294.99±2.18	>1000
BHA	47.44±0.60	16.20±0.20
α-TOC	48.37±0.58	16.19±0.17
BHT	203.50±0.66	41.56±0.57

(i) In DPPH radical scavenging assay, the tested molecules showed antioxidant activities in the range of 283.24 and 532.79 μM. Among these molecules, compound **7** (IC₅₀=283,24 μM), which is a Schiff base derivative based on 3-hydroxy benzaldehyde, exhibited the best antioxidant activity. However, these molecules indicated weaker antioxidant activities than BHT (IC₅₀=203.50 μM), BHA (IC₅₀=47.44 μM) and α-TOC (IC₅₀=48.37 μM).

(ii) In ABTS radical scavenging assay, all Schiff base derivatives except for compound **10** demonstrated activities in the range of 24.88 and 64.82 μM. Among these molecules in the series, compounds **7** (IC₅₀=25.67 μM), **8** (IC₅₀=37.79 μM), and **9** (IC₅₀=24.88 μM) showed higher antioxidant activity than BHT (IC₅₀=41.56 μM). When the results given in Table 2 were investigated, we found that compound **9** exhibited high antioxidant activity. However, all tested compounds displayed lower activities than BHA (IC₅₀=16.20 μM) and α-TOC (IC₅₀=16.19 μM).

4. Conclusion

AD is the most common age-related neurodegenerative disease and has become an important public health problem in most areas of the world. Substantial progress has been made in understanding the basic neurobiology of AD and, as a result, novel drugs for its therapy have become available. ChEIs, which increase the availability of ACh in central synapses, has become the main approach to symptomatic therapy. In this research, we synthesized and characterized five novel heterocyclic Schiff bases derived from 4-AAP as potential inhibitors of AChE and BChE with antioxidant activity. The inhibition potential of these molecules, which were characterized by three spectroscopic methods, against cholinesterases was investigated. We found that some of them inhibited these enzymes more than galanthamine. Amongst the screened molecules, compound **6** and **10** for AChE has been determined to be the most efficacious inhibitor. Compound **10** was also determined to be the best inhibitor for BChE. In ABTS radical scavenging assay, we determined that many compounds showed better antioxidant activities than BHT. In DPPH radical scavenging assay, we determined that the same molecules indicated lower antioxidant activities than standard antioxidants.

Conflict of interest:

The article's authors declare that there is no conflict of interest between them.

The Declaration of Ethics Committee Approval

The author declares that this document does not require ethics committee approval or any special permission. Our study does not cause any harm to the environment.

Authors' Contributions:

E. Ç: Conceptualization, Methodology, Validation, Formal analysis, Investigation, Writing-original draft preparation, Writing - review&editing (%30)

M. B: Validation, Writing-original draft preparation (%20)

G. T: Conceptualization, Investigation, Writing-original draft preparation (%20)

R. Ç: Conceptualization, Methodology, Validation, Formal analysis, Investigation, Writing-original draft preparation, Writing - review&editing (%30)

Compliance with Research and Publication Ethics

This study was carried out by obeying research and ethics rules.

References

- [1] Jarosova, R., Niyangoda, S.S., Hettiarachchi, P., Johnson, M.A., "Impaired dopamine release and latent learning in Alzheimer's disease model zebrafish", *ACS Chemical Neuroscience*, 13, 2924-2931, 2022. doi.org/10.1021/acscemneuro.2c00484.
- [2] Veluppal, A., "Differentiation of Alzheimer conditions in brain MR images using bidimensional multiscale entropy-based texture analysis of lateral ventricles", *Biomedical Signal Processing and Control*, 78, 103974, 2022. doi.org/10.1016/j.bspc.2022.103974.
- [3] Skovronsky, D.M., Lee, V.M.Y., Trojanowski, J. Q., "Neurodegenerative diseases: new concepts of pathogenesis and their therapeutic implications", *Annual Review of Pathology: Mechanisms of Disease*, 1, 151-170, 2006. doi.org/10.1146/annurev.pathol.1.110304.100113.
- [4] Pievani, M., de Haan, W., Wu, T., Seeley, W.W., Frisoni, G.B., "Functional network disruption in the degenerative dementias", *The Lancet Neurology*, 10, 829-843, 2011. doi.org/10.1016/S1474-4422(11)70158-2.
- [5] Li, R., Zhang, C., Rao, Y., Yuan, T.F., "Deep brain stimulation of fornix for memory improvement in alzheimer's disease: a critical review", *Ageing Research Reviews*, 79, 101668, 2022. doi.org/10.1016/j.arr.2022.101668.
- [6] Osmaniye, D., Ahmad, I., Sağlık, B.N., Levent, S., Patel, H.M., Ozkay, Y., Kaplancıklı, Z.A., "Design, synthesis, and molecular docking and ADME studies of novel hydrazone derivatives for AChE inhibitory, BBB permeability and antioxidant effects", *Journal of Biomolecular Structure and Dynamics*, 1-17, 2022. doi.org/10.1080/07391102.2022.2139762.
- [7] Jindal, H., Bhatt, B., Sk, S., Singh Malik, J., "Alzheimer disease immunotherapeutics: then and now", *Human vaccines & immunotherapeutics*, 10, 2741-2743, 2014. doi.org/10.4161/21645515.2014.970959.
- [8] Hardy, J., Bogdanovic, N., Winblad, B., Portelius, E., Andreasen, N., Cedazo- Minguéz, A., Zetterberg, H., "Pathways to Alzheimer's disease", *Journal of Internal Medicine*, 275, 296-303, 2014. doi.org/10.1111/joim.12192.
- [9] Parihar, M.S., Hemnani, T., "Alzheimer's disease pathogenesis and therapeutic interventions", *Journal of Clinical Neuroscience*, 11, 456-467, 2004. doi.org/10.1016/j.jocn.2003.12.007.
- [10] Parnetti, L., Mignini, F., Tomassoni, D., Traini, E., Amenta, F., "Cholinergic precursors in the treatment of cognitive impairment of vascular origin: ineffective approaches or need for re-evaluation?", *Journal of the Neurological Sciences*, 257, 264-269, 2007. doi.org/10.1016/j.jns.2007.01.043.
- [11] Başaran, E., Çakmak, R., Şentürk, M., Taskin-Tok, T., "Biological activity and molecular docking studies of some N-phenylsulfonamides against cholinesterases and carbonic anhydrase isoenzymes", *Journal of Molecular Recognition*, 35, e2982, 2022.

- [12] Craig, L.A., Hong, N.S., McDonald, R.J., “Revisiting the cholinergic hypothesis in the development of Alzheimer's disease”, *Neuroscience & Biobehavioral Reviews*, 35, 1397-1409, 2011. doi.org/10.1016/j.neubiorev.2011.03.001.
- [13] Cummings, J. L., Back, C., “The cholinergic hypothesis of neuropsychiatric symptoms in Alzheimer's disease”, *The American Journal of Geriatric Psychiatry*, 6, S64-S78, 1998. doi.org/10.1097/00019442-199821001-00009.
- [14] Rusanen, M., Kivipelto, M., Quesenberry Jr, C.P., Zhou, J., Whitmer, R.A., “Heavy smoking in midlife and long-term risk of Alzheimer disease and vascular dementia”, *Archives of Internal Medicine*, 171, 333-339, 2011. doi:10.1001/archinternmed.2010.393.
- [15] Van Marum, R.J., “Current and future therapy in Alzheimer's disease”, *Fundamental & Clinical Pharmacology*, 22(3), 265-274, 2008. doi.org/10.1111/j.1472-8206.2008.00578.x.
- [16] Wilkinson, D.G., Francis, P.T., Schwam, E., Payne-Parrish, J., “Cholinesterase inhibitors used in the treatment of Alzheimer's disease”, *Drugs & Aging*, 21, 453-478, 2004. doi.org/10.2165/00002512-200421070-00004.
- [17] Dawson, G.R., Iversen, S.D., “The effects of novel cholinesterase inhibitors and selective muscarinic receptor agonists in tests of reference and working memory”, *Behavioural Brain Research*, 57, 143-153, 1993. doi.org/10.1016/0166-4328(93)90130-I.
- [18] Grutzendler, J., Morris, J.C., “Cholinesterase inhibitors for Alzheimer's disease”, *Drugs*, 61, 41-52, 2001. doi.org/10.2165/00003495-200161010-00005.
- [19] Teixeira, J.P., de Castro, A.A., Soares, F.V., da Cunha, E.F., Ramalho, T.C., “Future therapeutic perspectives into the Alzheimer's disease targeting the oxidative stress hypothesis”, *Molecules*, 24, 4410, 2019. doi.org/10.3390/molecules24234410.
- [20] Markesbery, W.R., “Oxidative stress hypothesis in Alzheimer's disease”, *Free Radical Biology and Medicine*, 23, 134-147, 1997. doi.org/10.1016/S0891-5849(96)00629-6.
- [21] Leeuwenburgh, C., Heinecke, J.W., “Oxidative stress and antioxidants in exercise”, *Current Medicinal Chemistry*, 8, 829-838, 2001. doi.org/10.2174/0929867013372896.
- [22] Rao, A.V., Balachandran, B., “Role of oxidative stress and antioxidants in neurodegenerative diseases”, *Nutritional Neuroscience*, 5, 291-309, 2002. doi.org/10.1080/1028415021000033767.
- [23] Kerru, N., Gummidi, L., Maddila, S., Gangu, K.K., Jonnalagadda, S.B., “A review on recent advances in nitrogen-containing molecules and their biological applications”, *Molecules*, 25, 1909, 2020. doi.org/10.3390/molecules25081909.
- [24] Raman, N., Johnson Raja, S., Sakthivel, A., “Transition metal complexes with Schiff-base ligands: 4-aminoantipyrine based derivatives—a review”, *Journal of Coordination Chemistry*, 62, 691-709, 2009. doi.org/10.1080/00958970802326179.
- [25] Başaran, E., Çakmak, R., Akkoç, S., Kaya, S., “Combined experimental and theoretical analyses on design, synthesis, characterization, and in vitro cytotoxic activity evaluation of some novel imino derivatives containing pyrazolone ring”, *Journal of Molecular Structure*, 1265, 133427, 2022. doi.org/10.1016/j.molstruc.2022.133427.
- [26] Çakmak, R., Başaran, E., Şentürk, M., “Synthesis, characterization, and biological evaluation of some novel Schiff bases as potential metabolic enzyme inhibitors”, *Archiv der Pharmazie*, 355, 2100430, 2022. doi.org/10.1002/ardp.202100430.

- [27] Çakmak, R., Başaran, E., Boğa, M., Erdoğan, Ö., Çınar, E., Çevik, Ö., “Schiff base derivatives of 4-aminoantipyrine as promising molecules: synthesis, structural characterization, and biological activities”, *Russian Journal of Bioorganic Chemistry*, 48, 334-344, 2022. doi.org/10.1134/S1068162022020182.
- [28] Başaran, E., “Some aryl sulfonyl ester-based heterocyclic schiff bases: synthesis, structure elucidation and antioxidant activity”, *Journal of the Institute of Science and Technology*, 11, 2967-2978, 2021. doi.org/10.21597/jist.963129.
- [29] Çınar, E., Başaran, E., Erdoğan, Ö., Çakmak, R., Boğa, M., Çevik, Ö., “Heterocyclic Schiff base derivatives containing pyrazolone moiety: Synthesis, characterization, and in vitro biological studies”, *Journal of the Chinese Chemical Society*, 68, 2355-2367, 2021. doi.org/10.1002/jccs.202100357.
- [30] Alam, M.S., Lee, D.U., Bari, M., “Antibacterial and cytotoxic activities of Schiff base analogues of 4-aminoantipyrine”, *Journal of the Korean Society for Applied Biological Chemistry*, 57, 613-619, 2014. doi.org/10.1007/s13765-014-4201-2.
- [31] Esmer, Y.İ., Çınar, E., Başaran, E., “Design, docking, synthesis and biological evaluation of novel nicotinohydrazone derivatives as potential butyrylcholinesterase enzyme inhibitor”, *ChemistrySelect*, 7, e202202771, 2022. doi.org/10.1002/slct.202202771.
- [32] Ellman, G.L., Courtney, K.D., Andres Jr, V., Featherstone, R.M., “A new and rapid colorimetric determination of acetylcholinesterase activity”, *Biochemical Pharmacology*, 7, 88-90, 1961. doi.org/10.1016/0006-2952(61)90145-9.
- [33] Çakmak, R., Çınar, E., Başaran, E., Boğa, M., “Synthesis, characterization and biological evaluation of ester derivatives of 4-(diethylamino) salicylaldehyde as cholinesterase, and tyrosinase inhibitors”, *Middle East Journal of Science*, 7, 137-144, 2021. doi.org/10.51477/mejs.947973.
- [34] Blois, M.S., "Antioxidant determinations by the use of a stable free radical", *Nature*, 181, 1199-1200, 1958. doi.org/10.1038/1811199a0.
- [35] Re, R., Pellegrini, N., Proteggente, A., Pannala, A., Yang, M., Rice-Evans, C., “Antioxidant activity applying an improved ABTS radical cation decolorization assay”, *Free Radical Biology and Medicine*, 26, 1231–1237, 1999. doi.org/10.1016/S0891-5849(98)00315-3.

**SYNTHESIS OF NOVEL BIS(PHOSPHINO)AMINE-RU^{II}(ACAC)₂ COMPLEXES, AND INVESTIGATION OF CATALYTIC ACTIVITY IN TRANSFER HYDROGENATION**

Duygu ELMA KARAKAŞ¹ ^{*} Uğur IŞIK² ^{ID} Murat AYDEMİR³ ^{ID} Feyyaz DURAP⁴ ^{ID}
Akın BAYSAL ^{ID}⁵

¹Science and Technology Application and Research Center, Siirt University, Siirt, Turkey

²Medical-Aromatic Plants Application and Research Center, Artvin Coruh University, Artvin, Turkey

³Dicle University, Science Faculty, Department of Chemistry, 21280-Diyarbakır, Turkey

⁴Dicle University, Science Faculty, Department of Chemistry, 21280-Diyarbakır, Turkey

⁵Dicle University, Science Faculty, Department of Chemistry, 21280-Diyarbakır, Turkey

*Corresponding author: duyguelma@siirt.edu.tr

Abstract: In this study, reactions of $(PPh_2)_2NCH_2CH_2N(PPh_2)_2$ (**L**₁) and $\{(PPh_2)_2NCH_2CH_2\}_3N$ (**L**₂) with $[Ru^{II}(acac)_2(CH_3CN)_2]$ led to the production of new dinuclear complex $[Ru(acac)_2]_2(L_1)$ (**1**) and trinuclear complex $[Ru(acac)_2]_3(L_2)$ (**2**). Complex 1 and 2 are excellent candidates for the role of catalyst precursors in the transfer hydrogenation (TH) of acetophenone and its derivatives. Compared to complex (**1**), the trinuclear complex (**2**) is an exceptional catalyst, producing the corresponding alcohols in 98–99% yields in 20 minutes at 80 °C ($TOF \leq 300 h^{-1}$) for the TH process. A comparison of the catalytic properties of the complexes is also briefly discussed. Complex structures have also been characterized by combining nuclear magnetic resonance (NMR), Fourier Transform Infrared (FT-IR), and elemental analysis.

Keywords: Transfer Hydrogenation; Ruthenium Complex; Aminophosphine; Homogeneous Catalysis.

Received: September 26, 2022

Accepted: December 31, 2022

1. Introduction

One of the most crucial processes for creating high-value alcohols for academic research and commercial uses, notably in organic synthesis and the pharmaceutical sector, is TH catalysis. Catalytic TH is a valuable alternative approach for catalytic hydrogenation by molecular hydrogen. This method involves catalytic hydrogenation being carried out with the assistance of a stable hydrogen donor. The TH technique, in which formic acid and its salts or secondary alcohols have been utilized as hydrogen sources, is more desirable and safer than the direct hydrogenation method[1-4]. The catalytic transfer hydrogenation process results in the generation of minimal by-products eliminates the use of potentially dangerous chemicals and makes use of easily accessible and nonhazardous starting ingredients such as carbonyl compounds[2, 5]. The transfer hydrogenation process, which began with the use of main-group metals such as aluminum, has given way to complexes including transition metals such as ruthenium, rhodium, and iridium[6, 7].

The synthesis and coordination chemistry of bis(phosphino)amines $RN(PR_2)_2$ have gained much interest in recent years because of their varied donor-acceptor characteristics when a substituent is added to the ligand backbone[8-11]. The use of preparative pathways gives access to several structural alterations via the production of a straightforward P-N bond[12, 13]. P-N-P skeletons are more versatile

than P-C-P skeletons, and tiny modifications in substituents result in dramatic alterations in the P-N-P angle and structure around the whole P-centers[14-16]. As a result, by modifying the substituents, their coordination characteristics and structural features may be drastically altered. This property permits the synthesis of an extensive variety of novel transition metal complexes[17-19]. The synthesis of extremely effective transition metal-based catalysts derived from aminophosphines, which can be used in several catalytic processes, including the TH reaction, has lately attracted more attention[20].

In this study, new binuclear complex (**1**) and trinuclear complex (**2**) were obtained as a result of the reaction of $(\text{PPh}_2)_2\text{NCH}_2\text{CH}_2\text{N}(\text{PPh}_2)_2$ (**L**₁) and $\{(\text{PPh}_2)_2\text{NCH}_2\text{CH}_2\}_3\text{N}$ (**L**₂) aminophosphine ligands with $[\text{Ru}^{\text{II}}(\text{acac})_2(\text{CH}_3\text{CN})_2]$. The structures of the (**1**) and (**2**) complexes were characterized by ³¹P, ¹H NMR, ¹³C NMR, and FT-IR. Then, the applications of (**1**) and (**2**) complexes as catalysts in the TH of acetophenone derivatives to their respective 1-phenylethanol derivatives using isopropanol as a hydrogen source were investigated.

2. Materials and Methods

2.1. Materials

$\text{Ru}(\text{acac})_3$, Ethylenediamine, Tris(2-aminoethyl) amine, PPh_2Cl and Et_3N were purchased from Sigma-Aldrich. $[\text{Ru}^{\text{II}}(\text{acac})_2(\text{CH}_3\text{CN})_2]$ [21], N,N,N',N'-Tetrakis(diphenylphosphino)ethylenediamine $(\text{PPh}_2)_2\text{NCH}_2\text{CH}_2\text{N}(\text{PPh}_2)_2$ (**L**₁)[22, 23] and Tris[2-(N,N-bis(diphenylphosphino)aminoethyl)amine] $\{(\text{PPh}_2)_2\text{NCH}_2\text{CH}_2\}_3\text{N}$ (**L**₂) [24] were synthesized according to the literature procedures. Since the substances used in all reactions are sensitive to air and humidity, the glass materials and solvents were dried and the reactions were carried out using the standard Schlenk technique in a high-purity argon or nitrogen atmosphere. The solvents used (THF, diethyl ether, toluene, etc.) were dried by distillation with sodium-benzophenone, dichloromethane with di-phosphorus pentoxide, and 2-propanol with calcium hydride (CaH_2). Triethylamine is distilled with CaH_2 and dried with metallic sodium before use. Reaction monitoring of aminophosphine compounds was performed with ³¹P-¹H NMR. All synthesized complexes have their structures elucidated by ¹H (at 400.1 MHz), ¹³C (at 100.6 MHz), and ³¹P-¹H NMR (at 162.0 MHz) as well as elemental analysis. To conduct the GC analyses, a Shimadzu GC 2010 Plus Gas Chromatograph fitted with a capillary column was used.

2.2. The general hydrogen transfer procedure

Below is a sample procedure for TH of ketones: A degassed (5 mL) solution of catalysts (**1** and **2**) (0.005 mmol), potassium hydroxide (0.025 mmol), and corresponding ketone (0.5 mmol) in isopropanol was heated to reflux until the reactions were complete. Then, a specimen was taken from this medium, followed by dilution with acetone, and analyzed immediately by GC. The conversions are calculated depending on the remaining ketone. ¹H NMR spectra of the resulting products were as anticipated.

2.3. Synthesis and characterization of complexes

2.3.1 Preparation of complex (1)

Under a nitrogen atmosphere, 36 mg of $[\text{Ru}^{\text{II}}(\text{acac})_2(\text{CH}_3\text{CN})_2]$ (0.045 mmol), 36 mg of $(\text{PPh}_2)_2\text{NCH}_2\text{CH}_2\text{N}(\text{PPh}_2)_2$ (L_1) (0.045 mmol), and 20 mL of dry toluene were combined in a 100 mL two-neck flask and refluxed at 110 °C for 12 hours. The reaction was terminated after the samples taken at certain intervals during the reaction period were checked with ^{31}P $\{^1\text{H}\}$ NMR and the $(\text{PPh}_2)_2\text{NCH}_2\text{CH}_2\text{N}(\text{PPh}_2)_2$ (L_1) was depleted and the complex formation was observed. At the end of the reaction, the solvent was removed under vacuum until approximately 1-2 mL remained, petroleum ether was added to it and the crude products were precipitated. Next, the product was desiccated after being washed in a (1:1) mixture of diethyl ether-hexane. A dark red solid product was obtained. (yield: 0.05 g, 79 %); ^1H NMR (400.1 MHz, CDCl_3 , ppm) δ : 7.25-7.36 (m, 40 H, $\text{C}_6\text{H}_5\text{P}$), 4.98 (s, 4H, acac- CH), 3.78 (s, 4H, CH_2N), 1.58 (s, 24H, acac- CH_3); ^{13}C NMR (100.6 MHz, CDCl_3 , ppm) δ : 187.30, 185.65 (acac- $\text{C}=\text{O}$), (126.85, 128.65, 128.95, 131.50, 133.24, 138.52 ($-\text{C}_6\text{H}_5\text{P}$); 98.95 (acac- CH), 47.78 (CH_2N), 25.98 (acac- CH_3); ^{31}P - $\{^1\text{H}\}$ NMR (162.0 MHz, CDCl_3 , ppm) δ : 87.02 (s, $\text{NP}(\text{Ph})_2$); IR (KBr pellet cm^{-1}) ν : (P-N-P): 805, (P-Ph): 1438, (C-O) 1574; For element analysis $\text{C}_{70}\text{H}_{76}\text{N}_2\text{P}_4\text{O}_8\text{Ru}_2$ (1399.36gr/mol) calculated: C 60.08, N 2.00, H 5.47; found: C 59.70, N 1.95, H 5.08.

2.3.2 Preparation of complex (2)

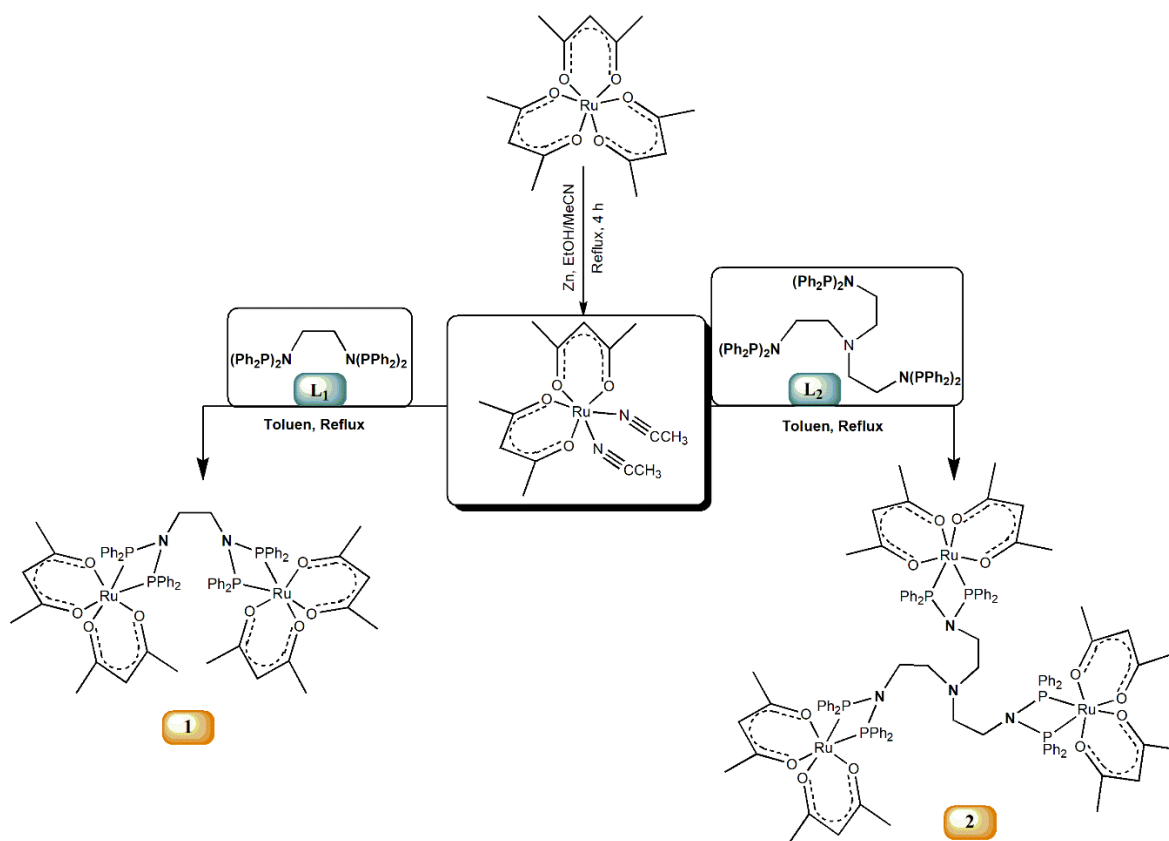
Under a nitrogen atmosphere, 400 mg of $[\text{Ru}^{\text{II}}(\text{acac})_2(\text{CH}_3\text{CN})_2]$ (1.06 mmol), 440 mg of $\{(\text{PPh}_2)_2\text{NCH}_2\text{CH}_2\}_3\text{N}$ (L_2) (0.35 mmol), and 20 mL of dry toluene were combined in a 100 mL two-neck flask and refluxed at 110 °C for 12 hours. The reaction was terminated after the samples taken at certain intervals during the reaction period were checked with ^{31}P $\{^1\text{H}\}$ NMR and the $\{(\text{PPh}_2)_2\text{NCH}_2\text{CH}_2\}_3\text{N}$ (L_2) ligand was depleted and the complex formation was observed. At the end of the reaction, the solvent was removed under vacuum until approximately 1-2 mL remained, petroleum ether was added to it, and the crude products were precipitated. Next, the product was desiccated after being washed in a (1:1) mixture of diethyl ether-hexane. A dark red solid product was obtained. (yield: 0.65 g, 86 %); ^1H NMR (400.1 MHz, CDCl_3 , ppm) δ : 7.94- 6.94 (m, 60H, $-\text{C}_6\text{H}_5\text{P}$), 4.81 (s, 6H, acac- CH), 5.22-5.53 (m, 12H, NCH_2-), 1.83 (s, 18H, acac- CH_3) 1.44 (s, 18H, acac- CH_3); ^{13}C NMR (100.6 MHz, CDCl_3 , ppm) δ : 186.29, 185.07 (acac- $\text{C}=\text{O}$), 134.32, 131.64, 130.71, 127.82 (aromatik karbonlar), 98.62 (acac- CH), 54.3 (NCH_2-), 53.48 (NCH_2-), 27.84 (acac- CH_3), 27.72 (acac- CH_3); ^{31}P - $\{^1\text{H}\}$ NMR (162.0 MHz, CDCl_3 , ppm) δ : 88.43 (s, $\text{NP}(\text{Ph})_2$); IR (KBr pellet cm^{-1}) ν : (P-N-P): 843, (P-Ph): 1435, (C-O) 1575; For element analysis $\text{C}_{108}\text{H}_{120}\text{N}_4\text{P}_6\text{O}_{12}\text{Ru}_3$ (2153.9 gr/mol) calculated: C 60.22, N 2.60, H 5.62; found: % C 59.78, N 2.45, H 5.36.

3. Results and Discussion

3.1. Synthesis and characterization of complex 1 and 2

For the manufacture of phosphinoamines and bis(phosphino)amines, many different methods have been established, however, aminolysis seems to be the one that is used the most often. The synthesis as well as the characterisation of the ligands (L_1) and (L_2) were discussed elsewhere[22, 24]. The coordination chemistry of these aminophosphines with $[\text{Ru}^{\text{II}}(\text{acac})_2(\text{CH}_3\text{CN})_2]$ precursor was investigated. Crystalline dark red powders (1) and (2) were obtained by reacting (L_1) and (L_2) with $[\text{Ru}^{\text{II}}(\text{acac})_2(\text{CH}_3\text{CN})_2]$ in molar ratios of 1:2 and 1:3, respectively, at room temperature for 1 hour

(Scheme 1). Singlet peaks at 61.33 and 62.20 ppm in the ^{31}P - $\{^1\text{H}\}$ NMR spectra of aminophosphine L_1 and L_2 ligands, respectively, show that the ligands were successfully separated by giving rise to singlets at 87.20 and 88.43 ppm in the formation of complexes **1** and **2**, as shown in Figure 1. In addition, when the ^1H and ^{13}C -NMR spectra of complexes are examined, the disappearance of the CH_3CN -peak of 2.49 ppm in ^1H -NMR and 27.66 ppm in ^{13}C -NMR of $[\text{Ru}^{\text{II}}(\text{acac})_2(\text{CH}_3\text{CN})_2]$ indicates that the structure was formed. In their ^1H -NMR spectra, compounds **1** and **2** are characterized by CH resonances of *acac* at $\delta \sim 4.90$ ppm, whereas in the ^{13}C - $\{^1\text{H}\}$ NMR spectra, resonance at $\delta \sim 98$ ppm correspond to CH resonances of *acac*. ^1H -NMR spectra of compounds **1** and **2** display the anticipated multiplets at ~ 8.00 - 7.00 ppm for protons of phenyls. Furthermore, other ^1H and ^{13}C -NMR data are in agreement with the proposed structures (for details see Experiment Section). The infrared spectrum of **1** and **2** exhibits the bands at 1574 and 1438 cm^{-1} due to $\nu(\text{C-O})$ and $\nu(\text{P-Ph})$, respectively[25]. Characterization of the complexes by infrared spectroscopy and elemental analysis revealed values that were in excellent accord with theoretical.



Scheme 1. Synthesis of complex **(1)** and **(2)**.

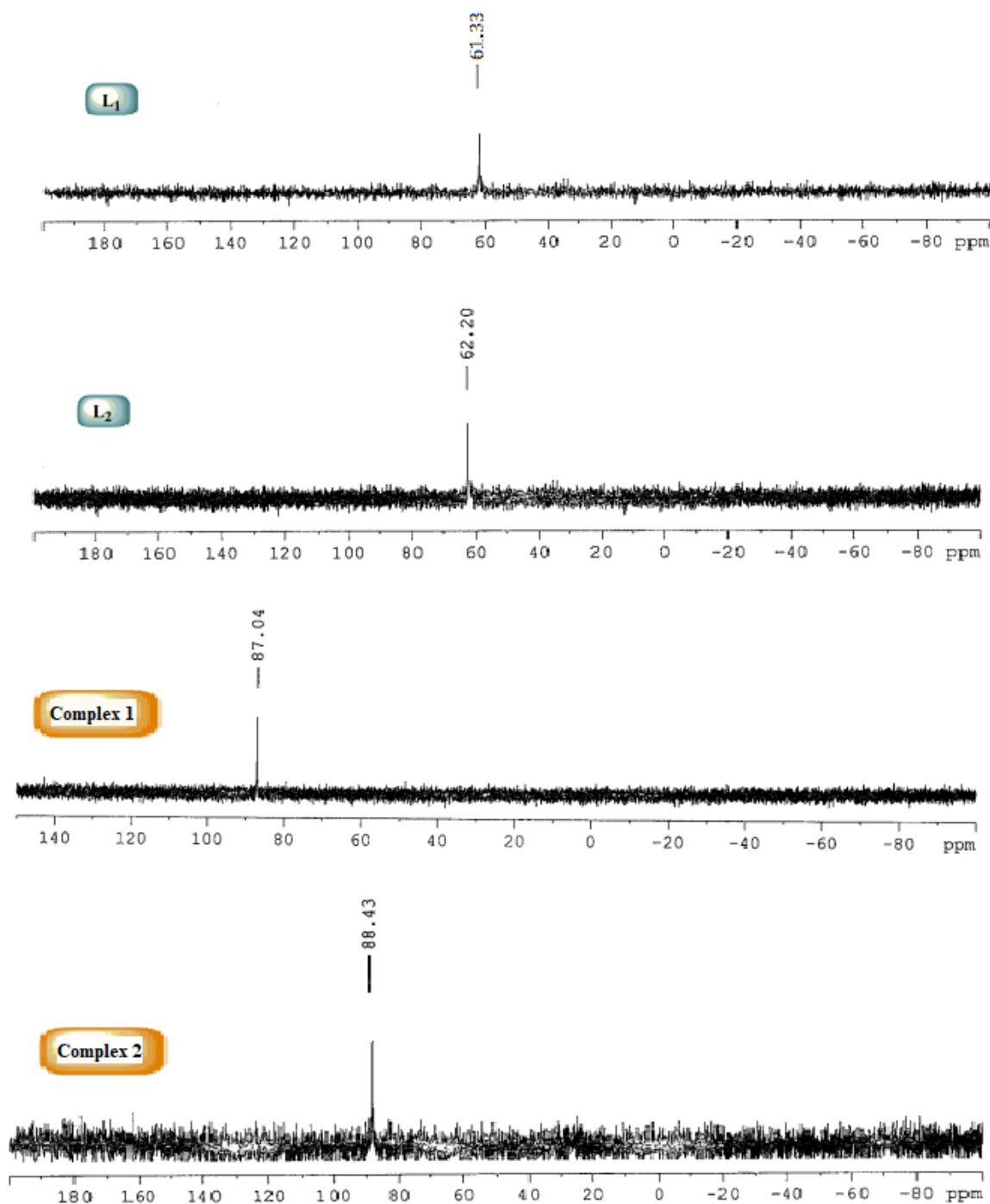


Figure 1. The $^{31}\text{P}\{-^1\text{H}\}$ NMR spectra of ligands (L1 and L2) and complexes (1 and 2).

3.2. Transfer hydrogenation studies

After complexes **1** and **2** had been well described, we examined their catalytic potential as a catalyst in the TH reaction that converts ketones to alcohols using the standard heating method. When selecting the beginning conditions, we took into account any past reports. Initially, acetophenone was hydrogenated in isopropanol with KOH as the base in the presence of a catalyst. Isopropanol is employed as a hydrogen source in the TH, and under these conditions, the process is governed by thermodynamics: when isopropanol releases hydrogen, acetone develops, and acetone may act as a hydrogen acceptor, so

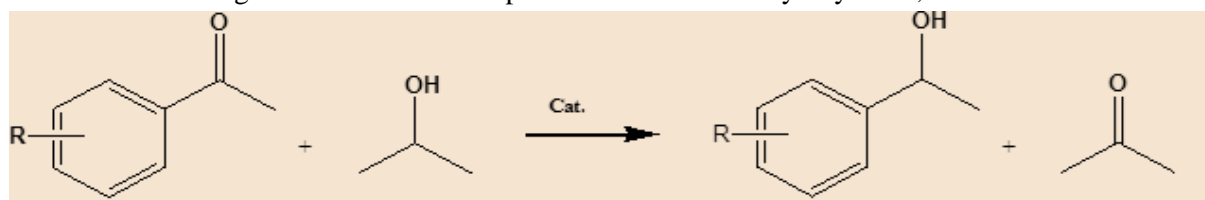
equilibrium is achieved. Due to the fact that the boiling point of 2-propanol is only 82 °C, the procedure may be successfully carried out at reflux temperature as well[26, 27]. The outcomes of the transfer hydrogenation are listed in Table 1. In Table 1, entries 2 and 6 clearly demonstrated that the procedure is impossible without a base. Consequently, it follows that a base is required for this reaction. In most cases, the quantity of base is approximately 5 equivalents with regard to the catalyst[28-30]. Therefore, complexes **1** and **2** are effective catalysts in the TH reaction of acetophenone when isopropanol is employed as a hydrogen donor at 82 °C, in the presence of a base, and after a specified amount of time (1 hour and 1/3 hour for complexes **1** and **2**, respectively) (Table 1 entry 1, entry 5). Accordingly, complex **2** effectively converts acetophenone to 1-phenyl-ethanol in high yields, as shown by GC monitoring of the reaction, which revealed a TOF of 294 h⁻¹ (Table 2, entry 5). The conversion of complex **1** was likewise satisfactory, with TOF values of 97 h⁻¹ (Table 2, entry 1). In addition, an increase in substrate quantity causes an increase in the reaction time, which in turn results in a decrease in TOF (Table 1 entries 3-4, entries 7-8).

Table 1. TH of acetophenone with isopropanol catalyzed by **1** and **2**.

Entry	Catalyst	S/C/KOH	Time	Conversion(%) ^[e]	TOF(h ⁻¹) ^[f]
1	1 ^[a]	100:1:5	1 h	97	97
2	1 ^[b]	100:1	24 h
3	1 ^[c]	500:1:5	6 h	92	15
4	1 ^[d]	1000:1:5	15 h	98	7
5	2 ^[a]	100:1:5	1/3 h	98	294
6	2 ^[b]	100:1	24 h
7	2 ^[c]	500:1:5	2 h	97	49
8	2 ^[d]	1000:1:5	5 h	95	19
9	[Ru(acac) ₃](CH ₃ CN) ₂	100:2:5	7 h	98	14

Reaction conditions:
^[a] Refluxing in 2-propanol; acetophenone/Ru/KOH, (100:1:5); ^[b] Refluxing in 2-propanol; acetophenone/Ru, in the absence of base; ^[c] Refluxing in 2-propanol; acetophenone/Ru/KOH, (500:1:5); ^[d] Refluxing in 2-propanol; acetophenone/Ru/KOH, (1000:1:5); ^[e] Determined by GC (three independent catalytic experiments); ^[f] Referred at the reaction time indicated in column; TOF= (mol product/mol Ru(II)Cat.)x h⁻¹.

In this TH reaction, the catalytic effects of acetophenone derivatives were investigated under the optimal circumstances that could be identified. When utilizing an acetophenone derivative containing an electron-withdrawing moiety, such as F, Cl, Br, or NO₂, the corresponding alcohol is found to form in a shorter amount of time (Table 2, entry 1-6, entry 9-14). Due to the fact that electron-withdrawing groups diminish the electron density of the ketone's C=O bond, the ketone is more readily hydrogenated[31, 32]. Second, the reaction time for TH of acetophenone derivatives containing o- and p-OCH₃ groups is longer, and the TOF values are lower. Also, it was seen that the TOF value is lower when there is an electron-donating substituent on the o-position (-OCH₃) than on the p-position. In fact, when 4-MeO was used in place of 2-MeO catalyzed by **2**, the reaction duration decreased from 3 h to 2 h (Table 2, entries 15-16).

Table 2. TH findings for substituted acetophenones with the catalyst systems, **1** and **2**.^[a]

Entry	R	Time	Conversion(%) ^[b]	TOF(h ⁻¹) ^[c]
Cat. 1				
1	2-F	1/2 h	99	198
2	4-F	1/3 h	98	294
3	4-Cl	1/3 h	94	282
4	2-Br	3/4 h	96	77
5	4-Br	1/3 h	97	194
6	4-NO ₂	1/2 h	95	190
7	2-MeO	4 h	98	25
8	4-MeO	3 h	99	33
Cat. 2				
9	2-F	1/4 h	98	392
10	4-F	1/6 h	99	594
11	4-Cl	1/4 h	95	380
12	2-Br	1/3 h	98	294
13	4-Br	1/4 h	94	376
14	4-NO ₂	1/4 h	96	384
15	2-MeO	3 h	95	32
16	4-MeO	2 h	98	49

^[a] Catalyst (0.0025 mmol), substrate (0.5 mmol), 2-propanol(5 mL), KOH (0.025 mmol %), 82 °C, the concentration of acetophenone derivatives is 0.1 M; ^[b]Purity of compounds is checked by ¹H NMR and GC (three independent catalytic experiments), yields are based on methyl aryl ketone; ^[c] TOF = (mol product/mol Cat.)xh⁻¹.

4. Conclusions

This study reports the synthesis of a novel series of Ru(II)(acac) compounds based on aminophosphine using amine precursors. The obtained results demonstrate that complexes **1** and **2** are effective catalysts for the TH reaction of aromatic ketones, indicating that desired alcohols can be produced in high yield. Trinuclear complex Catalyst **2** showed better catalytic activity for TH than dinuclear catalyst **1**. These catalysts are attractive because of their modular design and versatility in terms of transfer hydrogenation, and future reports will focus on the use of the complexes that we have synthesized in TH of other activated aryl and alkyl ketones.

Acknowledgment

Financial support from Siirt University Research Fund (Project number: 2017-SIULAB-48) is gratefully acknowledged.

Authors' Contributions:

D.E.K.: Investigation, Conceptualization, Methodology, Resources, Writing (30 %)

U. I: Conceptualization, Writing - Original draft preparation (15 %)

M. A: Conceptualization, Formal analysis - Original draft preparation (15 %)

F.D: Methodology, Conceptualization, supervision, and review. (25 %)

A.B.: Supervision and Review. (15 %)

All authors read and approved the final manuscript.

Conflict of Interest

The author declares no conflict of interest.

Compliance with Research and Publication Ethics

This work was carried out by obeying research and ethics rules.

The Declaration of Ethics Committee Approval

The authors declare that this document does not require ethics committee approval or any special permission. Our study does not cause any harm to the environment.

References

- [1] Aydemir M, Baysal A, Turgut Y., "Applications of transition metal complexes containing aminophosphine ligand to transfer hydrogenation of ketones", *Applied Organometallic Chemistry*, 25, 270-5, 2011.
- [2] Li F, France LJ, Cai Z, Li Y, Liu S, Lou H, et al., "Catalytic transfer hydrogenation of butyl levulinate to γ -valerolactone over zirconium phosphates with adjustable Lewis and Brønsted acid sites", *Applied Catalysis B: Environmental*, 214, 67-77, 2017.
- [3] Wang D, Astruc D., "The golden age of transfer hydrogenation", *Chemical reviews*, 115, 6621-86, 2015.
- [4] Gilkey MJ, Vlachos DG, Xu B., "Poisoning of Ru/C by homogeneous Brønsted acids in hydrodeoxygenation of 2, 5-dimethylfuran via catalytic transfer hydrogenation", *Applied Catalysis A: General*, 542, 327-35, 2017.
- [5] Gnanamgari D, Sauer EL, Schley ND, Butler C, Incarvito CD, Crabtree RH., "Iridium and ruthenium complexes with chelating N-heterocyclic carbenes: efficient catalysts for transfer hydrogenation, β -alkylation of alcohols, and N-alkylation of amines", *Organometallics*, 28, 321-5, 2009.
- [6] Yiğit M, Yiğit B, Özdemir İ, Çetinkaya E, Çetinkaya B., "Active ruthenium-(N-heterocyclic carbene) complexes for hydrogenation of ketones", *Applied organometallic chemistry*, 20, 322-7, 2006.
- [7] Elma D, Durap F, Aydemir M, Baysal A, Meric N, Ak B, et al., "Screening of C2-symmetric chiral phosphinites as ligands for ruthenium (II)-catalyzed asymmetric transfer hydrogenation of prochiral aromatic ketones", *Journal of Organometallic Chemistry*, 729, 46-52, 2013.
- [8] Chang Y-C, Hu C-Y, Liang Y-H, Hong F-E., "Computational and 31P NMR studies of moisture-metastable cyclic diamino-phosphine oxide preligands", *Polyhedron*, 105, 123-36, 2016.
- [9] Gholivand K, Kahnouji M, Maghsoud Y, Hosseini M, Roe SM., "Synthesis, structure, computational and catalytic activities of palladium complexes containing hydrazide based amino-phosphine ligands", *Journal of Organometallic Chemistry*, 880, 281-92, 2019.
- [10] Biricik N, Durap F, Gümgüm B, Fei Z, Scopelliti R., "Synthesis and reactivity of N, N-bis (diphenylphosphino) dimethylaniline compounds", *Transition Metal Chemistry*, 32, 877-83, 2007.
- [11] Aydemir M, Baysal A, Durap F, Gümgüm B, Özkar S, Yıldırım LT., "Synthesis and characterization of transition metal complexes of thiophene-2-methylamine: X-ray crystal

- structure of palladium (II) and platinum (II) complexes and use of palladium (II) complexes as pre-catalyst in Heck and Suzuki cross-coupling reactions", *Applied Organometallic Chemistry*, 23, 467-75, 2009.
- [12] Kaur N., "Copper catalysts in the synthesis of five-membered N-polyheterocycles", *Current Organic Synthesis*, 15, 940-71, 2018.
- [13] Sushev VV, Kornev AN, Min'ko YA, Belina NV, Kurskiy YA, Kuznetsova OV, et al., "Rearrangement of phosphinohydrazide ligand-NPh-N (PPh₂)₂ in transition metal coordination sphere: Synthesis and characterization of nickel and cobalt spirocyclic complexes M (NPh-PPh₂N-PPh₂)₂ and their properties", *Journal of organometallic chemistry*, 691, 879-89, 2006.
- [14] Fedotova YV, Kornev AN, Sushev VV, Kurskiy YA, Mushtina TG, Makarenko NP, et al., "Phosphinohydrazines and phosphinohydrazides M (-N (R)-N (R)-PPh₂)_n of some transition and main group metals: synthesis and characterization: Rearrangement of Ph₂P-NR-NR-ligands into aminoiminophosphorane, RNPh₂-NR-, and related chemistry", *Journal of organometallic chemistry*, 689, 3060-74, 2004.
- [15] Sarcher C, Lebedkin S, Kappes MM, Fuhr O, Roesky PW., "Bi- and tetrametallic complexes of the noble metals with PNP-ligands", *Journal of Organometallic Chemistry*, 751, 343-50, 2014.
- [16] Naktode K, Kottalanka RK, Adimulam H, Panda TK., "Tetra-nuclear copper complex having P-N-P ligand to P-O-P ligand-synthesis, structural, and mechanistic studies", *Journal of Coordination Chemistry*, 67, 3042-53, 2014.
- [17] Kama DV, Brink A, Visser HG., "Crystal structure of bis (μ₂-chlorido)-bis (di-p-tolylhydroxyphosphine-κP)-bis (di-p-tolylphosphite-κP) dipalladium (II), C₅₆H₅₈Cl₂O₄P₄Pd₂", *Zeitschrift für Kristallographie-New Crystal Structures*, 231, 1081-3, 2016.
- [18] Kornev AN, Sushev VV, Panova YS, Belina NV, Lukoyanova OV, Fukin GK, et al., "The Intramolecular Rearrangement of Phosphinohydrazides [R' 2P-NR-NR-M]→[RN □ PR' 2-NR-M]: General Rules and Exceptions. Transformations of Bulky Phosphinohydrazines (R-NH-N (PPh₂)₂, R= t Bu, Ph₂P)", *Inorganic Chemistry*, 51, 874-81, 2012.
- [19] Ok F, Aydemir M, Durap F, Baysal A., "Novel half-sandwich η⁵-Cp*-rhodium (III) and η⁵-Cp*-ruthenium (II) complexes bearing bis (phosphino) amine ligands and their use in the transfer hydrogenation of aromatic ketones", *Applied Organometallic Chemistry*, 28, 38-43, 2014.
- [20] Oomura K-i, Ooyama D, Satoh Y, Nagao N, Nagao H, Howell FS, et al., "Redox behavior of a binuclear ruthenium complex having a di-μ-nitrosyl ligand, [Ru (acac)₂ (μ-NO)₂](acac= acetylacetonato)", *Inorganica chimica acta*, 269, 342-6, 1998.
- [21] Akba O, Durap F, Aydemir M, Baysal A, Gümgüm B, Özkar S., "Synthesis and characterizations of N, N, N', N'-tetrakis (diphenylphosphino) ethylenediamine derivatives: Use of palladium (II) complex as pre-catalyst in Suzuki coupling and Heck reactions", *Journal of Organometallic Chemistry*, 694, 731-6, 2009.
- [22] Gümgüm B, Akba O, Durap F, Yıldırım LT, Ülkü D, Özkar S., "Synthesis, characterization, crystal and molecular structure of diphenyloxophosphinoethylenediamines", *Polyhedron*, 25, 3133-7, 2006.
- [23] Aydemir M, Baysal A, Gümgüm B., "Synthesis and characterization of tris {2-(N, N-bis (diphenylphosphino) aminoethyl) amine derivatives: Application of a palladium (II) complex as a

- pre-catalyst in the Heck and Suzuki cross-coupling reactions", *Journal of Organometallic Chemistry*, 693, 3810-4, 2008.
- [24] Tokgun O, Karakas DE, Tan S, Karagür ER, İnal B, Akca H, et al., "Novel ruthenium and palladium complexes as potential anticancer molecules on SCLC and NSCLC cell lines", *Chemical Papers*, 74, 2883-92, 2020.
- [25] Mannu A, Grabulosa A, Baldino S., "Transfer Hydrogenation from 2-propanol to Acetophenone Catalyzed by [RuCl₂ (η⁶-arene) P](P= monophosphine) and [Rh (PP) 2] X (PP= diphosphine, X= Cl⁻, BF₄⁻) Complexes", *Catalysts*, 10, 162, 2020.
- [26] Ak B, Elma D, Meriç N, Kayan C, Işık U, Aydemir M, et al., "New chiral ruthenium (II)–phosphinite complexes containing a ferrocenyl group in enantioselective transfer hydrogenations of aromatic ketones", *Tetrahedron: Asymmetry*, 24, 1257-64, 2013.
- [27] Kayan C, Meriç N, Rafikova K, Zazybin A, Gürbüz N, Karakaplan M, et al., "A new class of well-defined ruthenium catalysts for enantioselective transfer hydrogenation of various ketones", *Journal of Organometallic Chemistry*, 869, 37-47, 2018.
- [28] Ak B, Aydemir M, Durap F, Meriç N, Elma D, Baysal A., "Highly efficient iridium catalysts based on C₂-symmetric ferrocenyl phosphinite ligands for asymmetric transfer hydrogenations of aromatic ketones", *Tetrahedron: Asymmetry*, 26, 1307-13, 2015.
- [29] Uğur I, Meriç N, Aydemir M., "Novel Mononuclear Metal-Phosphinite Compounds And Catalytic Performance In Transfer Hydrogenation Of Ketones", *Middle East Journal of Science*, 8, 1-15, 2022.
- [30] Faller J, Lavoie AR., "Catalysts for the asymmetric transfer hydrogenation of ketones derived from L-prolinamide and (p-cymeneRuCl₂)₂ or (Cp* RhCl₂)₂", *Organometallics*, 20, 5245-7, 2001.
- [31] Ödemir I, Yaşar S, Çetinkaya B., "Ruthenium (II) N-heterocyclic carbene complexes in the transfer hydrogenation of ketones", *Transition metal chemistry*, 30, 831-5, 2005.



Review

HIROTA METHOD AND SOLITON SOLUTIONS**Barış YAPIŞKAN** 

Mimar Sinan Fine Arts University Department of Science and Letters, Istanbul, Turkey

Corresponding Author: baris.yapiskan@msgsu.edu.tr

Abstract: Solitons are an important class of solutions to nonlinear differential equations which appear in different areas of physics and applied mathematics. **In this study, we provide** a general overview of the Hirota method which is one of the most powerful tools in finding the multi-soliton solutions of nonlinear wave and evaluation equations. Bright and dark soliton solutions of the nonlinear Schrödinger equation are discussed in detail.

Keywords: Nonlinear differential equations, integrable systems, Hirota method, solitons, nonlinear Schrödinger equation.

Received: November 30, 2021

Accepted: August 25, 2022

1. Introduction

Solitons are particular exact solutions of some nonlinear partial differential equations. Although there is no strict definition of solitons or solitary waves, they are characterized mainly by some common features: A solitary wave is a local disturbance or pulse which retains its shape during propagation. A soliton is a solitary wave that preserves its shape and velocity after interacting with other solitary waves. They are only affected by a phase shift after interactions and in this sense, they behave like particles. There are many nonlinear integrable differential equations that have soliton solutions such as the Korteweg-de Vries (KdV) equation, Boussinesq equation, nonlinear Schrödinger equation, sine-Gordon equation, et cetera.

Soliton theory begins with a phenomenon that the Scottish engineer J. Scott Russell observed by chance. Russell detected that a body of water set in motion by a canal boat, travels a long distance along the canal maintaining its shape and speed. As a result of later experiments done on this observation, he empirically derived a relation between the speed and the amplitude of the wave: $c^2 = g(h + a)$, where c is the speed, a is the maximum amplitude, h is the depth of the water and g is the acceleration due to gravity. This equation implies that the speed of the wave is related to its amplitude and a larger wave moves faster than a small one. Russell's work [1] triggered many debates on the subject, many of which were critical of his results. In the 1870s both Boussinesq [2] and Rayleigh [3] independently obtained similar results, which confirm Russell. They also showed that these long water waves have a $sech^2$ wave profile. Whereas the differential equation which is satisfied by this function remained unknown for about two more decades. Thus, the explanation of the phenomenon observed by Russell remained unsolved for more than 60 years. Finally, in 1895, a mathematical model proposed by Korteweg and de Vries achieved this task. This model is known as the KdV equation [4] and has been studied extensively in every aspect ever since. In its standard form, the equation is given by

$$u_t + \alpha uu_x + \beta u_{xxx} = 0. \quad (1)$$

Here the constants α and β are arbitrary and can be set to any values by scaling transformations of u , x , and t . The conventional choice is given by $\alpha = 6$ and $\beta = 1$. This is one of the most important equations in the soliton theory and it is ubiquitous in physics problems, such as water waves, fluid mechanics, and plasma physics. There are two competing terms in this equation as in other nonlinear wave models. These terms ensure the coherence of the wave so that, it maintains the waveform and continues to propagate over a long period of time. The last linear term in the equation is the origin of the dispersion observed. On the other hand, the second term is a nonlinear term, and it steepens the wave and finally causes disintegration. When these competing effects are balanced, a stable waveform is formed.

The modern era of solitary waves began in 1955 with the studies of Fermi, Pasta, and Ulam (FPU) on a numerical model of a discrete nonlinear mass-spring system [5]. They tried to show that a smooth initial state would eventually relax to an equipartition of energy among all modes because of nonlinearity. Contrary to the expectations, results showed that the equipartition of energy among the modes did not occur. They put all the energy in a few lowest modes of the corresponding linear model at the beginning. In the linear problem, the energy in each mode would stay unchanged and no new mode would be excited. In the nonlinear problem, the energy is transferred from low modes to higher ones, and the expectation was a continuation of this process until the energy is completely distributed over all modes. Whereas, when the model starts to process, the energy is exchanged between various low-order modes, and it eventually returns to the lowest mode again. Hence, in the end, a series of recurring states show up. The next milestone is the work done by Zabusky and Kruskal on FPU results in 1965 [6]. In this study, they tried to understand why the recurrence phenomenon occurs and for this aim, they investigated a continuous model of the nonlinear mass-spring system. In fact, they analyzed the initial value problem of the KdV equation (1) in the form $q_t + 6qq_\xi + \delta^2 q_{\xi\xi\xi} = 0$ with a finite and small δ^2 , i.e., for a weak nonlinear modulational term. What they get when starting with a smooth initial state $q(\xi, 0) \sim \cos(2\pi\xi)$, was summarized as follows: *“Initially the wave steepened in regions where it had a negative slope, a consequence of the dominant effects of nonlinearity over the dispersive term. As the wave steepens, the dispersive effect then becomes significant and balances the nonlinearity. At later times, the solutions develop a series of eight well-defined waves, each like sech^2 functions with the taller waves ever catching up and overtaking the shorter waves. These waves undergo nonlinear interaction according to the KdV equation and then emerge from the interaction without a change of form and amplitude, but with only a small change in their phases. Another surprising fact is that the initial profile reappears very similarly to the FPU recurrence phenomenon”* [6]. All these strange phenomena led the researchers to think that there are some conservation laws that operate in the background and somehow the KdV equation is integrable. After that, several conserved quantities were calculated by Zabusky-Kruskal, Whitham, and Miura. Miura also found one of the last pieces of the puzzle by introducing the famous Miura transformation [7]. He proved that another important integrable nonlinear differential equation, which is called the modified KdV (mKdV) equation, also has an infinite number of conserved quantities. Moreover, all these conserved quantities can be related to the corresponding counterparts in the KdV equation via the Miura transformation. The next step toward the integrability of the equation was the construction of an inverse scattering transformation method. Consequently, the complete integrability of the KdV equation was shown in a series of papers by Gardner et al. [8-10] and Zakharov and Faddeev [11].

Ryogo Hirota introduced another powerful method to find the exact solutions of the KdV equation [12,13] in 1971. Hirota's method is the most suitable method for obtaining multi-soliton solutions of nonlinear differential equations. Soliton solutions can also be studied by using other methods like inverse scattering transformation, Bäcklund transformation, Darboux transformation, or Painlevé expansion method. Especially, the inverse scattering method is a very powerful technique to obtain exact

solutions to nonlinear equations; nevertheless, its application to practical problems requires a bit of cumbersome work. On the other hand, Hirota's method is much more manageable in this sense. After all these great achievements, soliton solutions of many nonlinear differential equations in 1-dimension, as well as higher dimensions, were studied extensively by using various methods [14-19].

In this study, we introduce the Hirota direct method to obtain the multi-soliton solutions of various differential equations. The plan of the paper is as follows. We will review the method in detail in the second section. In that section, the method is explained on a well-known example, the KdV equation. The soliton solutions up to the third order are constructed explicitly and then solutions are generalized to the N-soliton case. The third section is devoted to the nonlinear Schrödinger equation where focusing and defocusing nonlinear Schrödinger equations are presented. The soliton solutions of these equations are called bright and dark solitons respectively. Both, bright and dark soliton solutions of focusing and defocusing nonlinear Schrödinger equations, up to the two-solitons are calculated by the Hirota direct method. The fourth section includes a conclusion and discussions.

2. Hirota Direct Method

In this section, we will discuss the Hirota direct method to find the N-soliton solutions of any integrable nonlinear differential equation by following [13]. We will explain the method by reviewing its application to the KdV equation, which is also important for historical reasons in the sense that, it is the first introduced equation for explaining the previously observed solitary wave phenomenon. Having equipped with these tools our next goal will be to handle the nonlinear Schrodinger equation.

Multi-soliton solutions can be obtained by the inverse scattering transform [8-11], the dressing method [20-23] and the Hirota method [13]. The Hirota method is algebraic rather than analytic which can be treated as one of its advantages. The Hirota direct method also called bilinear method was first proposed by Hirota to obtain the N-soliton solutions of the KdV equation [12]. It is an efficient method for searching soliton solutions of the nonlinear evolution equations.

First, we will introduce the Hirota differential operator (from now on we will use D-operator in short) and then show how a nonlinear differential equation can be brought into the Hirota bilinear form by using those operators. The D-operator is a bilinear operator which acts on a pair of functions to produce a new function. We will work in 2-dimensional spacetime (t, x) , but definitions can be extended to higher dimensions.

The Hirota D-operator is given by

$$D_{x_i}^m = \left(\frac{\partial}{\partial x_i} - \frac{\partial}{\partial x_i'} \right)^m, \quad x_i = (t, x) \quad (2)$$

where m is a positive integer. It acts as a product of a pair of functions:

$$D_{x_i}^m(f \cdot g) = \left(\frac{\partial}{\partial x_i} - \frac{\partial}{\partial x_i'} \right)^m f(x, t) \cdot g(x', t')|_{x'=x, t'=t} \quad (3)$$

In what follows, we give some properties of the D-operator for later convenience. Equation (3) can be written for $x_i = x$ more explicitly as:

$$D_x^m(f \cdot g) = \sum_{k=0}^m (-1)^k \binom{m}{k} f_k g_{(m-k)}, \quad (4)$$

where f_k stands for $f_k \equiv \partial_x^k f$ and $\binom{m}{k}$ is the binomial coefficient. The anti-symmetrization property of the D-operator with respect to the second function is

$$D_{x_i}^m(g \cdot f) = (-1)^m D_{x_i}^m(f \cdot g). \quad (5)$$

Because of these properties, if we take the first or second function as a constant function, for example, if $g = 1$, we get

$$D_{x_i}^m(f \cdot 1) = \partial_{x_i}^m f. \quad (6)$$

On the other hand, if we take $f = g$ we then obtain

$$D_{x_i}^m(f \cdot f) = 0, \text{ if } m = \text{odd} \quad (7)$$

and for even m , the first few equations are

$$\begin{aligned} m = 2: \quad & D_{x_i}^2(f \cdot f) = 2(ff_{x_i x_i} - f_{x_i}^2), \\ & D_x D_t(f \cdot f) = 2(ff_{xt} - f_x f_t), \\ m = 4: \quad & D_{x_i}^4(f \cdot f) = 2(ff_{x_i x_i x_i x_i} - 4f_{x_i} f_{x_i x_i x_i} + 3f_{x_i}^2), \\ & \vdots \end{aligned} \quad (8)$$

The following properties are especially useful for studying soliton solutions. Using the definition $\phi_i = k_i x + \omega_i t + \alpha_i$, where constant coefficients k_i , ω_i and α_i denote the wave number, angular momentum, and phase factor respectively, then

$$D_x^m D_t^n (e^{\phi_1} \cdot e^{\phi_2}) = (k_1 - k_2)^m (\omega_1 - \omega_2)^n e^{\phi_1 + \phi_2}, \quad (9)$$

and

$$D_{x_i}^m (e^{\phi_1} \cdot e^{\phi_1}) = 0. \quad (10)$$

The second part of the Hirota method includes the transformation of the dependent variable of the equation. The underlying motivation for such a transformation is to express the original equation as a quadratic equation of the dependent variable so that, the leading order derivative and the nonlinear term have the same degree and the same number of derivatives. Mainly three kinds of transformations are commonly used: logarithmic, rational, or arctan transformations. Once the equation is brought into a quadratic form it can be bilinearized via D-operators.

Now, let us assume that a nonlinear differential equation is brought into the Hirota bilinear form by using one of the above transformations of the dependent variable and any combination of D-operators. This bilinear form is expressed by the equation $B(f \cdot f) = 0$ where B denotes a polynomial of D-operators. The N-soliton solution is obtained by taking a perturbative expansion for the function f such that

$$f = 1 + \sum_{i=1}^{\infty} \epsilon^i f_i, \quad (11)$$

where the parameter ϵ is a formal parameter, which can be set equal to 1 after getting all order solutions. When this expansion is plugged into the bilinear equation $B(f \cdot f) = 0$ and then grouped in order of the powers of ϵ one gets the following set of equations:

$$\epsilon^0: B(1 \cdot 1) = 0 \quad (12.0)$$

$$\epsilon^1: B(f_1 \cdot 1 + 1 \cdot f_1) = 0 \quad (12.1)$$

$$\epsilon^2: B(f_2 \cdot 1 + f_1 \cdot f_1 + 1 \cdot f_2) = 0 \quad (12.2)$$

$$\epsilon^3: B(f_3 \cdot 1 + f_2 \cdot f_1 + f_1 \cdot f_2 + 1 \cdot f_3) = 0 \quad (12.3)$$

$$\begin{aligned} & \vdots \\ \epsilon^n: \quad & B \left(\sum_{j=0}^m f_{(m-j)} \cdot f_j \right) = 0. \end{aligned} \quad (12.n)$$

This procedure is quite general and can be applied to any explicit bilinear operator expression. It can be proved that if the original equation admits an N-soliton solution, then the perturbative expansion (11) will truncate at the $n = N$ term, and hence, the convergence problem will be solved automatically.

2.1. KdV equation

In this section we will review the application of the Hirota method for the KdV equation as our first example, obtaining solutions up to 3-solitons explicitly. Then N-soliton solutions are given. In this section, we follow [13]. Let us recall Equation (1) in its standard form

$$u_{xxx} + 6uu_x + u_t = 0 \quad (13)$$

with the boundary condition $u \rightarrow 0$ as $|x| \rightarrow \infty$. To bring this equation into a quadratic form we will apply two successive transformations for the dependent variable u . We define $u = v_x$ and after integrating with respect to x we get the potential KdV equation

$$v_t + 3v_x^2 + v_{xxx} = c(t), \quad (14)$$

where $c(t)$ is an arbitrary function of t and it can be set to 0 after applying boundary conditions $v, v_x, v_t, v_{xx}, v_{xxx} \rightarrow 0$ as $|x| \rightarrow \infty$. Now, if we choose a logarithmic transformation for the new variable such that

$$v(x, t) = 2 \ln (f(x, t))_x \quad (15)$$

and insert this into Equation (14), we find

$$f f_{xxxx} - 4f_x f_{xxx} + 3f_{xx}^2 + f f_{xt} - f_x f_t = 0. \quad (16)$$

As it can be seen from Equation (16), this is a quadratic equation of the dependent variable f and it satisfies the previously mentioned property. Equation (16) can be written in terms of D-operators:

$$(D_x D_t + D_x^4)(f \cdot f) = 0. \quad (17)$$

Hence, the bilinearization operator B can be written as $B \equiv D_x D_t + D_x^4$.

2.2. Soliton solution:

The 1-soliton solution can be obtained by choosing the leading order term in the expansion (11) to contain only one exponential factor, and then solving the set of Equations (12) by orderwise iteration. For this aim, the following ansatz can be used:

$$f_1 = e^{\theta_1} \quad ; \quad \theta_1 = k_1 x + \omega_1 t + \alpha_1 \quad (18)$$

where k_1, ω_1 and α_1 are constants. Since Equation (12.0) is trivial, we start with Equation (12.1):

$$f_{1,xt} + f_{1,xxxx} = 0. \quad (19)$$

Ansatz (18) satisfies Equation (19) provided that the dispersion relation $\omega_1 = -k_1^3$, ($k_1 \neq 0$) is satisfied. Equation (12.2) corresponds to

$$f_{2,xt} + f_{2,xxxx} = -(D_x D_t + D_x^4)(f_1 \cdot f_1) \quad (20)$$

and if we use the results of the previous order here, we see that the right-hand side of Equation (20) vanishes. Hence, we can choose $f_2(x, t) = 0$. Continuing to the next-order equations with these results, one can show that all the next-order solutions can be fixed to zero, $f_i(x, t) = 0$, for $i \geq 2$. Consequently, by setting $\epsilon = 1$ we end up with

$$f = 1 + e^{\theta_1} \quad (21)$$

for the 1-soliton solution. It is an easy task to obtain the original function $u(x, t) = 2(\ln f)_{xx}$ by going backward starting from the result (21)

$$u(x, t) = \frac{k_1^2}{2} \operatorname{sech}^2 \frac{\theta_1}{2}. \quad (22)$$

2.3. Soliton solution:

In a similar way, the 2-soliton solution needs two exponential factors for the leading order term in the expansion of the function f . One can start with the ansatz

$$f_1 = e^{\theta_1} + e^{\theta_2}, \quad (23)$$

where

$$\theta_i = k_i x + \omega_i t + \alpha_i \quad (24)$$

with constant coefficients k_i, ω_i, α_i . Equation (12.1) again gives the relations

$$\omega_i = -k_i^3, \quad (k_i \neq 0), \quad (25)$$

but the right-hand side of Equation (12.2) is not zero anymore and we have

$$f_{2,xt} + f_{2,xxxx} = 3k_1k_2(k_1 - k_2)^2 e^{\theta_1 + \theta_2}. \quad (26)$$

It can be shown that the solution to this equation is given by

$$f_2 = e^{A_{12}} e^{\theta_1 + \theta_2}, \quad (27)$$

with the constant coefficient

$$e^{A_{12}} = \left(\frac{k_1 - k_2}{k_1 + k_2} \right)^2. \quad (28)$$

The next order Equation (12.3) is

$$f_{3,xt} + f_{3,xxxx} = -B(f_1 \cdot f_2 + f_2 \cdot f_1), \quad (29)$$

and the right-hand side of this equation is zero, since $B(f_1 \cdot f_2) = B(f_2 \cdot f_1) = 0$. In that case one can choose $f_3 = 0$ and similarly all higher order terms can be set to zero as well, i.e. $f_i = 0, (i \geq 3)$. Finally, we get

$$f = 1 + e^{\theta_1} + e^{\theta_2} + e^{\theta_1 + \theta_2 + A_{12}}, \quad (30)$$

and hence the 2-soliton solution is given by

$$u(x, t) = -2 \frac{k_1^2 e^{\theta_1} + k_2^2 e^{\theta_2} + (k_1^2 e^{\theta_2} + k_2^2 e^{\theta_1}) e^{\theta_1 + \theta_2 + A_{12}} + 2(k_1 - k_2)^2 e^{\theta_1 + \theta_2}}{(1 + e^{\theta_1} + e^{\theta_2} + e^{\theta_1 + \theta_2 + A_{12}})^2} \quad (31)$$

This result can also be rearranged in terms of hyperbolic trigonometric functions however, for later convenience we keep it in this form. Now, let us continue with the 3-soliton solution.

2.4. Soliton solution and generalization:

The 3-soliton solution goes in a similar way, except that the ansatz for the first term of the expansion (11) has one more exponential factor:

$$f_1 = e^{\theta_1} + e^{\theta_2} + e^{\theta_3} \quad (32)$$

When this form is inserted into Equation (12.1), dispersion Equations (25) are obtained. After a few algebraic calculations, the next-order term in the expansion can be written as

$$f_2 = e^{A_{12}} e^{\theta_1 + \theta_2} + e^{A_{13}} e^{\theta_1 + \theta_3} + e^{A_{23}} e^{\theta_2 + \theta_3} \quad (33)$$

from Equation (12.2). Here, the coefficients are

$$e^{A_{ij}} = \left(\frac{k_i - k_j}{k_i + k_j} \right)^2, \quad i, j = 1, 2, 3 \text{ and } i < j. \quad (34)$$

If we proceed with Equation (12.3), we see that the right-hand side of Equation (29) does not vanish anymore, and the solution to Equation (12.3) can be given by

$$f_3 = e^{A_{123}} e^{\theta_1 + \theta_2 + \theta_3} \quad (35)$$

with the constant coefficient

$$e^{A_{123}} = e^{A_{12}} e^{A_{13}} e^{A_{23}}. \quad (36)$$

The perturbative expansion will cease at this order as stated before. It can be checked that since

$$B(f_1 \cdot f_3 + f_2 \cdot f_2 + f_1 \cdot f_3) = 0 \quad (37)$$

the next order equation (12.4)

$$f_{4,xt} + f_{4,xxxx} = 0 \quad (38)$$

can be solved by setting $f_4 = 0$ indeed. Finally, all following orders can be set to zero in the same fashion. Hence, we reach the 3-soliton solution by setting the expansion parameter $\epsilon = 1$:

$$f = 1 + e^{\theta_1} + e^{\theta_2} + e^{\theta_3} + e^{A_{12}} e^{\theta_1 + \theta_2} + e^{A_{13}} e^{\theta_1 + \theta_3} + e^{A_{23}} e^{\theta_2 + \theta_3} + e^{A_{123}} e^{\theta_1 + \theta_2 + \theta_3}. \quad (39)$$

We see that this solution includes no additional freedom and is totally obtained from the preceding parameters. We will not get into details but, unlike the previous orders, the 3-soliton solution is quite restrictive and closely related to the integrability of the equation. The 3-soliton solution guides us to obtain the N-soliton solution which contains a finite polynomial of exponential factors given below

$$f(x, t) = \sum_{\substack{\mu_i=0,1 \\ 1 \leq i \leq N}} \exp \left(\sum_{1 \leq i < j \leq N} A_{ij} \mu_i \mu_j + \sum_{j=1}^N \mu_j \theta_j \right). \quad (40)$$

Proof of this can be found in [13]. Here, it should be noted that the combination of lower-order solutions in the form given above to get higher-order solutions is possible only for integrable equations. For a detailed discussion see [24], [25]. This is called the Hirota integrability condition. Hirota integrability can be used equivalently instead of the usual integrability because no counterexamples have been found so far.

3. Nonlinear Schrödinger equation

In this section, we will present another important class of nonlinear differential equations, the nonlinear Schrödinger (NLS) equation. The NLS equation is an extension of the well-known linear Schrodinger equation, and it can be defined as an approximation to a wide class of nonlinear wave equations [26] that arise in many branches of physics such as plasma physics, nonlinear optics, and fluid dynamics. The most common applications of the NLS equation include self-focusing of beams in nonlinear optics, modeling of the propagation of electromagnetic pulses in nonlinear optical fibers which act as waveguides, and stability of Stokes waves in water. In hydrodynamics, the NLS equation describes the dynamics of surface gravity waves in finite or infinite depth, depending on the ratio between the water depth and wavelength. It is also shown that the nonlinear modulation of a quasi-monochromatic wave is described by the NLS equation. For a further discussion see [27], [28] and references therein. The integrability of the NLS equation has been shown by Zakharov and Shabat by using the inverse scattering method [20].

In this section, we mainly follow the references [13] and [28]. The derivation of the NLS equation and the related definitions can be found in detail in [28]. Soliton solution technic can be found in [13] and [29].

The NLS equation is given by

$$iq_t + \frac{1}{2}q_{xx} + p|q|^2q = 0, \quad (41)$$

where p is a parameter that takes values $p = \mp 1$. The equation for $p = 1$ is called the focusing NLS (fNLS) equation and it has an N-envelop solution [20, 30]. The case for $p = -1$ is called defocusing NLS (dNLS) equation and it is shown that it has a dark pulse solution [30]. We will keep this parameter undetermined and at the end, possible values of the parameter will be considered separately. Bilinearization of the NLS equation goes as follows: a transformation of the dependent variable is defined as follows

$$q(x, t) = \frac{u(x, t)}{v(x, t)}, \quad (42)$$

where $u(x, t)$ is a complex function and $v(x, t)$ is a real function. Exploiting Equation (42) and D-operators, Equation (41) can be split into two distinct equations:

$$\left(iD_t + \frac{1}{2}D_x^2 \right) (u \cdot v) = 0 \quad (43)$$

and

$$\frac{1}{2}D_x^2(v \cdot v) - p|u|^2 = 0. \quad (44)$$

Now let us expand new functions u and v into series

$$\begin{aligned} u(x, t) &= \epsilon u_1 + \epsilon^2 u_2 + \epsilon^3 u_3 + \dots, \\ v(x, t) &= 1 + \epsilon v_1 + \epsilon^2 v_2 + \dots, \end{aligned} \quad (45)$$

with the assumption that all the functions $u_1, u_2, \dots, v_1, v_2, \dots$ go to zero as $|x| \rightarrow \infty$, which is the boundary condition also satisfied by the original function q . Keeping in mind that, $B = iD_t + \frac{1}{2}D_x^2$ for Equation (43) and $B = \frac{1}{2}D_x^2$ for Equation (44), one can expand the equations in powers of ϵ as before. This gives us

$$\begin{aligned} \epsilon^n: B \left(\sum_{k=1}^n u_k \cdot v_{n-k} \right) &= 0 \\ \Rightarrow iu_{n,t} + \frac{1}{2}u_{n,xx} &= -B \left(\sum_{k=1}^{n-1} u_k \cdot v_{n-k} \right), \end{aligned} \quad (46)$$

and

$$\begin{aligned} \epsilon^n: B \left(\sum_{k=0}^n v_k \cdot v_{n-k} \right) &= p \sum_{k=1}^{n-1} u_k \cdot u_{n-k}^* \\ \Rightarrow v_{n,xx} &= p \left(\sum_{k=1}^{n-1} u_k \cdot u_{n-k}^* \right) - \frac{1}{2}D_x^2 \left(\sum_{k=1}^{n-1} v_k \cdot v_{n-k} \right). \end{aligned} \quad (47)$$

respectively.

3.1. Soliton solutions

3.1.1 Soliton solution:

After getting the bilinearization of the equation, one can now start seeking the soliton solutions. As we saw in the previous section the N -soliton solution is given by defining the first order function of the expansion (45) as a sum of N exponential term: $u_1 = \sum_{i=1}^N e^{\theta_i}$ where θ_i is defined as in Equation (24). Let us start by taking $N = 1$ for the 1-soliton solution. If one takes $n = 1$ in Equation (46) it gives the following linear equation

$$iu_{1,t} + \frac{1}{2}u_{1,xx} = 0. \quad (48)$$

Inserting the ansatz for the 1-soliton solution into Equation (48) gives the condition $\omega_1 = \frac{i}{2}k_1^2$ which defines the dispersion relation of the wave. The equation for the function v at the same order of ϵ , i.e., taking $n = 1$ in Equation (47),

$$v_{1,xx} = 0 \quad (49)$$

allows us to choose $v_1 = 0$. Hence, we have

$$\begin{aligned} u_1 &= e^{\theta_1}, \\ v_1 &= 0. \end{aligned} \quad (50)$$

For the next order, taking $n = 2$, Equations (46) and (47) can be read as

$$iu_{2,t} + \frac{1}{2}u_{2,xx} = -B(u_1 \cdot v_1), v_{2,xx} = p|u_1|^2 - B(v_1 \cdot v_1) \quad (51)$$

respectively. It can be shown that, since $B(u_1 \cdot v_1) = 0 = B(v_1 \cdot v_1)$, one can choose $u_2 = 0$ from the first of Equation (51). On the other hand, the second equation gives the solution

$$v_2 = e^{\theta_1 + \theta_1^* + A_{11}} \quad (52)$$

with

$$e^{A_{11}} = \frac{p}{(k_1 + k_1^*)^2}. \quad (53)$$

Therefore, one can see that the function v is real as assumed. It can be verified that all the next order terms in the expansion (45) can be set to zero, $u_i = v_i = 0$, ($i \geq 3$). In this way, the 1-soliton solution is obtained by setting $\epsilon = 1$ as

$$q = \frac{u}{v} = \frac{e^{\theta_1}}{1 + e^{\theta_1 + \theta_1^* + A_{11}}}. \quad (54)$$

Now, let $k_1 = a + ib$ as a general complex number. Plugging this definition into Equation (54) and setting $p = +1$ to deal with the fNLS solution gives

$$q(x, t) = ae^{i\left[bx + \frac{a^2 - b^2}{2}t\right]} \operatorname{sech}[a(x - bt) + \alpha_2] \quad (55)$$

where α_2 is a constant. If one chooses $p = -1$, i.e., if the dNLS case is considered, one can see that the coefficient (53) becomes negative, and one gets

$$q(x, t) = -a \frac{e^{i\left[bx + \frac{a^2 - b^2}{2}t\right]}}{\sinh[a(x - bt) + \alpha_2]}. \quad (56)$$

This solution has a singularity and therefore does not yield a soliton solution for the dNLS equation. This situation will be considered in detail in section 3.2, before that let us continue investigating the 2-soliton solution.

3.1.2 Soliton solution

As one can see above, since the 1-soliton solution contains ϵ^2 terms, it is reasonable to expect that for the 2-soliton solution we should go up to the ϵ^4 orders. For $N = 2$ one starts with the ansatz

$$u_1 = e^{\theta_1} + e^{\theta_2}, \quad (57)$$

which satisfies Equation (48) with the dispersion relation $\omega_i = \frac{i}{2}k_i^2$, ($i = 1, 2$). Equation (49) gives $v_1 = 0$ as before. Since the right-hand side of the first equation and the second term in the right-hand side of the second equation in (51) vanish, these equations give us

$$u_2 = 0, \quad (58)$$

$$v_2 = e^{\theta_1 + \theta_1^* + A_{11}} + e^{\theta_1 + \theta_2^* + A_{12}} + e^{\theta_2 + \theta_1^* + A_{21}} + e^{\theta_2 + \theta_2^* + A_{22}}$$

respectively. The constant factors are given by

$$e^{A_{ij}} = \frac{p}{(k_i + k_j^*)^2}. \quad (59)$$

If we proceed to the third-order equations by taking $n = 3$ in Equations (46) and (47) we get

$$iu_{3,t} + \frac{1}{2}u_{3,xx} = -B(u_1 \cdot v_2 + u_2 \cdot v_1), v_{3,xx} \\ = p(u_1 u_2^* + u_2 u_1^*) - D_x^2(v_1 \cdot v_2) \quad (60)$$

respectively. One can show that the right-hand side of the second equation in (60) vanishes. On the other hand, the non-vanishing part on the right-hand side of the first equation can be written as

$$B(u_1 \cdot v_2) = p \frac{(k_1 - k_2)^2}{(k_1 + k_1^*)(k_2 + k_1^*)} e^{\theta_1 + \theta_2 + \theta_1^*} + p \frac{(k_1 - k_2)^2}{(k_1 + k_2^*)(k_2 + k_2^*)} e^{\theta_1 + \theta_2 + \theta_2^*}. \quad (61)$$

One can solve the set of equations (60) to obtain the following results:

$$u_3 = e^{\theta_1 + \theta_1^* + \theta_2 + B_{121}} + e^{\theta_1 + \theta_2 + \theta_2^* + B_{122}}, \quad (62)$$

$$v_3 = 0,$$

where

$$e^{B_{ijk}} = \frac{p(k_i - k_j)^2}{(k_i + k_k^*)^2 (k_j + k_k^*)^2}. \quad (63)$$

For $n = 4$ one can write the fourth-order equations as

$$iu_{4,t} + \frac{1}{2}u_{4,xx} = 0, v_{4,xx} = p(u_1u_3^* + u_3u_1^*) - \frac{1}{2}D_x^2(v_2 \cdot v_2). \quad (64)$$

The solution of the first equation is obvious and after a bit of long but straightforward calculations the solution of the second equation can be obtained as

$$u_4 = 0, \quad v_4 = e^{\theta_1 + \theta_1^* + \theta_2 + \theta_2^* + C_{1212}}, \quad (65)$$

where

$$e^{C_{ijkl}} = \frac{p^2(k_i - k_j)^2 (k_k^* - k_l^*)^2}{(k_i + k_k^*)^2 (k_i + k_l^*)^2 (k_j + k_k^*)^2 (k_j + k_l^*)^2}. \quad (66)$$

We should emphasize that because of the symmetry of constant factors in the solutions, both v_2 and v_4 are real functions as it is stated at the beginning. On the other hand, it can easily be shown that the coefficient $e^{C_{1212}}$ is positive. The perturbative expansion is truncated at this order and all the higher order terms can be chosen as zero; indeed, $u_n = v_n = 0$, for $n \geq 5$. Therefore, we end up with

$$q(x, t) = \frac{u_1 + u_3}{1 + v_2 + v_4} \quad (67)$$

for 2-soliton solution. After taking $p = 1$ and rearranging the terms one can write the solution for the fNLS equation as

$$q = \frac{\Lambda_{122} e^{i\xi_1} \cosh \zeta_2 + \Lambda_{121} e^{i\xi_2} \cosh \zeta_1}{\Lambda_{1212} \cosh(\zeta_1 + \zeta_2) + \Lambda_{11}\Lambda_{22} \cosh(\zeta_1 - \zeta_2) + \Lambda_{12}\Lambda_{21} \cos(\xi_1 - \xi_2)}, \quad (68)$$

where coefficients Λ_{ijkl} stand for the square root of the exponential coefficients with the same index structure in Equations (59), (63) and (66), $\zeta_i = \frac{\theta_i + \theta_i^*}{2}$ and $\xi_i = \frac{\theta_i - \theta_i^*}{2}$ are the real and the imaginary parts of θ parameters respectively. This solution is nonsingular since the condition $\Lambda_{1212} + \Lambda_{11}\Lambda_{22} > \Lambda_{12}\Lambda_{21}$ is satisfied by definitions of the coefficients. If we look at the dNLS solution, we encounter the same problem as in the 1-soliton case. Namely, for the case of $p = -1$, the second term in the denominator takes a minus sign and therefore the solution again includes a singularity.

3.2. Soliton solution to the dNLS equation

The soliton solutions obtained in the previous subsection are called bright solitons and they are characterized by the vanishing boundary values at infinity. Although the dNLS equation does not admit bright soliton solutions, it has been shown that by changing the boundary conditions it can support other kinds of soliton solutions which are called dark and gray solitons. They are typically in the form $q \sim e^{ikx} \tanh(\omega t)$ and $q \sim e^{ikx} (\cos \alpha + i \sin \alpha \tanh \theta)$ respectively and in this sense, dark solitons are a special case of the gray solitons in the limit $\cos \alpha \rightarrow 0$. Such solitons satisfy the boundary conditions $|q|^2 \rightarrow \text{constant}$ as $|x| \rightarrow \infty$ and appear as localized dips on the finite background [28]. These kinds of solutions have been detected in various experiments [31-35].

To bring the equation into bilinear form, an appropriate redefinition of the dependent variable with the above-mentioned boundary condition is given by

$$q(x, t) = \rho e^{i\theta} \frac{u(x, t)}{v(x, t)}, \quad \theta = \alpha x - \beta t \quad (69)$$

where u and v are real functions, α and ρ are real constants, and $\beta = \alpha^2 - p\rho^2$. One can choose $u/v \rightarrow 1$ as $|x| \rightarrow \infty$ without loss of generality. Substituting this definition into Equation (41) leads to two distinct equations as follows

$$\begin{aligned} (iD_t + i\alpha D_x + \frac{1}{2}D_x^2)(u \cdot v) &= 0, \\ (\frac{1}{2}D_x^2 + p\rho^2)(v \cdot v) &= p\rho^2|u|^2. \end{aligned} \tag{70}$$

Choosing the following ansatzes for the functions

$$\begin{aligned} u &= 1 + \epsilon u_1 + \epsilon^2 u_2 + \dots, \\ v &= 1 + \epsilon v_1 + \epsilon^2 v_2 + \dots \end{aligned} \tag{71}$$

one obtains,

$$\epsilon^n: (i\partial_t + i\alpha\partial_x)(u_n - v_n) + \frac{1}{2}\partial_x^2(u_n + v_n) = -(iD_t + i\alpha D_x + D_x^2) \sum_{k=1}^{n-1} u_k \cdot v_{n-k}, \tag{72}$$

and

$$\epsilon^n: v_{n,xx} + 2p\rho^2 v_n = -\frac{1}{2}D_x^2 \left(\sum_{k=1}^{n-1} v_k \cdot v_{n-k} \right) - p\rho^2 \left(\sum_{k=1}^{n-1} v_k \cdot v_{n-k} - \sum_{k=1}^{n-1} u_k \cdot u_{n-k}^* \right) \tag{73}$$

3.2.1 Soliton solution

Compared to section 3.1, we reached a different set of equations that require different ansatzes for solutions. We see that the leading order equation in Equation (72) contains both functions u and v on the left-hand side. Thus, one can assume

$$\begin{aligned} u_1 &= e^{\eta_1 + 2i\phi_1}, \\ v_1 &= e^{\eta_1}, \end{aligned} \tag{74}$$

where $\eta_1 = \kappa_1 x + \omega_1 t + \tau_1$ and all the coefficients $\kappa_1, \omega_1, \tau_1$ and ϕ_1 are real constants. If one solves the first order ϵ equations, which assume $n = 1$ in Equations (72) and (73), one obtains

$$\begin{aligned} \omega_1 &= \frac{\kappa_1^2}{2} \cot \phi_1 - \alpha \kappa_1, \\ \kappa_1^2 &= -4p\rho^2 \sin^2 \phi_1. \end{aligned} \tag{75}$$

As it can be seen from Equations (75), these coefficients and hence the related functions are real only for $p = -1$. Therefore, we proceed with this p -value. One can easily show that solving the second-order equations, which are given by $n = 2$ in Equations (72) and (73), gives $u_2 = 0 = v_2$. All the higher-order terms in the expansion (71) can be set to zero by the same reasoning. Hence, after a few easy calculations one obtains the 1-soliton solution as

$$q(x, t) = \rho e^{i(\theta + \phi_1)} \left(\cos \phi_1 + i \sin \phi_1 \tanh \frac{\eta_1}{2} \right), \tag{76}$$

which defines a gray soliton.

3.2.2 Soliton solution

In order to derive the 2-soliton solution we take two exponential functions in the ansatzes for the leading order functions

$$\begin{aligned} u_1 &= e^{\eta_1 + 2i\phi_1} + e^{\eta_2 + 2i\phi_2}, \\ v_1 &= e^{\eta_1} + e^{\eta_2}, \end{aligned} \tag{77}$$

where $\eta_i = \kappa_i x + \omega_i t + \tau_i$. When these ansatzes plugged into Equations (72) and (73) with $n = 1$, it gives the dispersion relations

$$\begin{aligned}\omega_i &= \frac{\kappa_i^2}{2} \cot \phi_i - \alpha \kappa_i, \\ \kappa_i^2 &= -4p\rho^2 \sin^2 \phi_i.\end{aligned}\quad (78)$$

The next order terms in the expansion (71) can be obtained with $n = 2$ in equations (72) and (73) and with the help of Equation (77), as

$$\begin{aligned}u_2 &= e^{\eta_1 + \eta_2 + 2i(\phi_1 + \phi_2)}, \\ v_2 &= e^{\eta_1 + \eta_2 + A_{12}}.\end{aligned}\quad (79)$$

Also, one can show that the coefficient in v_2 is given by

$$e^{A_{12}} = \frac{\left[\sin\left(\frac{1}{2}(\phi_1 - \phi_2)\right) \right]^2}{\left[\sin\left(\frac{1}{2}(\phi_1 + \phi_2)\right) \right]^2}.\quad (80)$$

The perturbative expansion is truncated at this level and all the higher-order terms can be set to zero as before, $u_n = 0 = v_n$, $n \geq 3$. Here we see that the coefficient given by the equation (80) is positive for real ϕ 's and by using that, one can write the solution as

$$q = \frac{\rho e^{i(\theta + 2\phi_+)}}{\Delta_{12} \cosh \eta_+ + \cos \eta_1} \{ \Delta_{12} \cosh \eta_+ \cos(2\phi_+) + \cosh \eta_- \cos(2\phi_-) + i \Delta_{12} \sinh \eta_+ \sin(2\phi_+) + i \sinh \eta_- \sin(2\phi_-) \},\quad (81)$$

where the coefficient Δ_{12} stands for the square root of the coefficient given by equation (80), $\eta_{\mp} = \frac{\eta_1 \mp \eta_2}{2}$ and $\phi_{\mp} = \frac{\phi_1 \mp \phi_2}{2}$. Consequently, one obtains the 2-soliton solution of the dNLS equation as in Equation (81), and this procedure can be repeated in each following order to obtain the N-soliton solution. Although the calculations become more cumbersome and complex as more terms are added at each higher level, the application of the method is quite systematic and clear. In this sense, the Hirota direct method is one of the most powerful methods to obtain N-soliton solutions of any integrable nonlinear differential equation.

4. Conclusion

Solitary wave solutions of nonlinear differential equations are an active research topic. These solutions appear in a variety of types, such as solitons, kinks, peakons, cuspons, and others. They play a significant role in almost every branch of physics from fluid dynamics [36] and oceanography [37] to Bose-Einstein condensation [38] and cosmology [39]. Solitons are a special type of solitary wave solutions due to their particle-like properties and because of that, they attract a great deal of interest. It is now quite well understood that solitons appear as a result of a balance between the competing properties, weak nonlinearity, and dispersion. Soliton solutions can be obtained by various methods. Although the inverse scattering technic is the most powerful one, its applicability to practical problems is a bit troublesome. Bäcklund transformation, Darboux transformation, Painleve expansion method can be mentioned as other solution technics. However, the Hirota method is the most efficient way to obtain the multi-soliton solutions of nonlinear differential equations. Many soliton equations, such as the nonlinear Schrödinger equation [18], the 2-dimensional Toda lattice [40], the AKNS hierarchy [41] and some equations constrained from the high-dimensional KP hierarchy [42] admit solutions in Hirota forms. Recent researches have shown that the Hirota method can also be used to construct soliton solutions with rogue-like phenomena [43]. These are localized waves both in time and in space and Peregrine solution [44] was the first example of this kind of solution. They represent an unexpected wave event on an otherwise flat background and are observed in water waves [45] and in optical fibers [46]. Because of that property, they are called “waves that appear from nowhere and disappear without

a trace". Recently, for high-dimensional soliton equations, there are a lot of work on lump solutions by the Hirota method [47]. Furthermore, the Hirota method can also be used to solve the nonlinearization systems of Lax pairs [48, 49]. The advantage of the Hirota method is that it does not depend on Lax pairs.

Recently, the supersymmetric (susy) extensions of integrable systems are another hot topic that has been studied a lot. $N=1$ susy extension of the KdV equation is defined by Manin and Radul [50], and Mathieu [51]. $N=2$ susy extension of the KdV equation is defined in [52] and later other susy extensions of the KdV equation have also defined [53]. In a similar fashion, susy extensions of the other integrable systems are defined as well [54, 55]. The integrability of these susy extended models have been proved by similar methods to the original bosonic counterparts: infinite number of conservation laws, a bihamiltonian structure, the Lax operator etc. Another method of integrability is the existence of soliton solutions and for this aim, Hirota method has also been adapted to bilinearize supersymmetric systems [56-58].

In this study, we give an overview of the Hirota direct method. We construct the bilinear forms and study the multi-soliton solutions of the KdV and the nonlinear Schrödinger equations by using Hirota's method. We explicitly demonstrate how both bright/dark one and two-soliton solutions of the nonlinear focusing/defocusing Schrödinger equations can be obtained. We showed that fNLS equation admits bright soliton solutions for the vanishing boundary value at infinity. An appropriate redefinition of the dependent variable splits up the equation into a set of bilinear equations which are to be solved to obtain the term of the solution by term. On the other hand, dNLS equation admits dark soliton solutions by changing both the boundary condition and the definition of the dependent variable. The powerful property of Hirota's method is that it gives solutions in terms of a series of exponential functions and this series expansion truncates at a certain finite order for any soliton degree. Hence, one can obtain soliton solutions of any degree directly without dealing with the initial value problem of the related differential equation.

References






- [1] Russell, J.S., "Report on waves", report of the 14th meeting of the British Association for the Advancement of Science, John Murray, London, 311–390, 1845.
- [2] Boussinesq, J., "Theorie de l'intumescence liquid appelee onde solitaire ou de translation, se propageant dans un canal rectangulaire", *C. R. Acad. Sci.*, Paris, 1872.
- [3] Rayleigh, Lord, "On waves", *Phil. Mag. (5)*, 1, 257-279, 1876.
- [4] Korteweg, D.J., De Vries, G., "On the change of form of long waves advancing in a rectangular canal, and on a new type of long stationary waves", *Phil. Mag.*, 39(240), 422-443, 1895.
- [5] Fermi, A., Pasta, J., Ulam, S., "Studies of nonlinear problems", *I. Los Alamos Report LA-1940*, Los Alamos National Laboratory, May 1955.
- [6] Zabusky, N.J., Kruskal, M.D., "Interaction of solitons in a collisionless plasma and the recurrence of initial states" *Phys. Rev. Lett.*, 15, 240-243, 1965.
- [7] Miura, R.M., "Korteweg-de Vries equation and generalizations I. A remarkable explicit nonlinear transformation", *J. Math. Phys.*, 9, 1202-1204, 1968.
- [8] Gardner, C.S., Greene, J.M., Kruskal, M.D., Miura, R.M., "Method for solving the Korteweg-de Vries equation", *Phys. Rev. Lett.*, 19(19), 1095-1097, 1967.

- [9] Gardner, C.S., “Korteweg-de Vries equation and generalizations IV. The Korteweg-de Vries equation as a Hamiltonian system”, *J. Math. Phys.*, 12, 1548–1551, 1971.
- [10] Gardner, C.S., Greene, J.M., Kruskal, M.D., Miura; R.M., “Korteweg-de Vries equation and generalizations VI. Methods for exact solution”, *Comm. Pure Appl. Math.*, 27, 97-133, 1974.
- [11] Zakharov, V.E., Faddeev, L.D., “Korteweg-de Vries equation: a completely integrable Hamiltonian system”, *Funct. Anal. Appl.*, 5, 280-287, 1971.
- [12] Hirota, R., “Exact solutions of the Korteweg-de Vries equation for multiple collisions of solitons”, *Phys. Rev. Lett.*, 27 (18), 1192-1194, 1971.
- [13] Hirota, R., *The direct method in soliton theory*, Cambridge University Press, 2004.
- [14] Wadati, M., Konno, K., Ichikawa, Y.H., “A generalization of inverse scattering method”, *J. Phys. Soc. Japan*, 46(6), 1965-1966, 1979.
- [15] Matveev, V.B., Salle, M.A., *Darboux transformation and soliton*, Springer, Berlin, 1991.
- [16] Ito, M., “An extension of nonlinear evolution equations of the KdV (mKdV) type to higher orders”, *J. Phys. Soc. Japan*, 49(2), 771–778, 1980.
- [17] Freeman, N.C., Nimmo, J.J.C., “Soliton solutions of the Korteweg-de Vries and Kadomtsev-Petviashvili equations: The wronskian technique”, *Phys. Lett. A.*, 95(1), 1–3, 1983.
- [18] Freeman, N.C., Nimmo, J.J.C., “A method of obtaining the n-soliton solutions of the Boussinesq equation in terms of a wronskian”, *Phys. Lett. A.*, 95(1), 4–6, 1983.
- [19] Nimmo, J.J.C., “A bilinear Bäcklund transformation for the nonlinear Schrodinger equation”, *Phys. Lett. A.*, 99(6-7), 279–280, 1983.
- [20] Nimmo, J.J.C., Yilmaz, H., “Binary Darboux transformation for the Sasa-Satsuma equation”, *J. Phys. A.*, 48(42), 2015.
- [21] Zakharov, V.E., Shabat, A.B., “Exact theory of two-dimensional self-focusing and one-dimensional self-modulation of waves in nonlinear media”, *Sov. Phys. JETP*, 34, 62, 1972.
- [22] Zakharov, V.E., Shabat, A.B., “A scheme for integrating the nonlinear equations of numerical physics by the method of the inverse scattering problem. I”, *Funk. Anal. Prilozh.* 8, 43-53, 1974 [*Funct. Anal. Appl.* 8, 226-235 (1974)],
- [23] Zakharov, V.E., Shabat, A.B., “Integration of the nonlinear equations of mathematical physics by the method of the inverse scattering problem. II”, *Funk. Anal. Prilozh.*, 13 (3), 13-22, 1979 [*Funct. Anal. Appl.* 13, 166-174 1979].
- [24] Ablowitz, M.J., Ramani, A., Segur, H., “A connection between nonlinear evolution equations and ordinary differential equations of P-type. II”, *J. Math. Phys.*, 21, 1006, 1980.
- [25] Ablowitz, M.J., Clarkson, P.A., “Solitons non-linear evolution equations and inverse scattering”, Cambridge University Press, 1991.
- [26] Hietarinta, J., “A search for bilinear equations passing Hirota’s three-soliton condition. I. KdV type bilinear equations”, *J. Math. Phys.*, 28, 1732, 2094, 1987.
- [27] Hietarinta, J., “Hirota’s bilinear method and its generalization”, *Inter. J. Mod. Phys. A*, 12(1), 43-51, 1997.

- [28] Hietarinta, J., "Introduction to the bilinear method," in Integrability of nonlinear systems. Lecture notes in physics (Ed. Y. Kosman-Schwarzbach, K.M. Tamizhmani, B. Grammaticos), 638, 95-105, Springer, Berlin, 2004.
- [29] Taniuti, T., Yajima, N., "Perturbation method for a nonlinear wave modulation I", *J. Math. Phys.*, 10, 1369-1372, 1969.
- [30] Debnath, L., *Nonlinear partial differential equations for scientists and engineers*, Birkhauser, 2012.
- [31] Ablowitz, M.J., *Nonlinear dispersive waves. Asymptotic analysis and solitons*, Cambridge University Press, 2011.
- [32] Hirota, R., "Exact envelope-soliton solutions of a nonlinear wave equation", *J. Math. Phys.*, 14, 805-809, 1973.
- [33] Hasegawa, A., Tappert, F., "Transmission of stationary nonlinear optical pulses in dispersive dielectric fibers. II. Normal dispersion", *Appl. Phys. Lett.*, 23, 171-172, 1973.
- [34] Weiner, A.M. *et al.*, "Experimental observation of the fundamental dark soliton in optical fibers", *Phys. Rev. Lett.*, 61, 2445, 1988.
- [35] Tlidi, M., Gelens, L., "High-order dispersion stabilizes dark dissipative solitons in all-fiber cavities", *Opt. Lett.*, 35, 306-308, 2010.
- [36] Carr, L.D., Brand, J., Burger, S., Sanpera, A., "Dark-soliton creation in Bose-Einstein condensates", *Phys. Rev. A*, 63, 051601(R), 2001.
- [37] Shukla, P.K., Eliasson, B., "Formation and dynamics of dark-solitons and vortices in quantum electron plasmas", *Phys. Rev. Lett.*, 96, 245001, 2006.
- [38] Heidemann, R. *et al.*, "Dissipative dark soliton in a complex plasma", *Phys. Rev. Lett.*, 102, 135002, 2009.
- [39] Zakharov, V.E., "Stability of periodic waves of finite amplitude on a surface of deep fluid", *J. Appl. Mech. Tech. Phys.*, 9, 190-194, 1968.
- [40] Osborne, A., "Nonlinear ocean waves and the inverse scattering transform", Academic Press, 2010.
- [41] Gross, E.P., "Structure of a quantized vortex in boson systems", *Nuovo Cimento*, 20, 454, 1961.
- [42] Pitaevskii, L.P., "Vortex lines in an imperfect Bose gas", *Sov. Phys. JETP*, 13, 451, 1961.
- [43] Lidsey, J.E., "Scalar field cosmologies hidden within the nonlinear Schrödinger equation", <https://arxiv.org/abs/1309.7181>, 2013.
- [44] Hirota, R., Ohta, Y., Satsuma, J., "Wronskian structures of solutions for soliton equations", *Progr. Theor. Phys. Suppl.*, 94, 59-72, 1988.
- [45] Liu, Q.M., "Double wronskian solutions of the AKNS and classical Boussinesq hierarchies", *J. Phy. Soc. Jpn.*, 59, 3520-3527, 1990.
- [46] Zhang, Y. J., Cheng, Y., "The Wronskian structure for solution of the k-constrained KP hierarchy", *J. Phys. A: Math. Gen.*, 27, 4581-4588, 1994.
- [47] Zhang, J.B., Gongye, Y.Y., Chen, S.T., "Soliton solutions to the coupled Gerdjikov- Ivanov equation with rogue-wave-like phenomena", *Chin. Phys. Lett.*, 34(9), 090201, 2017.

- [48] Peregrine, D.H., “Water waves, nonlinear Schrödinger equations and their solutions”, *J. Australian Math. Soc. Ser. B*, 25, 16, 1983.
- [49] Chabchoub, A., Hoffmann, N.P., Akhmediev, N., “Rogue wave observation in a water wave tank”, *Phys. Rev. Lett.*, 106, 204502, 2011.
- [50] Kibler, B., Fatome, J., Finot, C. *et al.*, “The Peregrine soliton in nonlinear fiber optics”, *Nat. Phys.*, 6, 790-795, 2010.
- [51] Zhang, J.B., Ma, W.X., “Mixed lump-kink solutions to the BKP equation”, *Comput. Math. Appl.*, 74(3), 591–596, 2017.
- [52] Zhang, J.B., Zhang, D.J., Shen, Q., “Bilinear approach for a symmetry constraint of the modified KdV equation”, *Appl. Math. Comput.*, 218, 4497–4500, 2011.
- [53] Zhang, J.B., Zhang, D.J., Chen, D.Y., “Solving the KdV equation under Bargmann constraint via bilinear approach”, *Commun. Theor. Phys.*, 53, 211–217, 2010.
- [54] Manin, Y.I., Radul, A.O., “A supersymmetric extension of the Kadomtsev-Petviashvili hierarchy”, *Comm. Math. Phys.*, 98, 65-77, 1985.
- [55] Mathieu, P., “Supersymmetric extensions of the Korteweg-de Vries equation”, *J. Math. Phys.*, 29, 2499, 1988.
- [56] Laberge, C.A., Mathieu, P., “N=2 superconformal algebra and integrable O(2) fermionic extensions of the Korteweg-de Vries equation”, *Phys. Lett. B*, 215, 718, 1988.
- [57] Labelle, P., Mathieu, P., “A new N=2 supersymmetric Korteweg-de Vries equation”, *J. Math. Phys.*, 32, 923, 1991.
- [58] Popowicz, Z., “Odd bihamiltonian structure of new supersymmetric N=2, 4 Korteweg-de Vries equation and odd SUSY Virasoro-like algebra”, *Phys. Lett. B*, 459, 150, 1999.
- [59] Das, A., Popowicz, Z., “New nonlocal charges in SUSY integrable models”, *arXiv:nlin/0004034*, 2000.
- [60] Yamanaka, I., Sasaki, R., “Super Virasoro algebra and solvable supersymmetric quantum field theories”, *Prog. Theor. Phys.*, 79, 5, 1167, 1988.
- [61] Popowicz, Z., “A 2-component or N=2 supersymmetric Camassa–Holm equation”, *Phys. Lett. A*, 354, 1-2, 110-114, 2006.
- [62] Popowicz, Z., “Odd Hamiltonian structure for supersymmetric Sawada–Kotera equation”, *Phys. Lett. A*, 373, 37, 3315-3323, 2009.
- [63] Mc Arthur, I.N., Yung, C.M., “Hirota bilinear form for the super-KdV hierarchy”, *Modern Phys. Lett. A*, 8, 1739-1745, 1993.
- [64] Carstea, A.S., “Extension of the bilinear formalism to supersymmetric KdV-type equations”, *Nonlinearity*, 13, 1645-1656, 2000.
- [65] Carstea, A.S., Ramini, A., Grammaticos, B., “Constructing the soliton solutions of the N=1 supersymmetric KdV hierarchy”, *Nonlinearity*, 14, 1419-1423, 2001.
- [66] Ghosh, S., Sarma, D., “Bilinearization of N=1 supersymmetric modified KdV equations”, *Nonlinearity*, 16, 411-418, 2002.

**THE CHEMISTRY MECHANISM OF HAIR DYES**

Arzu YILDIRIM¹  **Belinda DEMİR¹**  **Berfin AK İZGİ¹**  **Büşra Nur ERKOL¹** 
Çağla ÖZSU¹  **Gülşah EŞLİK AYDEMİR¹**  **Mine MUSTAFAOĞLU¹**  **Murat KIZIL¹** 
Nubar AYHAN¹  **Sevil EMEN¹**  *

¹Lila Cosmetics, Diyarbakır, Turkey, 21010

*Corresponding Author: ar-ge@lilafix.com

Abstract: *One of the oldest and most well-known cosmetics, hair color has been used by numerous ancient cultures throughout history on both men and women. It involves treating hair with various chemical compounds for changing hair color. According to how long they remain in the hair, these products are primarily divided into two categories: temporary and permanent. This classification is consistent with the types of active substances used in the dyeing process as well as the dyeing method itself, which are referred to as non-oxidative and oxidative hair dye products, respectively. Permanent hair dyes often consist of active chemicals that are not dyed but are oxidized to provide the desired color. As a result, the phrase "oxidative hair dye" was emerged. The precursor part and coupler part are the two main ingredients in formulations for oxidative hair dyes. Quinonediimine intermediates are momentary compounds that are generated when combined with hydrogen peroxide (developer). As a result, the coupler agent and these compounds interact to form the appropriate hair dye molecule. Notably, the entire dyeing process requires both an alkaline medium and an oxidizing agent, often hydrogen peroxide, to ensure that the staining agents reach the cuticle widely. This review's objective is to provide information about hair dye formulations and mechanisms of action as well as repairing damaged hair and new applications.*

Key words: *Hair dyes; temporary; semipermanent; permanent; chemical mechanism*

Received: September 08, 2022

Accepted: December 05, 2022

1. Introduction

Since the dawn of human civilisation, people have used vegetable and animal fats in cosmetics and other items [1,2]. It is well known that both men and women frequently utilize a combination of natural materials, such as original hair color changes with chemical dye application [3,4]. Colors are crucial to human existence. Previously, dyes were used for clothing coloring, cosmetics, medicine, and a variety of other uses, but recently, due to biodegradability and environmental concerns, the usage of natural dyes has grown significantly [5]. Hair dyes are currently in a crucial stage of development, and substantial advancements are being made in the discovery and use of numerous new synthetic dyes.

The oxidation behavior of dyes falls under two categories. These can be divided into two groups: oxidative and non-oxidative hair dyes [6]. Some hair dyes are referred to as "non-oxidative" dyes because they produce color without the use of oxidation chemicals. Contrarily, oxidative hair colors feature oxygen release in their formula and make up about 90% of the hair dyes on the market today. The oxygen that is produced helps to oxidize the dye substance, start the reaction process, and also provide the desired color in the hair [7]. For cream and lotion-based hair dyes, a variety of oxidizing agents are available. These agents are also employed in liquid form, with hydrogen peroxide serving as

the finest illustration. The reaction mechanism greatly depends on the concentration of the oxidizing agent. Faster color integration and reaction mechanism are provided by higher concentrations [8].

Numerous people utilize hair cosmetics, which alter the hair's structural characteristics [9]. It alters the hair's protein composition and structure while also changing the physical characteristics of the hair. Long polyhedral hair strands are encased in cuticle cells. Cortical cells are arranged structurally in it. The majority of the mechanical properties of the hair are determined by the cortical layer [10]. The usual structure of the hair shaft must be altered chemically in order for the hair to change color when dyed. This allows color pigments to enter the hair and provides a coloring process [11].

When hair colors are applied continuously, the hair strands are repeatedly exposed to the dye, which makes them more sensitive. Therefore, even if you've colored your hair before, it could be difficult to do so again without experiencing difficulties. Some hair colors can give sensitive people adverse reactions that result in skin discomfort and hair loss [12]. Before applying the color, the user must adhere to the user's instructions. Before using the hair dye, the consumer is required to carefully follow the user instructions each time. This reduces the likelihood of allergic reactions in the user.

2. Hair Biology and Chemistry

The term "hair" refers generally to the cluster of hairs on a person's scalp. A human embryo's skin begins to develop hair follicles during the eighth and twelfth weeks of gestation as the epidermis invades the dermis. A hair fiber's 50-100 μm in diameter serves both defensive and aesthetic purposes. The skin's hair follicles create hair, which is a highly keratinized tissue. Dermal stem cells in hair follicles modify the kind of hair and renew the dermal sheath and dermal papilla [13].

The three distinct components of the hair's composition are as follows: the medulla, which is the innermost layer of the hair shaft and is made of an amorphous, soft, greasy substance. The nourishing part necessary for hair growth is found within the cuticle, a thin protective outer layer. The main component of the hair, the cortex, is highly keratinized and is made up of cells that resemble scales that are layered one over the other, measuring roughly 60 micrometers long and 6 micrometers wide. Long keratin chains in the cortex give the hair its elasticity, suppleness, and resistance [14,15]. A lipid- and protein-rich intercellular cement holds the cortex's cells together. Each cell is made up of bundles called macrofibrils, which are composed of microfibrils and lie in the direction of the hair length. (Fig 1).

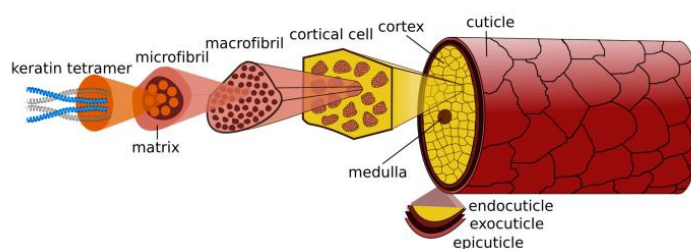


Figure 1. An illustration of a hair strand in cross-section. Adapted from ref. [15].

Human hair is composed of proteins called keratins. The family of fibrous structural proteins includes the complex natural composites known as keratins, which have varied morphological structures. As the cells develop and create the hair fiber, keratin, which is present in the cells during hair creation, crystallizes. The majority of the time, the hair surface contains a negative charge because keratin, which makes up the majority of the hair fiber, has an acidic isoelectric point. The molecular weight of keratins ranges from 40 to 70 kDa. Alpha-keratins are primarily in the α -helical conformation and are found in tissues like hair, nails, and claws of animals, including humans [14].

Alpha keratins come in type I and type II varieties. Human hair keratins are typically Type I keratins, bigger (50 to 60 kDa), neutral to slightly basic (pI range: 6.5-7.5), and larger than other keratins (50 to 60 kDa). The most notable variation is in the quantity of cysteine and glycine residues. The increased amount of cystine in human hair keratin, which converts to a higher amount of disulfide bonds, results in a tougher and more robust structure with good mechanical, thermal, and chemical properties.

All keratin forms, however, contain a lot of aspartic and glutamic acid residues, which explains why these proteins are relatively acidic. For proteins' structural stability to be maintained, water is a crucial component. As a result, while considering the physical and aesthetic qualities of hair, the water content is a crucial factor.

The amount of lipids and pH of the hair both affect how much water is absorbed. With an average amount of 4% by weight of the fiber, hair lipids are dispersed throughout the hair fiber. Cholesterol, cholesterol esters, cholesterol sulfate, free fatty acids, triglycerides, paraffins, squalene, and ceramides make up the majority of lipids. 18-MEA, which is a crucial part of exogenous lipids and is covalently attached to the cuticle surface, when this lipid is absent, the sensory sense of the hair is affected, leading to dry hair or difficulty combing, as it acts as a lubricant to reduce friction between hair fibers. Inorganic elements can also be found in hair, though they typically make up less than 1% of the total composition [15].

The most prevalent are metalloids (Hg, Cd, Pb, As, and Se), other metals (Ca, Zn, Fe, Mn), alkaline earth elements (K and Na), and alkaline earth metals (Mg, Ca, and Sr) (Si). & P If the scalp is lengthy, hair can reveal long-term information about drug use and toxin exposure over the course of months or even years. The connections between and within the protein chains are what keep the keratins' macromolecular structure stable and hold it all together.

From stronger contacts like hydrogen bonds, Coulomb interactions, Van der Waals forces, and hydrophobic interactions to weaker ones like covalent bonds like disulfide bonds and isopeptide cross-links, these interactions span the entire chemical spectrum. Reactive groups must be present in the fiber for these interactions to occur, but they must also be present due to the fiber's shape and molecular structure. Although weak and quickly disrupted by water, hydrogen bonds are the most prevalent in hair, and interchain hydrogen bonding along the polypeptide chain is crucial for the integrity of the -keratin structure. Coulombic interactions are rather stable in an aqueous media due to the high amount of acidic and basic side chains but are easily broken by acids or alkalis.

All along the keratin, nonpolar groups interact hydrophobically. Keratin's stability depends on disulfide bonds. A bridge between two chains or two sections of the same chain is created when two adjacent cysteines link together to produce cystine. The majority of chemical alterations in the hair and the resulting change in its physicochemical qualities are caused by these bonds' vulnerability to reduction and oxidation [14,15].

Changes in disulfide bonds are a negative side effect of some other cosmetic procedures, including oxidative hair coloring, bleaching, and hair damage. In both situations, redox chemical reactions have an inadvertent or intentional impact on the physicochemical characteristics of the hair. There are 18 methyleicosanoic acid-based covalently linked lipids that attach to proteins in the cuticle cells' outer layer. Involved in the penetration of substances into the fibers, including the breakdown of the cell membrane complex by persistent waves, sunlight, hair bleaches, and cyclic elongation stresses, they contribute to the surface characteristics of the fibers.

3. Pigmentation of Hair

The quantity and distribution of melanosomes in the cuticle, cortex, and medulla determine the color of hair. Vesicular organelles called melanosomes hold the melanin pigments eumelanin (brown to black) or pheomelanin (yellow or red). The density, location, and relative amounts of various melanin

granules might vary depending on the age of the person and the stage of hair growth [16, 17]. The colour variations between hair strands collected from the same person are shown in Figure 2. These two hair strands were taken from a person's top of the head; however, it is obvious that they differ in terms of color, diameter, and medullation. Researchers examining genotype-phenotype connections can obtain a quantitative color assessment by spectrophotometric measurement, chemical analysis, and microscopic examination [18].

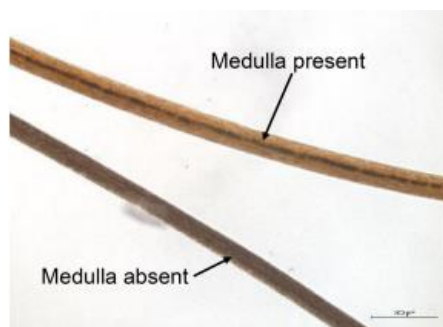


Figure 2. Two hairs from the same person are shown in a photomicrograph with different colour and medulla presence/absence. Adapted from ref. [18].

Studies on hair color employ handheld spectrophotometers to classify the various hair hues and examine mass hair samples [19, 20]. Blond, red, brown, and dark brown/black hairs can all be classified quantitatively using spectrophotometry, although there are detection limits that make it impossible to study a single hair strand [21]. Examining melanin and the genes responsible for various phenotypes using reflection spectrophotometry can provide quantitative information about hair color. This kind of study might be constrained, though, by the quantity of hair and the differences in the sample hair used for such investigations [22].

It is possible to investigate hair color and composition at the chemical level quantitatively by analyzing the kind and quantity of melanin in hair. It has been demonstrated that there is a correlation between the hair color and the amount of melanin in the hair when the melanin in the hair is chemically examined with the High-Performance Liquid Chromatography instrument [23]. Pheomelanin, although it cannot be seen, the ratio of eumelanin to pheomelanin can be established chemically. It should be noted that brown to dark hair consistently has a pheomelanin content of 11–17% [24].

In order to take advantage of and interpret the numerous procedures available, it would be more acceptable to combine multiple techniques in studies on hair color and melanin. Investigating the superstructure of the hair, hair pigmentation, color, and shape, and linking chemical and genetic data are all advantages of this sort of integrated study [25]. This combined approach will also result in a more precise approach when examining the variations in hair pigment hue.

Using natural or synthetic hair dye, such as henna, indigo, strawberry, and other herbs, it is possible to temporarily alter the color of hair. Changes in hair pigmentation can be temporary or semi-permanent by coating the hair cuticle or introducing color molecules to the hair cuticle. Additionally, more lasting alterations in hair color are made possible by the color molecules' penetration of the deeper cortical layer. An essential component is hydrogen peroxide, which penetrates the cortical layer, oxidizes melanin, and eliminates color. The cuticle is opened by high pH (alkaline) substances like ammonia, allowing the dye to penetrate the cortex and bond to the keratin. The cuticle is closed by substances with a pH between 4 and 5.5, which helps the new desired color permeate the hair [26, 27].

4. Hair Dyes

According to the chemistry involved, modern commercial hair coloring products can be simply separated into two primary groups: the oxidative process and the nonoxidative process. Semipermanent hair dyes are included in the nonoxidative category. Oxidative dyeing products are classified into two subcategories: permanent hair dyes, and demipermanent hair dyes, which lighten hair less and cause colors to fade over time.

4.1. Non-oxidizing Hair Dyes

Hair coloring is a widely popular process, particularly among ladies. Temporary, semi-permanent, demipermanent and permanent hair colors are categorized according to their color resistance. Based on colored molecules, the first two dye classes (Table 1). Semi-permanent dyes can somewhat penetrate the hair cortex; therefore, the color permanence may resist up to six washes, in contrast to temporary dyes, which affect hair by accumulating on the cuticles [12].

Table 1. Contemporary hair dyes' classification and ingredients. Adapted from ref. [28].

Dyes category	Hair coloring process	Composition	Hair coloring type
Temporary	Non-oxidative	Water-soluble acidic and basic dyes containing azo or anthraquinone groups	Build up on hair
Semi-permanent	Non-oxidative	Azo groups, anthraquinones, triphenylmethanes and nitro derivatives as chromophores.	Ionic interactions or Van der Waals forces
Permanent	Oxidative	Precursor, binder and oxidizer	Hair penetration

4.2. Temporary (Non-Oxidative) Hair Dyes

Because the dye cannot penetrate the cortex, non-oxidative temporary hair dyes have a shorter lasting period on the hair fiber and start to wash out of the hair after the first shampoo. Because of its heavy molecular structure, it leaves deposits on the hair's surface.

Due to the fact that this kind of dye cannot bleach the hair, it is only used to add new nuances to the existing color of the hair. Once the color is at least one shade lighter than the original hair color, these dyes are ready for use. If the hair was born black, the color is not immediately apparent [29].

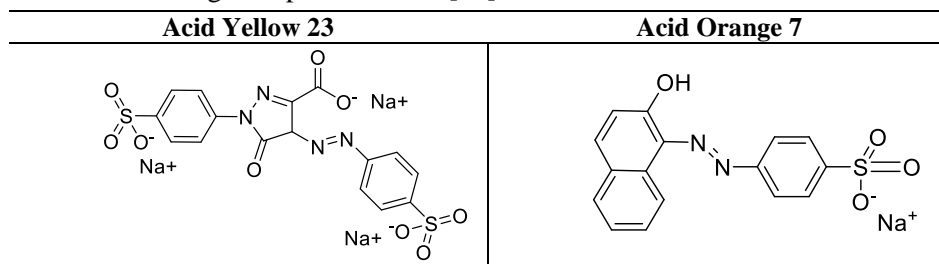
The color appears better on white, blond, or bleached hair because the original color of the hair strand allows the appearance of the new color applied. Temporary dyes work by building up in the hair strands and can colour hair that contains up to 15% white hair fiber. These colors have acidic characteristics. Typically, they have a large molar mass. Their effects on the hair are gone after the first wash since they exhibit anionic qualities, act with maximal water solubility, and penetrate the hair very minimally [30]. These colors function in aqueous solutions with a pH range of 2.5 to 4.0. Generally, no metal salts are used in their use (Table 3) [31].

Table 2. A few samples and reflections of temporary dye pigments. Adapted from ref [30].

Pearl Name	Ci Number	Cas Number	Color/Reflection
Acid yellow 23	CI19140	1934-21-0	Yellow

Acid Orange No. 7	CI15510	633-96-5	Orange
Acid Yellow No. 1	CI10316	846-70-8	Yellow

Table 3. A selection of anionic dyes with their structural and molecular formulations that are used in semi-permanent hair coloring. Adapted from ref [12].



Because extra dye molecules are rapidly removed by shampooing, higher concentrations of temporary color pigments should be used in temporary hair dyes to produce the desired color on the hair without exceeding the usage limit [29].

Because it is impossible to achieve the necessary tones with a single pigment, temporary dyes typically require at least two or five pigments in order to achieve the ideal hair color. Some types mix four to five colours to obtain red, brown, and black tones, and some types utilize two pigments to conceal the whiteness of the hair. Temporary non-oxidative dyes are stronger stains and have higher dye concentrations between 0.1% and 2.0% (w/w).

4.3. Semi-Permanent (Non-Oxidative) Hair Dye

The term "semi-permanent hair dye" refers to colors that can permanently change hair color without the use of hydrogen peroxide for up to 4 to 6 shampoos [29].

These hair colours have a strong affinity for the keratin in hair. These dyes have a low molar mass and are basic cationic dyes. Because of their straightforward application, semi-permanent hair dyes do not contain oxidation processes. After waiting for 10 to 40 minutes, they are rinsed out of the hair and dried. Nitroaniline, nitrophenylenediamines, nitroaminophenols, azoic compounds, and anthraquinone compounds are the general categories for semi-permanent colorants (Table 4) [32].

Semi-permanent hair dye products have higher wash resistance than temporary dyes because the semi-permanent dye molecules are in a form that can be applied with other oxygen-release agents without hydrogen peroxide or alkali solution. Robbins and Crawford only examined the diffusion pattern of semi-permanent color and found that weak Van der Waals bonds are formed in the semi-permanent coloring mechanism [29].

Table 4. A few illustrations of cationic semi-permanent hair color. Adapted from ref. [12, 33].

Name	Color/Reflection
2-Nitro-P-Phenylenediamine	Rejection
Basic Blue No.99	blue
Basic Yellow No.57	yellow

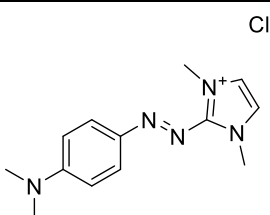
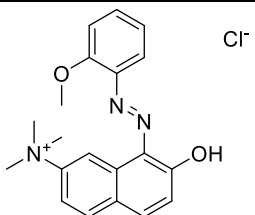
Given the high affinity of both dye families for hair, another type of product is that it might be essential to combine nitro aniline dyes with basic or acidic dyes, which offer a better color outcome and improved wash resistance. Nitro anilines are extremely polar compounds with mono, di, or tri nuclear rings that are made up of a neutral aromatic amine or anthraquinone derivatives. These colors are held by flimsy Van der Waals connections and spread throughout the hair fiber. Larger molecules with three

aromatic rings are expelled from the hair more slowly than smaller mononuclear molecules under the same circumstances.

The cationic molecules' identical sizes provide the hair a uniform permanence that promotes even color replication and washing resistance. In other words, during this procedure, all colours from the hair are washed away simultaneously (Table 5) [12].

Ionic bonds between the positive areas of the dye molecule and the negative sites on the hair fiber make cationic dyes more resistant to washing than nitro anilines, they are particularly useful for treating damaged hair [34].

Table 5. Cationic dyes used in various semi-permanent hair dyes, including their structural and molecular compositions. Adapted from ref [12].

Basic Red 51	Basic Red 76
	

4.4. Semi-Permanent Hair Dyes

Hemi-Cyanin is the abbreviation for "HC Dyes" in semi-permanent hair dye. These Hemi-Cyanine dyes, sometimes referred to as Nitro dyes, are a secondary source of amines. HC dyes are direct dyes because they belong to the semi-permanent dye class, but they are not direct dye color indicators (Fig 3). These HC dyes can be combined with oxidative dyes or used independently. These dyes have low molar extinction coefficients (approximately $10,000 \text{ L mol}^{-1} \text{ cm}^{-1}$). For better color results, use more of it in general (Table 6) [35].

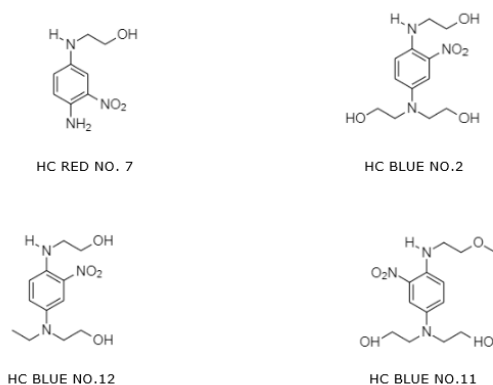


Figure 3. The Most Popular HC Dyes. Adapted from ref [35].

Table 6. Some HC Dyes containing secondary amine group. Adapted from ref [35].

Dye	Contains A Secondary Amin Group	Maximum Concentration Allowed %
HC Blue NO.16	+	No Limited

4.5. The Effect of pH on the physical properties of the hair structure

One of the variables that fundamentally affects the physical characteristics of the hair structure is pH. The outer layer of the hair develops pores as a result of acidic pH dyes, and the hair strands become positively charged. On the other hand, when negative charges are present and the pH is basic, the fibers swell and produce more holes [32].

As a result, a change in pH can affect how colors are distributed in the hair fiber's outer and interior layers. Ballarin, Galli, and Morigi (2007) described the Basic Red 76 pigment's state and the staining process, which took 30 minutes. In this situation, he noticed that the color deposited more on the hair surface at basic pH values compared to acid pH values. pH regulation is a crucial component of color stability. For instance, to produce a pH of 9.0, a weak base like monoethanolamine must be added, and to reduce the pH to 6.0, a weak acid like 10% citric acid solution must be used [32].

This results in the creation of a buffer system that preserves the pH of the finished product during the course of its shelf life. [36]

4.6. Oxidative (Permanent) Hair Dyes

Because this category offers better permanent dyeing efficacy, resistance to shampoo washes, and resistance to other environmental elements including drying, friction, light, and others, permanent hair dyes are frequently used [37]. This category receives any colour and covers up to 100% of grey hair strands, accounting for around 80% of commercial hair dyes [38]. Additionally, the combination of the oxidizing chemicals and the ammonia hydroxide allows for the creation of both dark and light natural hair colors. In the presence of an oxidizing agent, color production occurs upon combination and involves intricate interactions between precursors [12].

Precursors can be divided into two groups: couplers or reaction modifiers and oxidation basis [12, 39]. The reaction takes place in an alkaline environment that encourages the cuticles to open, allowing the molecules of the dyes to enter the cortex. The oxidizing agent allows the reaction to start in the cortex, which produces a colorful complex with a large molar mass and prevents formed molecules leaving from hair. The cuticles also participate in the process, and the first washes remove the molecules [40, 41].

An aromatic amine with ortho or para substitutions (hydroxy or amino) as coupling bases, reaction modifiers, an alkalizing material, and an oxidizing agent are the four primary components needed for redox reactions, which are used to make permanent dyes.

Three essential elements are needed for permanent hair coloring. The primary intermediate, oxidation base, or developer is an o- or p-substituted (hydroxy or amino) aromatic amine (by analogy with color photography). p-phenylenediamine (Fig 4), p-aminophenol (Fig 5), and their derivatives are examples of primary intermediates [12, 39].

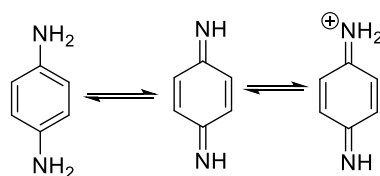


Figure 4. Formula structural for p-phenylenediamine (PPD).

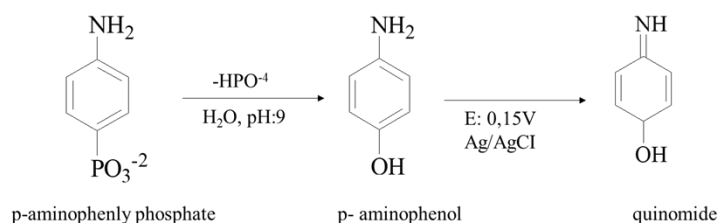


Figure 5. The structural formula of p-aminophenol (PPD).

The coupler, the second component, is often an aromatic compound with electron-donating groups organized in a meta-to-meta arrangement. Examples of such compounds include m-phenylenediamines, resorcinol, naphthols, and their derivatives (Table 8). When combined with the primary intermediates and an oxidant, these chemicals, which by themselves do not create noticeable hues by oxidation, can change color. According to the color produced in the fiber with the primary intermediates, couplers are divided into three groups: yellow-green, red, and blue. The third component is an alkali, typically ammonia, and an oxidant, nearly always hydrogen peroxide (although ambient oxygen can be used under some circumstances) [42].

To promote the right pH level for the start of the oxidation reaction, alkalizing substances must be added throughout the hair colouring process. Ammonia, in the form of ammonium hydroxide, monoethanolamine, and sodium silicate, when the formulation comprises water, are the most often employed alkalizing substances (powder) [12].

To delay the interaction between bases and reaction modifiers and to stop the reaction from starting in the packaging tube during storage, reducing agents are added to formulations of oxidative dyes. Sodium metabisulfite is one of the compounds most frequently utilized for such purposes (MBS) [12].

Antioxidants are required to stop the reaction from starting before the actual oxidant is added. It is advised to employ a water-soluble antioxidant since adjusting bases and reaction modifiers may start an oxidative process that could affect the product's final color. Erythorbic acid is one of the compounds that is most frequently utilized for this purpose (AEB). Additionally, it is advised to add an oil-soluble antioxidant when using an emulsion as a carrier for hair dyes in order to prevent wax from turning yellow and bases and reaction modifiers from oxidizing. The most often utilized chemical is t-butylquinone (TBQ) [36].

Sodium persulfate is used when the vehicle is a powder, while hydrogen peroxide is used when the vehicle is water. Because the peroxides are so unstable, stabilizers such sodium stannate and pentasodium pentetate must be used. They are typically used as an emulsion, or "creamy hydrogen peroxide." [36].

4.6.1 Mechanism of Action

Precursors and peroxide diffuse into the hair shaft, where chemical processes lead to the creation of color. The p-benzoquinone imines/diimines, which are reactive intermediates in color synthesis, are created when hydrogen peroxide oxidizes the dye precursors. The intermediates and couplers, which are both relatively stable to hydrogen peroxide, quickly react to form dinuclear, trinuclear, or polynuclear colorant molecules [43] (Fig 6).

The size of these molecules prevents them from escaping the hair structure. In oxidative hair dyeing formulations, hydrogen peroxide also acts as a bleaching agent for the hair's natural pigment. The precursors and direct dyes present in the dyeing solution, the pH of the dyeing solution, and the length of time the dyeing solution was in contact with the hair all affect the color creation (shades).

Couplers prevent the formation of self-coupling compounds like Bandrowski's base, which are the major reaction products produced by precursor and coupler combinations. The kinetics of reaction products production have not been observed to be impacted by the additional ingredients contained in the formulas of contemporary commercial hair dyes, including direct dyes like HC Yellow 2 and 2-Amino-6-chloro-4-nitrophenol. In addition, no new reaction products were discovered beyond those that were predictable [43].

A study using three couplers (2-methylresorcinol, 4-amino-2-hydroxytoluene, and p-toluenediamine) and three precursors (1-hydroxyethyl-4,5-diaminopyrazole, aminophenol, and 2,4-diaminophenoxyethanol) in a hair dye formulation showed that the oxidative coupling reaction products agreed with theoretical expectations based on the reaction kinetics and that the chemistry in the formulation is dominated by the fastest coupling reactions [43] (Fig 6).

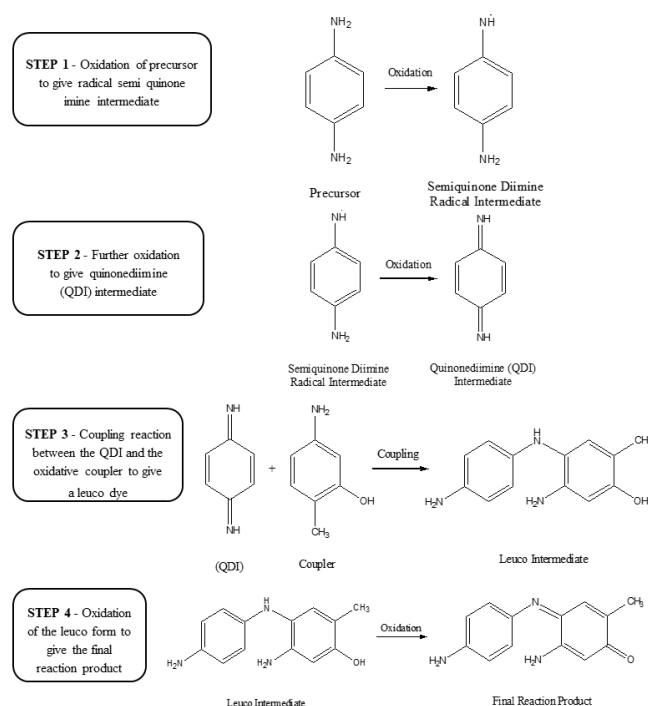


Figure 6. Proposed mechanism of oxidative hair dye formation. Adapted from ref. [43].

5. Repairing Damaged Hair

Hair can become damaged by a variety of things in daily life. In addition to problems including sun exposure, air pollution, improper product usage, hair dye, high styling temperatures, combing, drying, and even gathering hair can harm skin and hair strands. Depending on the amount of damage, mending products must be used to lessen all these negative effects or to treat damaged hair. Different shampoos, conditioners, and serums that contain lipids and protein can replace the elements that have been removed from the structure of healthy hair. For instance, Lee et al. (2022) examined the impact of applying a rinse-off conditioner made with argan and camellia oil on bleach-damaged hair. It has been demonstrated that using a conditioner with argan or camellia oil while washing can protect bleached hair from breakage, boost tensile strength, and lower protein leakage to pre-bleaching levels [44].

This had a stronger impact on conditioner with argan oil, and it was found that argan oil also lengthened the duration that color stayed in the hair. Studies were done on bleached hair to determine

the specific effects of each of the four fatty acids (stearic acid, palmitic acid, oleic acid, and linoleic acid) used in the formulation of the rinse-off conditioners (Fig 7) [44]. The rinse-off conditioner made with palmitic acid had the best results in repairing the surface characteristics of the hair and retaining the color, whereas the conditioner made with oleic acid had the worst results when these effects were studied. Additionally, it has been found that conditioners designed with linoleic acid first, then palmitic acid, and finally stearic acid, boost the tensile strength of the hair. Currently, it is believed that the high palmitic acid and linoleic acid concentration in argan oil's composition is what contributes to color protection [44].

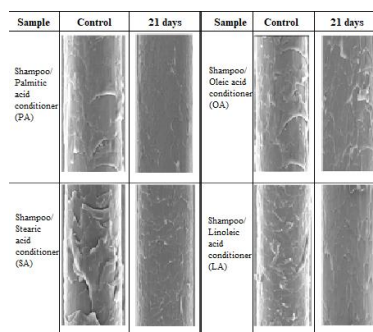


Figure 7. SEM images of bleached hair treated with rinse-off conditioner formulated with four different fatty acids. Adapted from ref. [44].

Morita et al. (2010) synthesized mannosylerythritol lipids (MELs) from *Pseudozyma* based on the effects of lipids on hair restoration and the advantages of glycolipids for the hair cuticle. The tensile strength of damaged hair was shown to be much higher after treatment with these biosurfactants, MEL-A (122.0 13.5 gf/p), MEL-B (119.4 7.6 gf/p), and ceramide (100.7 15.9 gf/p), than it was after treatment with lauryl glycoside (96.7 12.7 gf/p) alone. The mean friction coefficient of damaged hair was shown to be conserved by MEL-A (0.108 0.002), MEL-B (0.107 0.003), and ceramide (0.111 0.003), but it was increased by lauryl glucoside treatment (0.126 0.003). In contrast to lauryl glucoside (0.204 0.002), it was discovered that MEL-A (0.129 0.002), MEL-B (0.176 0.003), and ceramide (0.164 0.002) all prevented the rise in hair bending stiffness. These findings reveal that MELs can efficiently repair hair fibers in place of 18-methyleicosanoic acid. They also demonstrate their potential for improving the smoothness and elasticity of hair strands [45, 46].

In addition to the lipids' healing power, proteins, one of the hair's structural constituents and present in high concentrations in the hair, are known to have a significant part in the health of damaged hair. Transglutaminase (TG) enzyme is now employed in the restoration of protein-based materials like silk, wool, and hair. The reaction between the -hydroxyamide group on the glutamic acid residue and the -amino group on the lysine residue, which results in the formation of crosslinking between proteins or peptides, is catalyzed by the TG enzyme, a commonly used enzyme preparation (Fig 8). In order to repair hair, Xiao et al. (2021) created keratin repair solution (KRS), TG enzyme repair solution (TGRS), and a combination of keratin-TG enzyme repair solution (TG-KRS), all of which were based on the information above and the fact that hair is primarily made of keratin and contains similar lysine and glutamic acid residues. The combination of TG-KRS produced the best results in smoothing the damaged hair's surface using AFM pictures, it was determined (Fig 9). It demonstrates that the application of the TG-KRS combined repair solution to damaged hair induces a significant amount of keratin or keratin peptides to cross-link into those places under the control of the TG enzyme or by protein disulfide bond recombination [47].

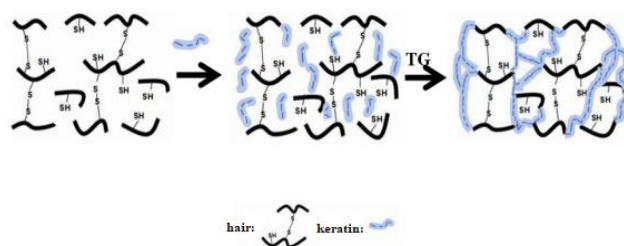


Figure 8. Hair repair mechanism with the combination of keratin and TG enzyme. Adapted from ref. [47].

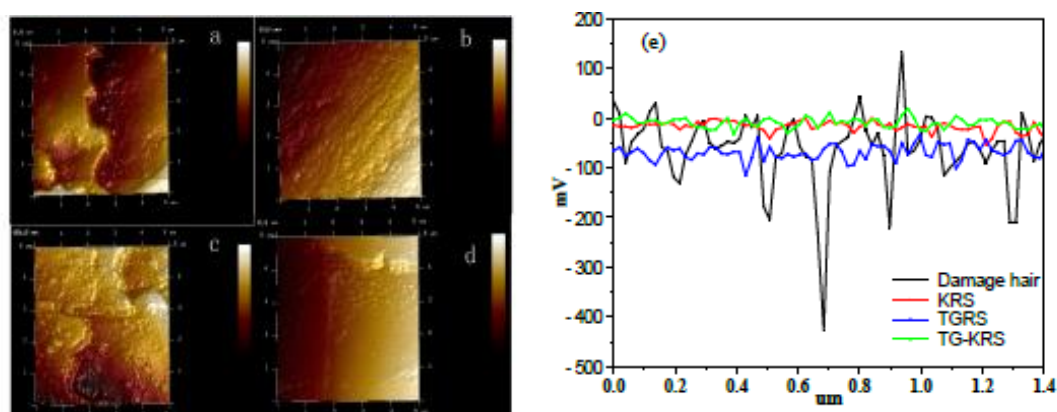


Figure 9. AFM images of (a) damaged hair, (b) KRS, (c) TGRS, and (d) TG-KRS, and (e) surface roughness graph. Adapted from ref. [47].

Another study looked at the effects of five different pentapeptide types with varied amino acid sequences on hair restoration. The STTSS (Ser-Thr-Thr-Ser-Ser), LIILL (Leu-Ile-Ile-Leu-Leu), CMMCC (Cys-Met-Met-Cys-Cys), DEEDD (Asp-Glu-Glu-Asp-Asp), and RKKRR (Arg-Lys-Lys-Arg-Arg) peptides were synthesized by Kang et al. (2020) (53). After being exposed to the fluorescent dye 5(6)-carboxytetramethyl-rhodamine, succinimidylester (5(6)-TAMRA), it was shown that these peptides bound to TAMRA. Due to their extra carboxyl or amine groups, DEEDD and RKKRR showed increased binding affinity to the hair in damaged hair treated with pentapeptide alone or pentapeptides containing crosslinking agents such 1-ethyl-3-(3-imethylaminopropyl) carbodiimide (EDC) and polymeric carbodiimide (PCI). By increasing the number of bonds in the hair by the carbodiimide coupling process, the hair was strengthened. With the exception of DEEDD, which can reach the innermost part of the hair, all peptides have been determined to have hair repair ratios that are appropriate for average fluorescence yield (Fig 10). The polymerizations within the peptide and between the peptide-hair might be claimed to perhaps aid in hair healing for DEEDD and RKKRR [48].

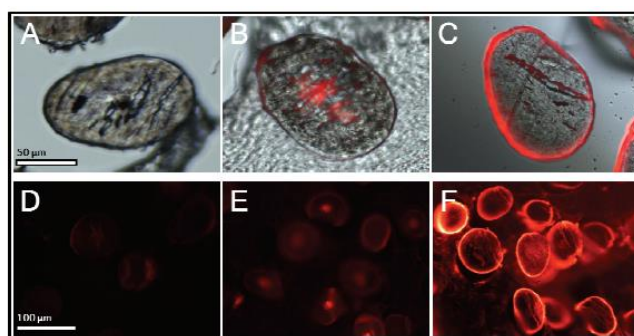


Figure 10. Representative fluorescent microscope images (400 X, 200 X) of hair treated with (A, D) TAMRA-STTSS, (B, E) TAMRA-DEEDD treated and (C, F) TAMRA-RKKRR treated hair after EDC solutions. Adapted from ref. [48].

Antioxidants, immunocosmetics, nanoparticles, as well as lipids and amino acids that can penetrate the hair shaft, are known to be employed in hair cosmetic products. According to Fernandez et al. (2012), rice and artichoke natural antioxidants were employed to prevent UV-induced chemical and physical harm. While the larger molecular weight peptides produced a protective layer to stop tryptophan from degrading and discoloring, the low molecular weight peptides of the rice formulation increased the mechanical qualities of the cortex by permeating the hair. The hydroxycinnamic characteristic of the artichoke formulation, on the other hand, has been demonstrated to improve the integrity of the hair fiber and exhibit better antioxidant qualities, greatly reducing lipid peroxidation and protein degradation of the hair. Both formulations have been demonstrated to be effective at lessening the negative effects of UV [49].

The impact of immunocosmetic use on removing hair damage was assessed in a different study. Human hair was used as the antigen to produce an egg yolk antibody, which was then used to make a hair care product. The anti-hair antibody formed from egg yolk, according to the present invention, has remarkable effects including elasticity, smoothness, gloss, hair renewal, moisturizing even in dry conditions, and a permanence that does not vanish even with repeated washes [50].

Nanotechnology's applications in cosmetic products have become more varied as a result of the technology's evolving and increasing effects. The nanostructured lipid carriers (NLCs) and NLCs loaded with vitamin E's (Vit E-NLCs) influences on the prevention of hair damage and discoloration induced by UV radiation and heat impacts were examined using cutting-edge nanotechnology. Using a process called high-pressure homogenization, NLCs and Vit E-NLCs were created. It was noted that creams containing Blank-NLCs (NLC's cream) and Vit E-NLCs (Vit E-cream) NLC's were protectively effective. On hair exposed to heat and UV radiation, both NLC creams have offered surface smoothness comparable to that of unharmed hair and the least amount of color loss as compared to other treatments. It was understood that, when compared to Blank-NLCs, the cream containing antioxidant Vit-E showed reduced protein loss and a greater photoprotective action against hair discoloration, but it had no additional effect for heat protection [51].

We can see from this information and the research that has been done that the damage to the hair can be reversed with the right kind of treatment. In order to restore damaged hair strands, proper maintenance and the use of products with suitable ingredients are essential considerations. The therapies of the future are emerging as a beacon of hope for the cosmetic industry as well as in every other industry thanks to science's unrelenting advancement.

6. Patch Test for Toxicity, Allergic Effect, and Hyperoxidative Hair Colors

Hair colors are primarily divided into two categories: oxidative and non-oxidative colors. The group of non-oxidative hair dyes includes temporary and semi-permanent colors that do not remain in the hair permanently and create dye accumulation; the dye does not penetrate the cortex and instead just interacts with the hair cuticles. Deep penetration of the hair shaft by chemicals is necessary to achieve permanent color. The cuticles must be opened for this.

Ammonia and other alkaline solutions are frequently employed for this purpose. In addition to opening the hair fibers, this alkaline solution makes the hair expand, which facilitates easier colour absorption. The next step is to mix these monomers with binding compounds and polymerize them using an oxidizing agent (like hydrogen peroxide). Due to this, colorful complexes are created that are too big to spread back out from the hair shaft [12].

Recently, studies on the chemistry and types of hair dyes have been conducted [52]. These are the several types of hair dyes: (Fig 11).

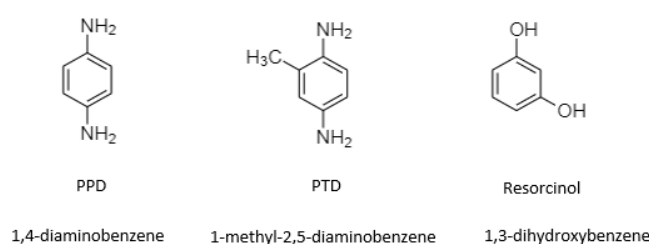


Figure 11. Paraphenylenediamine (PPD), paratoluendiamine (PTD), and resorcinol (binder): primary oxidative hair dye intermediates [52].

Similar compounds are still present in the majority of hair dyes today, despite the fact that their compositions have changed since the day they were originally produced. Depending on the type of metal and its concentration, or the extent of its harmful effects, it can cause a variety of health issues when consumed, including skin damage, allergic reactions, disorders of the tissue or organs, and occasionally even death [53].

The majority of the time, permanent hair dyes are linked to health hazards. These products often include binding molecules, oxidizing agents, primary intermediates, such as p-phenylenediamine (PPD), alkalizing agents, such as ammonia, and oxidizing agents, such as hydrogen peroxide (e.g. resorcinol). The other chemicals in the product stimulate a chemical reaction inside the hair shaft to generate color molecules, and the alkalizing agent aids in the product's penetration of the hair shaft's outer layer [54].

A common issue for hair colorists worldwide is allergic contact dermatitis (ACD), which is brought on by hair dyes [55, 56].

7. Acute Toxicity of PPD - Contact Allergy and Dermatitis

When a person is exposed to the same allergen again after being sensitized to it, they develop allergic contact dermatitis (ACD). T-cell (cellular-type) immunity mediates the hypersensitive reaction, which is of the delayed kind. Even while individual immune responses and clinical manifestations differ depending on the allergen, it typically worsens until itchy, eczematous-like sores develop at the point of contact [57].

PPD products like permanent hair dye, black henna, and permanent eyelashes have been linked to contact allergy and eczema. It encompasses symptoms including erythema multiforme, hyperpigmentation, lichenification, blepharoconjunctivitis, systemic contact allergy, and dermatitis syndromes [56, 58].

A colorless substance called p-phenylenediamine is used mostly in black hair dyes and is oxidizable by hydrogen peroxide. When PPD is administered to the skin, complications might range from contact dermatitis to allergic responses [59, 60]. PPD is permitted at hair dye quantities of up to 0.5% by the European Parliament and the Union of the European Commission. The harmful effects become more pronounced when this concentration is exceeded [61].

A hypersensitive response to chemicals that come into touch with the skin is known as allergic contact dermatitis (ACD). To find the allergens that induce ACD, a patch test is utilized [62].

7.1. Patch Test

Patch testing; sometimes known as allergic contact dermatitis; is a skin examination performed to identify eczema (contact eczema). Allergic eczema that appears 48–96 hours after frequent contact with an allergic person is known as allergic contact dermatitis (ACD), a type-IV hypersensitivity reaction to chemicals in touch with the skin [62].

A diagnostic technique for identifying allergies that can cause disease is patch testing. Patch testing is a crucial and secure technique for identifying allergic contact eczema [63].

7.1.1 Application

On the back, allergens formulated in pure vaseline are applied. The upper portion of the back is covered with tape. An alcohol wipe is used to clean the back's skin if it is oily or sweaty. The patient should be advised not to bathe, perspire, or perform any physical activity that would cause the bands to separate because the attached test will stay on the back for 48 hours. One week prior to the test, creams applied to the back should be stopped, and anti-allergic or cortisone-containing medications should not be taken due to their potential to stifle the reaction. A doctor should record the bands' placements with a pencil after 48 hours and do an evaluation after at least 30 minutes. A doctor should reevaluate the test site at 72 and 96 hours due to late-reactive allergens (Table 7) [63].

Table 7. Patch Test Interpretation and Evaluation. Adapted from ref. [63]

	Evaluation	Clinical Comment
IR	Irritation	Contact Allergies
+++	Vesiculobullous and/And Ulcerative Reaction	Allergic Contact Dermatitis (Definite)
++	Vesiculobullous, Erythema and Infiltration	Allergic Contact Dermatitis
+	Edema, Erythema and Infiltration	Contact Allergies
0	No Reaction	No Contact Allergies
+/-	Mild Erythema	Suspicious Reaction

The last 48 hours are when irritant effects are most notable. Lesions that are clearly outlined and barely infiltrating are present here. It has been documented that erythematous and follicular irritant reactions might manifest as papules, pustules, bullae, and necrosis. Another common observation is the emergence of wrinkled skin that is restricted to the region of the applied substance. After the test strips were removed from the skin, the majority of irritating reactions quickly subsided [64].

8. Conclusion

We have tracked changes in the past few decades about the interactions between the physical and chemical characteristics of the structure of the hair and the mechanisms underlying the hair-coloring process. The development of existing dye precursors and new technologies is aided by extensive knowledge of the makeup of the hair fiber, particularly the chemical composition of its outer layer and the factors influencing the dye diffusion pathways and process kinetics.

The oxidative treatment will continue to work best in an optimal form due to widespread technological advancements that do not appear to slow down in the near future, a considerable number of novel dye precursors patented over the years, and some examples of commercial success. Additionally, addressing worries about toxicological problems linked to commercial permanent hair-dyeing technology based on the oxidative process, originating from Hofmann's discovery about 150 years ago, has received a lot of attention [34].

This issue was addressed by Im et al. (2017) using a mordant staining-type method in which iron (II) sulfate and "synthetic melanin" (i.e. polydopamine (PDA)) oxidized via oxidative self-coupling of dopamine (DA) are applied combined [65]. According to Gao et al. (2019), by covering the hair with polydopamine, oxidative self-coupling of dopamine enhanced by copper (II) sulfate and peroxide provided quick and effective coloring [66]. According to Battistella et al. (2020), in situ polymerization

and deposition of polydopamine nanoparticles on the surface of the hair can produce permanent coloration [67].

One of the key priorities in the beauty and care sector is ensuring the safety of hair dyes and all cosmetic products. Consumers should feel assured of the safety of today's hair dye formulas based on the considerable safety data that is already accessible. To give customers, clients, and hairdressers a higher degree of confidence and certainty, hair dye makers are also continuing their studies into safety. It is crucial to inform consumers and hairdressers about the potential hazards of hair dyes, increase collaboration with experts (dermatologists), and reduce risk in order to fulfill the consistently high consumer demand for hair coloring products. There are already controls in place to safeguard vulnerable people [68].

9. New Applications

Oxidative coloring first rose to commercial popularity over a century ago, and it still reigns supreme in the professional and retail hair dye industries today. The popularity of oxidative hair dying is a result of its quick and inexpensive means of achieving long-lasting coloration [69].

Additionally, the entry of new dye precursors will likely be restricted to those for which there is unambiguous proof of a commercial return on investment due to the costs associated with the licensing procedure of new formulation ingredients as demanded by social norms and legislation. Systems that support natural, biotechnological, or semi-synthetic hair repigmentation may benefit from the fast-evolving genetics and growing understanding of the molecular basis of hair pigmentation [34].

Synthetic methods that are influenced by biology are gaining popularity [70]. Important research has been done in this regard on polydopamine (PDA)-based techniques for coloring human hair [66].

According to research by Battistella et al. (2020), optimal conditions for PDA coating can be combined with the oxidation of dopamine utilizing oxygen in the air to produce a protective and colored layer in the hair coating [70].

Sun et al. (2021) were able to collect polydopamine groups on the hair surface through metal chelation and hydrogen bond adsorption by oxidizing dopamine to polydopamine, an imitation of human eumelanin [71].

Gao et al. (2019) obtained the black color faster (within 5 minutes) than was feasible with commercial items using PDA coatings made from copper ions and hydrogen peroxide [66].

The findings demonstrate the potential of these innovative, simple, and efficient techniques for biomaterial-based hair cosmetics, and more crucially, they show that built systems behave similarly to natural materials [67].

The scientific community has become interested in natural dyes for use in a number of conventional and recently found application disciplines since they are typically believed to be non-toxic, affordable, renewable, and sustainable resources with minimum environmental impact [72]. Although the efficient use of colorants generated from natural sources has seen substantial technological advancement in recent years, there are still some technical obstacles that must be removed in all parts of natural dye application before these technologies can be put to use. Due to the great range of natural dye sources, it is currently difficult to develop extraction and application procedures and construct cost-effective processes [73].

Nanotechnology researchers have created natural and non-harmful hair surface engineering techniques to create hair coloring formulations that no longer rely on chemical reactions but rather only on physical forces acting at a very close distance thanks to recently published scientific papers and patents [73]. Long-lasting hair dyes using carbon nanotubes, which have volumizing and damage-prevention benefits, are among these works. The hair dye business will undoubtedly continue to pay attention to this amazing advancement in nanotechnology [74].

Considering the subject heading of the European Green Deal, which is the new growth strategy of the EU, which includes the main objectives such as ending the dependence on the use of resources for economic growth, "Innovative, Systemic Zero Pollution Solutions Against the Negative Effects of Persistent and Mobile Chemicals on Human Health, Environment and Nature" [75], the most important result is undoubtedly the following: "The cost is not the only important issue, it is very important to apply alternative test methods for safety and toxicity, and also to be environmentally friendly".

Ethical Statements

The author declares that this document does not require an ethics committee approval or any special permission. Our study does not cause any harm to the environment.

Conflict of interest

The authors declare that they have no conflicts of interest.

Authors' Contributions

A. Y: writing-review and editing

B.D: writing-review and editing

B.A: writing-review and editing

B.N.E: writing-review and editing

Ç.Ö: writing-review and editing

G.E.A: writing-review and editing

M.M: writing-review and editing

M.K: writing-review and editing

N.A: writing-review and editing

S.E: writing-review and editing

All authors have read, reviewed the results and agreed to the final published version of the manuscript.

References

- [1] Sudhir, S.P., Kumarappan, A., Vyas, L.K., Shrivastava, D., Deshmukh, P., Verma, H.N., "Identification of Nigella sativa seed and its adulterants using DNA Barcode Marker", *American Journal of Life Sciences*, 4, 118-128, 2016. [<DOI>](#)
- [2] Sudhir, S.P., Kumarappan, A., Malakar, J., Verma, H.N., "Genetic diversity of Nigella sativa from different geographies using RAPD markers *American Journal of Life Sciences*, 4, 175-180, 2016. [<DOI>](#)
- [3] Sudhir, S.P., Deshmukh, V.O., Verma, H.N., "Nigella sativa seed, a novel beauty care ingredient: A review", *International Journal of Pharmaceutical Sciences Research*, 7, 3185-3196, 2016. [<DOI>](#)
- [4] Alam, M.M., Rahman, M.L., Haque, M.Z., "Extraction of henna leaf dye and its dyeing effects on textile fibre", *Bangladesh Journal of Scientific and Industrial Research*, 42, 217-222, 2007. [<DOI>](#)
- [5] Jayaganesh, S., Jainendra, M., Rawat, B.S., Venkataramana, A.P., "Influence of gamma radiation on microbial and viscosity parameters of henna-based hair colour", *International Journal of New Technology and Research*, 2, 11-15, 2016. [<DOI>](#)
- [6] Chisvert, A., Chafer, A., Salvador, A., "Hair dyes in cosmetics: regulatory aspects and analytical methods", *Analysis of Cosmetic Products*, 2, 159-173, 2018. [<DOI>](#)

- [7] Sankar, J., Rawat, B.S., Malankar, J., Padmanabha, V.A., “Estimation of available oxygen in powder form of oxygen releaser in henna-based hair dyes”, *SSRG International Journal of Applied Chemistry*, 4, 34-37, 2017. [<DOI>](#)
- [8] Sankar, J., Sawarkar, S., Malakar, J., Rawat, B.S., “Ali MA. Mechanism of hair dying and their safety aspects: a review”, *Asian Journal of Applied Sciences*, 10 (4), 190-196, 2017. [<DOI>](#)
- [9] Draelos, Z.K., “Hair cosmetics”, *Dermatol Clin*, 9, 19–27, 1991. [<URL>](#)
- [10] Bolduc, C., Shapiro, J., “Hair care products. Waving, straightening, conditioning, and coloring”, *Clin Dermatol*, 19(4), 431-436, 2001. [<DOI>](#)
- [11] Harrison, S., Sinclair, R., “Hair colouring, permanent styling and hair structure”, *Journal of Cosmetic Dermatology*, 2, 180-185, 2004. [<DOI>](#)
- [12] Da Franca, A.S., Dario M.F., Esteves, V.B., Baby, A.R., Velasco, M.V.R., “Types of hair dye and their mechanisms of action”, *Cosmetics*, 2, 110-126, 2015. [<DOI>](#)
- [13] Shimomura, Y., Christiano, A.M., “Biology and genetics of hair”, *Annual Review of Genomics and Human Genetics*, 11, 109-132, 2010. [<DOI>](#)
- [14] Westgate, E.G., Botchkareva N.V., Tobin, D.J., “The biology of hair diversity”, *International Journal of Cosmetic Science*, Citations: [37](#), 30, 2013. [<DOI>](#)
- [15] Cruz, C.F., Costa C.C., Gomes A.C., Matamá, T., Paulo, A.C., “Human hair and the impact of cosmetic procedures: A review on cleansing and shape-modulating cosmetics” *Cosmetics*, 2016. [<DOI>](#)
- [16] Kaplan, P.D., Polefka, T., Grove, G., Daly, S., Jumbelic, L., Harper, D., Bianchini, R., “Grey hair: Clinical investigation into changes in hair fibres with loss of pigmentation in a photoprotected population”, *International Journal of Cosmetic Science*, 33(2), 171-182, 2011. [<DOI>](#)
- [17] Park, A.M., Khan, S., Rawnsley, J., “Hair biology growth and pigmentation”, *Facial Plastic Surgery Clinics of North America*, 26(4), 415-424, 2018. [<DOI>](#)
- [18] Koch, S.L., Tridico, S.R., Bernard, B.A., Shriver, M.D., Jablonski, N.G., “The biology of human hair: A multidisciplinary review”, *American Journal of Human Biology*, 32(2), 2020. [<DOI>](#)
- [19] Ozeki, H., Ito, S., Wakamatsu, K., Thody, A.J., “Spectrophotometric characterization of eumelanin and Pheomelanin in hair”, *Pigment Cell Research*, 9(5), 265–270, 1996. [<DOI>](#)
- [20] Shekar, S.N., Duffy, D.L., Frudakis, T., Montgomery, G.W., James, M.R., Sturm, R.A., Martin, N.G., “Spectrophotometric methods for quantifying pigmentation in human hair influence of MC1R genotype and environment”, *Photochemistry and Photobiology*, 84(3), 719-726, 2008. [<DOI>](#)
- [21] Vaughn, M.R., Van Oorschot R.A.H., Baidur-Hudson, S., “A comparison of hair colour measurement by digital image analysis with reflective spectrophotometry”, *Forensic Science International*, 183(1–3), 97–101, 2009. [<DOI>](#)
- [22] Sealy, R.C., Hyde, J.S., Felix, C.C., Menon, I.A., Protá, G., “Eumelanins and pheomelanins: Characterization by electron spin resonance spectroscopy”, *Science*, 217, 545–547, 1982. [<DOI>](#)
- [23] Lasisi, T., Ito, S., Wakamatsu, K., Shaw, C.N., “Quantifying variation in human scalp hair fiber shape and pigmentation”, *American Journal of Physical Anthropology*, 160(2), 341-352, 2016. [<DOI>](#)

- [24] Ito, S., Miyake, S., Maruyama, S., Suzuki, I., Commo, S., Nakanishi, Y., Wakamatsu, K., “Acid hydrolysis reveals a low but constant level of pheomelanin in human black to brown hair”, *Pigment Cell & Melanoma Research*, 31(3), 393-403, 2018. [<DOI>](#).
- [25] Ito, S., Fujita, K., “Microanalysis of eumelanin and pheomelanin in hair and melanomas by chemical degradation and liquid chromatography”, *Analytical Biochemistry*, 144, 527–536, 1985. [<DOI>](#).
- [26] Zviak C, Milléquant J. ‘Hair coloring: non-oxidation coloring’ and ‘Oxidation coloring’, chapters 8 and 9 in *The Science of Hair Care*, 2nd edition, ed. C Bouillon and J Wilkinson. Taylor and Francis. Boca Raton. 2005.
- [27] Hefford, R., “Colourants and dyes for the cosmetics industry. Handbook of Textile and Industrial Dyeing”, 2, 175-203, 2011. [<DOI>](#).
- [28] He L., Michailidou, F., Gahlon H. L., & Zeng W., “Hair dye ingredients and potential health risks from exposure to hair dyeing”, *American Chemical Society*, 35(6),901–915, 2022. [<DOI>](#)
- [29] Sankar, J., Sawarkar, S., Malankar, J., Rawat, B. S., Ali, M. A., “Mechanism of hair dyeing and their safety aspects”, *Research Journal of Topical and Cosmetic Sciences*, 8(2),72-77, 2017.[<DOI>](#)
- [30] Barel A. O, Paye M, & Maibach H. I (Eds.). *Handbook of cosmetic science and technology*. CRC Press. 2014; 51. [<URL>](#)
- [31] Tucker, H. H., “The coloring of human hair with semipermanent dyes”, *Journal of the Society of Cosmetic Chemists*, 22,379-398, 1971. [<URL>](#)
- [32] Ballarin, B., Galli, S., Morigi, M., “Study of dyeing properties of semipermanent dyestuffs for hair”, *Internaional Journal of Cosmetics Science*, 29,49–57, 2007. [<DOI>](#)
- [33] Robbins, C.R., Crawford, R. J., “Cuticle damage and the tensile properties of human hair”, *Journal of the Society of Cosmetic Chemists*, 42(1), 59-67, 199. [<URL>](#)
- [34] Morel, O. J., Christie, R. M., “Current trends in the chemistry of permanent hair dyeing”, *Chemical Reviews*, 111(4),2537-2561, 2011. [<DOI>](#)
- [35] Lewis, D., Mama, J., Hawkes, J., “A review of aspects of oxidative hair dye chemistry with special reference to N-nitrosamine formation”, *Materials*, 6(2), 517-534, 2013. [<DOI>](#)
- [36] Les Colorants Wackherr (LCW). *Apresentação Técnica Sobre Tinturas Capilares*; LCW: São Paulo, Brazil, 2008. (In Portuguese)
- [37] Harrison S., Sinclair R., “Hair coloring, permanent styling and hair structure”, *J. Cosmet. Dermatol*, 2, 180–185, 2004. [<DOI>](#)
- [38] Brown, K.C., “Hair coloring. In *Hair and Hair Care*; Johnson D H, Marcel Dekker: New York, NY, USA, 1997.35 21 Draelos, Z.K.”, *Hair cosmetics. Dermatol. Clin.*, 9, 19–27, 1991.
- [39] More O., Christie R M., Greaves A., Morgan, K.M., “Enhanced model for the diffusivity of a dye molecule into human hair fibre based on molecular modelling techniques”, *Color. Technol.*, 124, 301–309, 2008.
- [40] Bolduc C., Shapiro, J., “Hair care products: Waving, straightening, conditioning and coloring”, *Clin. Dermatol.*, 19, 431–436, 2001. [<DOI>](#)

- [41] Kojima T., Yamada, H., Yamamoto, T., Matsushita, Y., Fukushima, K., “Dyeing regions of oxidative hair dyes in human hair investigated by nanoscale secondary ion mass spectrometry”, *Colloid Surf. B*, 106, 140–144, 2013. [<DOI>](#)
- [42] Wolfram, L. J., “Hair cosmetics”, In Handbook of Cosmetic Science and Technology, Barel, A O, Paye M, Maibach H I, Eds. Marcel Dekker, New York, NY, USA, 2001.
- [43] Scientific Committee on Consumer Products, SCCP/1198/08.
- [44] Lee, S. H., Ahn, C., “Effect of rinse-off hair conditioner containing argan oil or camellia oil on the recovery of hair damaged by bleaching”, *Fashion and Textiles*, 9(1), 1-24, 2022. [<DOI>](#)
- [45] Morita, T., Kitagawa, M., Yamamotoi, S., Sogabe, A., Imura, T., Fukuoka, T., Kitamoto, D., “Glycolipid biosurfactants, mannosylerythritol lipids, repair the damaged hair”, *Journal of Oleo Science*, 59(5), 267-272, 2010. [<DOI>](#)
- [46] Kojima, T., Tsuji, S., Niwa, M., Saito, K., Matsushita, Y., Fukushima, K., “Distribution analysis of triglyceride having repair effect on damaged human hair by TOF-SIMS”, *International Journal of Polymer Analysis and Characterization*, 17(1), 21-28, 2012. [<DOI>](#)
- [47] Li, Z., Xiao, J., “Repair of damaged hair protein fiber by jointly using transglutaminase and keratin”, *Scienceasia*, 47(2), 195-201, 2021. [<DOI>](#)
- [48] Choi, W., Son, S., Song, S. H., Kang, N. G., Park, S. G., “Repairing Damaged Hair Using Pentapeptides of Various Amino Acid Sequences with Crosslinking Reaction”, *Korea Journal of Cosmetic Science*, 2(1), 11-19, 2020. [<DOI>](#)
- [49] Fernández, E., Martínez-Teipel, B., Armengol, R., Barba, C., Coderch, L., “Efficacy of antioxidants in human hair”, *Journal of Photochemistry and Photobiology B: Biology*, 117, 146-156, 2012. [<DOI>](#)
- [50] Nojiri H., Naito, S., Takahasi, H., Fujiki, M., Kim, M., “Yolk antibody-containing hair care products”, US Patent, 5976519, 1-8, 1999.
- [51] Prasertpol, T., Tiyaboonchai, W. “Nanostructured lipid carriers: A novel hair protective product preventing hair damage and discoloration from UV radiation and thermal treatment”, *Journal of Photochemistry and Photobiology B: Biology*, 204, 111769, 2020. [<DOI>](#)
- [52] Nohynek, G.J., Fautz, R., Kieffer, F.B., Toutaina, H., “Toxicity and human health risk of hair dyes”, *Food and Chemical Toxicology*, 42(4), 517–543, 2004. [<DOI>](#).
- [53] Palisoc, S., Causing, A.M., Natividad, M., “Gold nanoparticle/hexammine/ruthenium/Nafion® modified glassy carbon electrodes for trace heavy metal detection in commercial hair dyes”, *Analytical Methods*, 9(29), 4240-4246, 2017. [<DOI>](#).
- [54] Concert About Hair Dye, <https://www.poison.org/articles/hair-dye> [<URL>](#).
- [55] Almeida PJ, Borrego L, Limiñana JM. Age-related sensitization to p-phenylenediamine. *Contact dermatitis* 2011;64: 172–174. [<DOI>](#).
- [56] Chey, W.Y., Kim, K.L., Yoo, T.Y., Lee, A.Y., “Allergic contact dermatitis from hair dye and development of lichen simplex chronicus”, *Contact Dermatitis*, 51(1), 5–8, 2004. [<DOI>](#).
- [57] Prof. Dr. Kirmaz, www.alerjiklinigi.com [<URL>](#).
- [58] Vogel, T.A., Coenraads, P.J., Bijkersma, L.M., Vermeulen, K.M., Schuttelaar, M.L., “p-Phenylenediamine exposure in real life – a case–control study on sensitization rate, mode and

- elicitation reactions in the northern Netherlands”, *Contact Dermatitis*, 72(6), 355-361, 2015. [<DOI>](#).
- [59] Yenigün, A., Cetemen, A., Pektaş, E., Karayel, E., Özcan, N., “Frequency of respiratory and skin findings in hairdresser's apprentices in Aydın”, *Asthma Allergy Immunology*, 8, 77-87, 2010. [<URL>](#).
- [60] Uçar, S., Özçelik, S., Akyol, M., “Allergic contact evaluation of patch test results in cases with dermatitis”, *Cumhuriyet Medical Journal*, 33(3), 299-306, 2011. [<DOI>](#).
- [61] Jung, Y., Kwon, S., Kang, S.Y., “Status epilepticus possibly caused by hair dye exposure in a diabetic man”, *Journal Neurocrit Care*, 1, 168–170, 2008. [<DOI>](#).
- [62] Sen, B.B., Rifaioglu, E.N., Ekiz, Ö., Doğramacı, A.C., Sen, T., “Contact Evaluation of Patch Test Results in Cases with Dermatitis”, *Bozok Medical Journal*, 5(2), 35-40, 2015. [<DOI>](#).
- [63] Allergen; Patch Test Standard Series 2018. [<URL>](#).
- [64] Turkish Dermatology Association: Patch Test. [Accessed July 26, 2022]. [<URL>](#).
- [65] Im, K.M., Kim, T.W., Jeon, J.R., “Metal-chelation-assisted deposition of polydopamine on human hair: a ready-to-use eumelanin-based hair dyeing methodology”, *ACS Biomaterials Science & Engineering*, 3, 628-636, 2017. [<DOI>](#).
- [66] Gao, Z.F., Wang, X.Y., Gao, J.B., Xia, F., “Rapid preparation of polydopamine coating as a multifunctional hair dye”, *RSC Advances*, 9, 20492-20496, 2019. [<DOI>](#).
- [67] Battistella, C., et al. “Mimicking natural human hair pigmentation with synthetic melanin”, *ACS Central Science*, 6, 1179-1188, 2020. [<DOI>](#).
- [68] Schlatter, H., Long, T., Gray J., “An overview of hair dye safety”, *Journal of Cosmetic Dermatology*, 6, 32-36, 2017. [<DOI>](#).
- [69] Towns, A., “A review of developments in industrial hair colorant actives for oxidative dyes”, *Coloration Technology*, 137, 301-335, 2021. [<DOI>](#).
- [70] Battistella, C., et al. “Bioinspired chemoenzymatic route to artificial melanin for hair pigmentation” *Chemistry of Materials*, 32, 9201-9210, 2020. [<DOI>](#).
- [71] Sun, Y., Wang, C., Sun, M., Fan, Z., “Bioinspired polymeric pigments to mimic natural hair coloring” *RSC Advances*, 11, 1694-1699, 2021. [<DOI>](#).
- [72] Verma, S., Gupta, G., “Natural dyes and its applications: A brief review” *International Journal of Research and Analytical Reviews*, 4, 57-60, 2017. [<DOI>](#).
- [73] Shahid, M., Mohammad, F., “Recent advancements in natural dye applications: a review” *Journal of Cleaner Production*, 53, 310-331, 2013. [<DOI>](#).
- [74] Mihranian, A., Ferraz, N., Strømme, M., “Current status and future prospects of nanotechnology in cosmetics” *Progress in Materials Science*, 57, 875-910, 2012. [<DOI>](#).
- [75] The European Green Deal. ESDN Report, December (2020). [<URL>](#).